THERMOELECTRIC POWER AND HEATS OF TRANSPORT OF THE ALKALI-HALIDES

Thesis submitted for the degree of
Doctor of Philosophy

by

Tan Poh Lin

B.Sc.(Hons), London.
A.R.C.S., Imperial College.

May 1968

Department of Metallurgy,
Imperial College of
Science and Technology,
University of London.

Contents

Abstract

In principle the most direct way of obtaining the experiment-tal heats of transport is by measuring the crystal thermo-power. This is done for pure NaCl single crystals using platinum electrodes in the temperature range of 870°K to 1060°K. However, the results of the alkali-halides measure-ments have not been succesfully analysed so far. This is because in the alkali-halides system irreversible electrodes (no common ion between electrodes and crystal) have to be used, and the existing theories for the irreversible electrode-crystal thermopower are unsatisfactory. The possibility that the heterogeneous thermopower might be caused by the electrons, which are transfered from the electrodes to the crystal, and which do not fall into any traps, is investigated. This model is also found to be unsatisfactory.

The dynamics of the diffusion of a vacancy in a linear chain is studied. A simple relationship between the heat of transport, Q^*, and the activation energy for thermal diffusion, E, is found, namely, $Q^* = (2+q/T)E$, where q is related to the dynamics of the system. The subsequent calculations show that q is negative in agreement with the experimental data for AgBr and AgCl.

In the course of calculating q to attempt to give theoretical heats of transport for the alkali-halides,

various force constants operating between the ions have to be evaluated. This is first done by evaluating the Schottky -pair formation energies by lattice calculations. This calculations, which prove. very successful, show that the basic Born-Mayer form of potential chosen here is realistic.

CHAPTER I: INTRODUCTION

Point defects exist in solids, and they are necessary to maintain thermodynamic equilibrium. In ionic crystals the point defects are charged and their movements account for a major portion of the conductivity of the crystals. [For a comprehensive account of ionic conductivity see Lidiard (1)]. The conductivity and other related phenomena (e.g. dielectric absorption and relaxation) of ionic crystals, especially of the alkali-halides, have been studied extensively. From these studies, the type of defects (Schottky or Frenkel type), their concentrations, and some of their properties (e.g. energies of formation, energies of activation, etc) have been found.

In contrast to the phenomena which occur when the crystal is under an electric gradient, those phenomena which occur when there is a concentration gradient, i.e. the Soret effect (see Reinhold(2), Reinhold and Schulz(3), Allnatt and Chadwick(4)), or when there is a temperature gradient, are not well understood.

I.1 THERMOELECTRIC POWER MEASUREMENTS

The measurements of the thermoelectric power of the silver halides by Christy et. al (5) and Christy (6) show good reproducibility. But the early measurements on the alkali halides by Nikitinshaya and Murin (7) show that the reproducibility is far from satisfactory. Allnatt and Jacobs(8), working on KCl, report various unexpected phenomena which they are not able to explain. Subsequent authors (9,10,11,12) have since confirmed the observations of these phenomena in

the other members of the alkali-halides.

It has been suggested that the experimental difficulties, and the non-reproducible anomalous phenomena encountered in the measurements of the thermoelectric power of the alkali-halides have in a large part been due to the necessity of using irreversible electrodes (i.e. no ions in common between the crystal and the electrode). Alkali metals are soluble in the salt and they are extremely volatile at the temperatures at which the measurements are carried out.

It is difficult to explain the results of the measurements of the steady state thermoelectric power. The total thermopower, Θ, is made up of the homogeneous, i.e. crystal, thermopower, Θ_{hom}, and the heterogeneous, i.e. crystal-electrode, thermopower, Θ_{het}. The four theories explaining the heterogeneous thermopower, namely Howards's (13) surface formation of metal phase theory, Allnatt and Jacobs's (14) F-centre theory, Jacobs and Maycock's (11) surface charge theory, and Shimoji and Hoshino's (15) combination of the F-centre and Lehovec space charge theory all arrives at a significant magnitude of the heterogeneous thermopower.

I.2 THE HOMOGENEOUS THERMOELECTRIC POWER

The theoretical expression for the homogeneous thermopower, Θ_{hom}, is obtained by first writing down the flux of ions in the two sublattices of the binary ionic system when

the crystal is in a temperature gradient. For the alkali-halides, the flux of the cations (alkali ions), j_+, is written as

$$j_+ = D_+ \left[\text{grad } n_{(+)} - \frac{en_{(+)}}{kT} \text{ grad } V - \frac{\Theta_+^* n_{(+)}}{kT^2} \text{ grad } T\right] \quad \ldots\ldots (I.1)$$

where D_+ is the diffusion co-efficient of the cation.

$n_{(+)}$ is the concentration of the cation vacancies per unit volume, V is the potential developed across the crystal, and Θ_+^* is the heat of transport of the cations.

For the derivation of Equation (I1) see Chapter II

There is a corresponding expression for the anion (halide ion) flux, j_-.

In the steady state,

$$j_+ - j_- = 0,$$

and consequently, the homogeneous thermopower is

$$\Theta_{hom} = \frac{\text{grad } V}{\text{grad } T} = - \frac{kT \text{ grad } n_{(-)}}{en_{(-)} \text{ grad } T} + \frac{\left\{(h_s - Q_+^*)\eta + \phi Q_-^*/\eta\right\}}{eT\,(\eta + \phi/\eta)} \quad \ldots\ldots (I.2)$$

where $\phi = D_-/D_+$, $\eta = n_{(+)}/n_0$, n_0 is the equilibrium cation vacancy of the pure crystal, and h_s is the enthalpy of formation of a Schottky pair.

In order to analyse the experimental results of the thermopower measurements according to Equation (I.2) an adequate theory of the heats of transport is required.

I.3 THE HEAT OF TRANSPORT

The heat of transport of an ion, or atom, is defined as the heat, or energy, which is carried by a unit flux of the ions, or atoms, when the temperature is uniform throughout.

The earliest theory of the heat of transport is done by Wirtz (16) who uses a simple kinetic argument. Wirtz pictures the jumping process as follows: An ion at temperature T is given a free energy Δg_1, to make the jump. At the end of the jump it gives up a free energy, Δg_3 at a temperature of $T + \Delta T$, to push the ions surrounding the vacancy apart. Midway, Δg_2 is given up at $T + \Delta T/2$ to let the ion through. On the basis of this analysis, Wirtz deduces that $Q^{\ddagger} = - \Delta h_3 + \Delta h_1$ where Δh_1 and Δh_3 are the enthalpies corresponding to the free energies Δg_1 and Δg_3 respectively.

Assuming that Δh_1 and Δh_3 are roughly the energies of activation and formation of a vacancy respectively, this theory deduces that for NaCl, $Q_+^{\ddagger} = -1.01 + 0.69$ eV $= -0.32$ eV and $Q_-^{\ddagger} = -1.01 + 0.91$ eV $= -0.1$ eV. These values are independent of temperature. Both the form and the magnitude of these results are contrary to the experimental evidence.

Since Wirtz's original theory, other authors have used both the kinetic approach (17,18,19,20,21,22,23), and the transition-state, or activated complex, approach (24, 25, 26) towards the understanding of the heat of transport. Most of the results predict that the heat of transport is equal to the activation energy. Experimental observations have not proved this prediction correct [See Chapter (VI)]

I.4 THE RICE-SHOTTKY APPROACH

Rice (27) evaluates the probability that an ion will move into a neighbouring vacant site under isothermal conditions. The probability is expressed as a function of a frequency factor and an activation energies factor. By using Slater's (29) results on the effects of the super-positions of various molecular vibrational modes, Rice relates the frequency factor to the basic dynamics of a lattice.

Schottky (30), following the Rice-Slater method, uses a linear chain model of the lattice to evaluate the rate that an ion will jump into a neighbouring vacancy under a thermal gradient. The thermal gradient causes an asymmetric distribution of the lattice phonons around the vacancy. This asymmetric distribution results in the use of the phonon relaxation time, t. Any temperature dependence of the heat of transport lies in the factor t.

Schottky obtains the general result that

$$Q^{*}/E = 2 - 2t^{w_1}/a \qquad \ldots\ldots (I.3)$$

where E is the activation energy of the jump, 'a' is the lattice spacing and w_1 is a factor which is expressible in terms of the dynamics of the lattice.

[Equation (I.3) is the modified form of Schottky's original general result.]

All the calculations are done in the harmonic approximations and in the final result only Q^{*}/E is meaningful.

I.5 THE PRESENT WORK

Following the revised Schottky's general result on the heat of transport, as expressed in Equation (I.3), attempts are made to apply it to a simple, but realistic, model of a vacancy in the NaCl type lattice.

The dynamics of both a perfect lattice and a lattice with a point defect are studied. Special attention is paid to the scattering of the lattice phonons by a vacancy.

In the course of the work on the dynamics of the lattice, various functions of the force constants have to be evaluated. Therefore a study is made of the various types of forces operating between the ions in the alkali-halide crystals. Some lattice calculations are made on the energies of formation of a Schottky pair in the various alkali-halides.

The various known models attempting to explain the irreversible electrode-crystal thermoelectric power are discussed. A new model is presented and its validity, or otherwise, is tested by using it to analyse the experimental results.

The thermoelectric power measurements of pure NaCl single crystals is made. A thorough observation of the various phenomena, which appear during the course of the measurements, is reported.

Finally, from the work on the heat of transport, the experimental results are accordingly analysed.

Figure 1 Thermopower measurements set-up. The leads and electrodes are of metal M^1. The crystal, MX, is in a thermal gradient. Potential difference measurements are taken between A and F. The total thermopower is the sum of the homogeneous and heterogeneous thermopowers.

Figure. 1.

THERMOELECTRIC POWER MEASUREMENT SET-UP

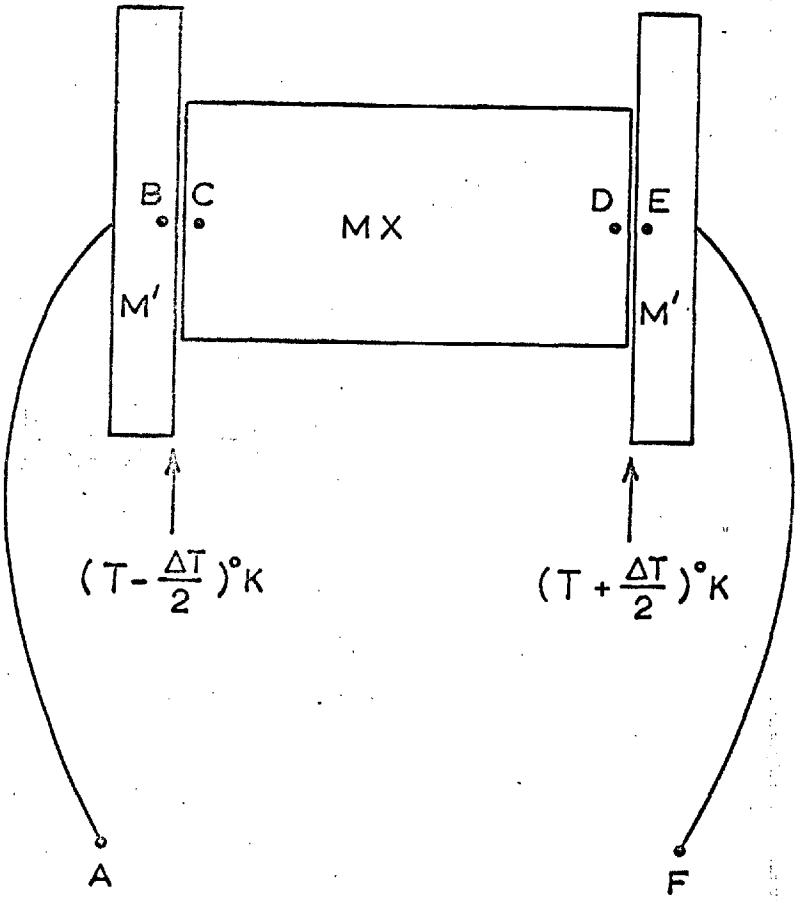

CHAPTER II

THE THERMOELECTRIC POWER (THEORY)

II.1 INTRODUCTION

When an ionic crystal is placed in a thermal gradient and sufficient time is allowed to elapse for the steady state to be established, an electrical potential difference is observed between the ends of the crystal.

Consider a crystal, MX, in a thermal gradient as in Figure (1). The total potential difference measured across A and F, say V(AF), is made up of several factors. It is given by

$$V(AF) = V(F) - V(A)$$
$$= V(AB)+V(BC)+V(CD)+V(DE)+V(EF)$$

where V(AB) and V(EF) are the potentials in the leads. They are small compared with the other factors and therefore can be neglected.

V(BC) and V(DE) are the contact potentials between the electrodes, M^1, and the crystal, MX.

V(CD) is the potential difference between the ends of the crystal.

Neglecting V(AB) and V(EF), the total thermoelectric power, σ_{Total} (T), defined as the potential difference divided by the thermal gradient between the electrodes, is given by

$$\Theta'_{Total}(T) = \left[\frac{V(BC)+V(DE)}{\Delta T}\right]_T + \left[\frac{V(CD)}{\Delta T}\right]_T$$

$$= \Theta'_{heterogeneous}(T) + \Theta'_{homogeneous}(T)$$

From a knowledge of the heterogeneous thermoelectric power, Θ'_{het}, the mechanism of the crystal-electrode contact potential can be determined.

From the homogeneous thermoelectric power, Θ'_{hom}, the basic dynamics of the ionic motions within the crystal lattice can be worked out.

II.2 THERMODYNAMICS OF IRREVERSIBLE PROCESSES

This branch of thermodynamics extends the concepts of reversible thermodynamics to the steady state irreversible processes under the assumption that the following three conditions hold:-

a) that throughout the fluctuations of the system the probability that the state variables, a_i, are in the ranges a_i to $a_i + da_i$ where $i = 1, \ldots n$, is

$$P da_1 da_2 \ldots da_n = \frac{\exp(\Delta S/k)\, da_1 \ldots da_n}{\int\int \ldots \int \exp(\Delta S/k)\, da_1 \ldots da_n}$$

where ΔS is the change in entropy of the system from its initial value.

b) that the microscopic processes are reversible. The average correlation between a_i at a time t and a_j at a time t later is the same as the average correlation between a_i at

the time t and a_j at a time $-t$ earlier. This time reversibility gives a normal sequence to the fluctuation.

c) that on the average, the decay of a fluctuation follows the ordinary phenomenological laws. The same laws apply to the microscopic as well as the macroscopic deviations.

For a detailed account of the above see De Groot (31).

Irreversible thermodynamics have been applied to fluids [De Groot and Mazur (32)] and also to solids [Bardeen and Herring (33)]

It can be shown that in an irreversible process the entropy produced is given by

$$T\sigma' = \underline{J}_q \cdot \underline{X}_q + \sum_{k=1}^{n} \underline{J}_k \cdot \underline{X}_k + \text{viscosity terms} \qquad \ldots\ (II.1)$$

where T is the temperature, σ' is the rate of change of entropy with respect to time, $\underline{J}_k$ is the flux of the $k^{\underline{th}}$ specie measured w.r.t. to the centre of mass, and $\underline{J}_q$ is the heat flux measured w.r.t. the centre of mass.

The forces $\underline{X}_k$'s and $\underline{X}_q$'s are defined as follows:

$$\left.\begin{aligned} \underline{X}_k &= \underline{F}_k - T\ \text{Grad}\left(\frac{\mu_k}{T}\right) \\ \underline{X}_q &= -\frac{1}{T}\ \text{Grad}\ T \end{aligned}\right\} \qquad \ldots\ (II.2)$$

where $\underline{F}_k$ is the external force, and μ_k is the chemical potential of the $\underline{k}$ specie.

The fluxes and forces are related, and they can be written as

$$\left.\begin{aligned} \underline{J}_k &= L_{kq}\,\underline{X}_q + \sum_{i}^{n} L_{ki}\underline{X}_i \\ \underline{J}_q &= L_{qq}\,\underline{X}_q + \sum_{i}^{n} L_{qi}X_i \end{aligned}\right\} \quad \ldots\ (II.3)$$

The main result of irreversible thermodynamics, indeed, the only new information that this approach can provide, is embodied in the Onsager's Theorem, which states that in the absence of a magnetic field,

$$L_{ik} = L_{ki} \quad \ldots\ (II.4A)$$

In the presence of a magnetic field, B, however, this becomes

$$L_{ik}(B) = L_{ki}\,(-B) \quad \ldots\ (II.4B)$$

II.2.1. THE HEAT OF TRANSPORT

The heat of transport, Q_k^*, expresses the inter-relationship between the co-efficients L_{ik} and L_{iq}, i.e.

$$L_{iq} = \sum_{k=1}^{n} L_{ik}\,Q_k^* \quad \ldots\ (II.5)$$

Substituting this result into Equation (II.3), the fluxes are re-expressed as:

$$\left.\begin{aligned} \underline{J}_k &= \sum_{i}^{n} L_{ki}\,(\underline{X}_i + Q_i^*\,\underline{X}_q) \\ \underline{J}_q &= \sum_{i}^{n} Q_i^*\,\underline{J}_i + \left(\underline{L}_{qq} - \sum_{i=1}^{n} L_{iq}Q_i^*\right)\underline{X}_q \end{aligned}\right\} \quad \ldots\ (II.6)$$

From the second of Equations (II.6) a physical interpretation is obtained for the heat of transport Q_i^*. It is the amount of heat which is carried by a unit flux of the i^{th} specie, when there is no thermal gradient.

If the fluxes and forces are represented by column matrices $\underline{J}$ and $\underline{X}$ respectively, and the fluxes are transformed, e.g. to represent a change of the coordinate system, to $\underline{J}^1 = A\underline{J}$, then these new fluxes, along with the forces $\underline{X}^1 = \tilde{A}^{-1}\,\underline{X}$ will satisfy the Onsager relations.

A physically useful transformation is:-

$$\left.\begin{aligned} \underline{J}_k^1 &= \underline{J}_k \\ \underline{J}_q^1 &= \underline{J}_q - \sum_k^n h_k \underline{J}_k \end{aligned}\right\} \quad .... \quad (II.7)$$

where h_k is the enthalphy of an atom of specie k.

This implies that

$$\left.\begin{aligned} \underline{X}_k^1 &= \underline{X}_k + h_k \underline{X}_q = \underline{F}_k - (\mathrm{Grad}\,\mu_k)_T \\ \underline{X}_q^1 &= \underline{X}_q \end{aligned}\right\} \quad .... \quad (II.8)$$

in which $(\mathrm{Grad}\,\mu_k)_T$ is that part of the gradient of u_k due to the pressure and concentration, but not the temperature. The flux $\underline{J}_q^1$ is called the reduced heat flow and the reduced heats of transport in the transformed system, Q_i^{*1}, are given by

$$Q_i^{*1} = Q_i^* - h_i \quad .... \quad (II.9)$$

II.2.2. THE HOMOGENEOUS THERMOELECTRIC POWER

Following Howard and Lidiard [83], in the case of the Schottky defects in the ionic crystals, the four species taken explicity into account are: (1) cation vacancies, (2) anion vacancies, (3) cations on cation lattice sites and (4) anions on anion lattice sites.

The forces in the "reduced heat flow" system are

$$\left.\begin{aligned} X^1{}_i &= -e_i \nabla V - (\nabla \mu i)_T \\ X_q &= -\frac{1}{T} \nabla T \end{aligned}\right\} \quad \ldots\ (II.10)$$

There is no exchange disorder and $e_1 = e_2 = 0$, $e_3 = -e_4 = e$, the electronic charge. Since the cations and anions are restricted to their own sub-lattices, the fluxes are related by

$$J_1{}^1 + J_3{}^1 = J_4{}^1 + J_2{}^1 = 0$$

Using Equations (II.6), and these relations, the fluxes become

$$\left.\begin{aligned} J_1{}^1 &= L_{11}(X_1{}^1 - X_3{}^1 + q_1^{*} X_q{}^1) + L_{12}\,(X_2{}^1 - X_4{}^1 + q_2^{*} X_q{}^1) \\ J_2{}^1 &= L_{21}(X_1{}^1 - X_3{}^1 + q_1^{*} X_q{}^1) + L_{22}\,(X_2{}^1 - X_4{}^1 + q_2^{*} X_q{}^1) \end{aligned}\right\} \quad \ldots\ (II.11)$$

where $q_1^{*} = Q_1^{*1} - Q_3^{*1}$

and $q_2^{*} = Q_2^{*1} - Q_4^{*1}$

and they are the heats of transport of the cation and anion vacancies.

Keeping in mind that

$$\mu_1 = g_1 + kT\ln\left(\frac{n_1}{N}\right)$$

and $$\mu_2 = g_2 + kT\ln\left(\frac{n_1}{N}\right)$$

and putting the total electric current to be zero in the steady state, i.e. $J_1 + J_2 = 0$, $\mathcal{O}_{hom}$ is obtained, namely,

$$\mathcal{O}_{hom} = \frac{kT}{e\,\mathrm{Grad}\ T}\ \frac{(D_1\,\mathrm{Grad}\ n_1 - D_2\,\mathrm{Grad}\ n_2)}{(n_1D_1 + n_2D_2)} + \frac{(n_1D_1q_1^{*} - n_2D_2q_2^{*})}{eT\ (n_1D_1 + n_2D_2)} \quad \ldots\ (II.12)$$

where D_1 and D_2 are the mobilities.

For a pure crystal, i.e. $n_1 = n_2 = n_o$, and from the law of mass action for thermal vacancies $\nabla n_1/n_1 = \nabla n_2/n_2 = h\nabla T/2kT^2$

where h is the enthalpy of formation of a Schottky pair, the homogeneous power reduces to

$$\mathcal{O}_{hom} = \frac{D_1(q_1^{*} + h/2) - D_2(q_2^{*} + h/2)}{eT\ (D_1 + D_2)} \quad \ldots\ (II.13)$$

For an impure crystal, i.e $n_1 \neq n_2$,

$$\mathcal{O}_{hom} = -\frac{kT\,\mathrm{Grad}\ n_1}{en_1\,\mathrm{Grad}\ T} + \frac{\{(q_2^{*} + h)\eta - \phi q_1^{*}/\eta\}}{eT\ (\eta + \phi/\eta)} \quad \ldots\ (II.14)$$

where $\phi = D_1/D_2$ and $\eta = n_2/n_o = n_o/n_1$.

Equation (II.13) is first given by Patrick and Lawson[34]. Equation (II.14) and its corresponding form for Frenkel defects are derived by Howard and Lidiard[35] and Haga[36].

II.3 REVIEW OF THE LITERATURE

The theory of the homogeneous thermoelectric power of ionic crystals, applicable to crystals with either Schottky or Frenkel defects, has been derived by various authors [Holtan, Mazur and de Groot(37), Patrick and Lawson(34), Howard and Lidiard(35), Haga(36), Allnatt and Jacobs(14) and Shimoji and Hoshino(15)]. They all agree in their final expressions. That is

$$\sigma_{hom}(\eta) = \frac{\text{Grad } V}{\text{Grad } T} = -\frac{kT \text{ Grad } n(-)}{e\, n(-) \text{Grad } T} + \frac{\{(h-Q_+^{\ddagger})n + \phi\, Q_-^{\ddagger}/n\}}{eT(n + \phi/n)} \quad \ldots\ldots \text{(II.15)}$$

where the notations are as in Chapter I.

Shimoji and Hoshimo(15) claim that the interactions of the cation vacancy-anion vacancy (in the systems where the intrinsic defects are of the Schottky type) cannot be entirely neglected even at high temperatures and therefore their analysis of the factors entering into Equation (II.15) is different. In view of the overwhelming evidence to the contrary provided by the ionic conductivity experiments [see Lidiard (1)], the author suggests that Shimoji and Hoshino's claim is doubtful.

II.3.1 THE HETEROGENEOUS THERMOPOWER: REVERSIBLE ELECTRODES

In the systems where the electrode is reversible (e.g. AgCl crystal with Ag electrodes) Howard and Lidiard(35) assume that there is a transference of the common ions

between the crystal and the electrodes. A contact potential builds up to prevent further flow of the common ions. The contact potential, $\mathcal{E}$, of a crystal MX, with electrodes M, is given by

$$\mathcal{E} = \frac{1}{e} \left[\mu_i - \mu(M^+ \text{ in } M)\right]$$

where μ_i is the chemical potential of the interstitial ion, and $\mu(M^+ \text{in } M)$ is the chemical potential of the metal ion in the electrode M.

Therefore the heterogeneous thermopower, Θ_{het}, is given by:

$$\Theta_{het} = \frac{\partial \mathcal{E}}{\partial T} = \frac{1}{e} \left[\frac{\partial \mu_i}{\partial T} + S(M^+ \text{ in } M)\right] \quad \ldots\ (II.16)$$

where $S(M^+ \text{ in } M)$ is the partial entropy of M^+ in M.

Howard and Lidiard obtain, for the difference between the thermopowers of the doped and pure crystals which contain intrinsic Frenkel defects, the expression

$$\Delta\Theta(\eta) \equiv \Theta'(\eta) - \Theta'(1) = \frac{(\eta^2-1)}{(\eta^2+\phi)} \frac{\phi}{(1+\phi)} \frac{(Q_i^* + Q_v^* + h)}{eT} - \frac{k}{e} \ln\eta \quad \ldots\ (II.17)$$

where η is the vacancy concentration relative to its value in the pure crystal at that temperature.

ϕ is the ratio of the interstitial mobility to the vacancy mobility

Q_i^* and Q_v^* are respectively the interstitial and vacancy heats of transport.

3.2 IRREVERSIBLE ELECTRODES

In cases where reversible electrodes are not used, as in the case of the alkali halides where the alkali metals are volatile and soluble in the salts, irreversible electrodes have to be resorted to. Theoretically the heterogeneous thermopower of the crystal-irreversible electrode is not clearly understood and various mechanisms have been proposed.

Howard's Model

Howard [26] suggests that, for the crystal MX in contact with electrodes M^1, electrons are transferred from M^1 to the surface of MX and the metal M is formed at the surface. Equating the electrochemical potentials, the difference between the electrode potential V_E and the surface potential, V_S, is

$$V_E - V_S = \frac{1}{e} \left[\mu_{M^+,S} + \mu_{e,E} - \mu_{M,S}\right] \quad \ldots\ldots \text{(II.18)}$$

where the μ's are the chemical potentials and the subscripts are self-explanatory e.g. $\mu_{M^+,S}$ is the chemical potential of the M^+ ion on the surface of the crystal.

Using this model Allnatt and Jacobs [14] then consider the transfer of one cation from the surface, S, to the bulk, B, of the crystal. The potential of the surface V_S relative to the potential of the bulk, V_B, of the crystal is then,

$$V_S - V_B = \frac{1}{e} \left(\mu_{M^+,B} - \mu_{(+),B} - \mu_{M^+,S}\right) \quad \ldots\ldots \text{(II.19)}$$

where $\mu_{(+),B}$ is just the chemical potential of the cation vacancy in the crystal.

From Equations (II.18) and (II.19) the heterogeneous thermopower is found to be

$$\sigma'_{het} = \frac{\partial}{\partial T}(V_E - V_B) = \frac{1}{e}(S_{m,s+} S_{(+)} - S_{e,E} - S_{m+,B}) \quad \ldots\ (II.20)$$

where the S's denotes the entropies.

The heterogeneous power cannot be calculated from Equation (II.20) because the terms are not known. For example the surface chemistry is not well understood and $S_{m,s}$ is not known. The difference in the total thermopower between the doped and the pure crystal is given by

$$\Delta\sigma'(\eta) = \sigma'(\eta) - \sigma'(1)$$

$$= \frac{1}{eT}\frac{\phi}{(1+\phi)}\frac{(\eta^2 - 1)}{(\eta^2 + \phi)}\left[h - Q_+^* - Q_-^*\right]$$

$$+ \frac{kT}{e}\frac{1}{\eta}\frac{\partial}{\partial T}\eta + T\Delta S_R \quad \ldots\ (II.21)$$

where ΔS_R denotes the change in entropies of Equation (II.20)

ϕ is the ratio of the anion to cation mobilities.

η is the ratio of the concentration of the cation vacancies to that of the pure crystal.

Lidiard and Howard [38] suggest that $\Delta S_R = 0$.

Allnatt and Jacobs Model

Allnatt and Jacobs [14] assume that the electrons are transferred between the electrodes and the crystal. Assuming that the electrochemical potentials of the electrons are the same everywhere, they obtain

$$-eV_E - \mu_{e,E} = -eV_S + \mu_{e,S} = -eV_B + \mu_{e,B} \quad \ldots\ldots \quad (II.22)$$

The heterogeneous power, therefore, becomes

$$e\Theta_{het} = S_{e,B} - S_{e,E} \quad \ldots\ldots \quad (II.23)$$

To evaluate $S_{e,B}$ Allnatt and Jacobs assume that the electrons in the crystal are distributed between the conduction electrons and the F-centers. The F-centers, they maintain, arise from the non-stoichiometry of the crystal.

Kroger (39) points out that if the F-centers exist uniformly throughout the bulk of the crystal then there should be an electronic contribution to the thermoelectric power.

Jacobs and Maycock (11) show that Allnatt and Jacobs have left out a term in their final expression for Θ_{het}. When this term is included, the number of non-stoichiometry electron becomes unreasonably high.

Allnatt and Chadwick (12) suggests that the F-center theory could be modified in such a way that instead of an excess of electrons, there are an excess of holes in the crystal. The holes react with the cation vacancy to form a V_k^x center. There is then an equilibrium between the holes and the V_k^x center as well as the equilibriums between the holes and electrons, and the V_k^x center and the $(V_k^x)_2$ center. In view of the complexity of the processes involved and the lack of information about the V_k^x centers in the alkali-halides, however, much work has to be done before this theory can be of any practical use.

Jacobs and Maycock Model

Jacobs and Maycock[11] suggest that the source of the heterogeneous thermopower lies in the temperature-dependent Frenkel-Lehovec[40] space charge. They assume that there is an excess of cation vacancies near the surface of the crystal. The excess cation vacancies form a negative space charge which induces an equal but opposite charge on the surface of the electrode. The electrons are transferred from the metallic side of the interface to the crystal side. The electrons do not actually enter into the crystal and the electrodes are ideally polarised. The equation of equilibrium is:

$$V_{M1} - V_{MX} = \frac{1}{e} (\mu_{M+} - \mu_{(+)}) \quad .... \quad (II.24)$$

the calculations on this model gives the heterogeneous thermopower as

$$\sigma_{het} = - kT \frac{d}{dT} \ln n_{(+)} \quad .... \quad (II.25)$$

The total power becomes, for the doped crystal,

$$\Theta (\eta) = - \frac{Q^*_+}{eT} \quad .... \quad (II.26)$$

and for the pure crystal,

$$\Theta (1) = \frac{1}{eT} \left[\frac{\phi(Q^*_- - h) - Q^*_+}{(1 + \phi)} \right] \quad .... \quad (II.27)$$

Shimoji and Hoshimo's Model

Shimoji and Hoshino[15], again, starting from the concept of the Frenkel-Lehovec surface charge, suggest that the electrons

are transferred across the interface. The electrons can do two things. It can wander about in the interface or it can be drawn by the space charge into the crystal. Should the first happen, the lack of knowledge about the interface prevents the chemical potential of the electrons to be expressed explicitly. The implication of this is that Jacobs and Maycock's starting point as expressed here in Equation (II.25) is incorrect. Therefore Shimoji and Hoshino suggest that the electrons actually enter into the crystal and, further, they are trapped by the anion vacancies to form F-centres. The heterogeneous thermopower is then divided into two parts,

$$\Theta'_{het} = \Theta'^{1}_{het} + \Theta'^{11}_{het}$$

Θ'^{1}_{het} is obtained by the electronic equilibrium between the metal electrode and the surface of the crystal. Θ'^{11}_{het} is the anion-vacancy equilibrium between the surface and the bulk of the crystal. The expression for Θ'^{1}_{het} is

$$\Theta'^{1}_{het} = (S_{e,s} - S_{e,M})/e$$

$S_{e,s}$ and $S_{e,M}$ are respectively the entropies of the electrons at the surface of the crystal and at the metal electrode.

The derivation of Θ'^{11}_{het} goes as follows: The potential between the surface and the bulk of the crystal is concentration-dependent. The presence of the electrons modifies the potential to a factor $\bar{m}^{11}(\eta)$, where η is, as before, the

ratio of the concentration of the cation vacancies of the impure crystal relative to that of the pure crystal at that temperature. The total heterogeneous thermopower is, eventuall

$$\Theta_{het}(\eta) = \frac{1}{eT}\left[kT\ln\left\{2(2\pi mkT/hs^2)^{3/2}\right\} - E_F - kT\ln(n_e^s(\eta)) + (h_{(-)}-h_{(+)})/2 + e\bar{\mathbb{m}}^{11}(\eta) - kT^2\frac{1}{T}\ln\eta\right] \quad \ldots\ldots \quad (II.28)$$

where $n_e^s(\eta)$ is the concentration of the electrons at the surface and $h_{(-)}$ and $h_{(+)}$ are the enthalphies of formation of anion- and cation-vacancies respectively.

There is one major difficulty with Shimoji and Hoshino's theory, namely the uncertainties of the modified potential $\bar{\mathbb{m}}^{11}(\eta)$ appearing in Equation (II.28). For example neither the form nor the magnitude of the potential $\bar{\mathbb{m}}^{11}(\eta)$ is known.

II.4 THE HETEROGENEOUS THERMOPOWER WITH IRREVERSIBLE ELECTRODES

The only species common to the electrode M^1 and the salt MX is the electrons. Owing to the difference between the Fermi levels of the electrode and the salt, the electrons are transferred from the electrodes to the crystal. Assume that the electrons are localised to a region in the crystal near the interface. An electrical double layer builds up across the interface to prevent any further transference of the electrons. Assume that the electrons do not get into traps, such as anion vacancies to form F-centres.

The electrical potential of the electrode relative to the crystal, V_{het}, is then given by

$$V_{het} = \frac{1}{e} (\epsilon_F^{M^1} - \epsilon_F^{MX}) \quad .... \quad (II.29)$$

where ϵ_F's are the Fermi levels.

Therefore, the heterogeneous thermopower is

$$\theta_{het} = \frac{\partial}{\partial T} V_{het} = \frac{1}{e} (S_e^{MX} - S_e^{M^1}) \quad .... \quad (II.30)$$

where S_e's are the entropies of the electrons.

II.4.1 THE ELECTRONIC ENTROPY IN METALS

The electronic entropy in metals is given by

$S_e^{M^1} = \int_o^T \frac{C_p^1}{N_a T^1} dT^1$ where C_p^1 is the molar specific heat of the electrons at constant pressure in the metal M^1, and N_a is the Avagadro's number.

Experimentally the electronic specific heat at constant volume, C_v, is determined at low temperatures and it is found to be given by

$C_v^1 = \gamma T$ where, for platinum $\gamma = 1.6 \times 10^{-3}$ cal/mole-deg^2 (Daunt (41)).

Assuming that the electrons in the metal is a perfect gas then the relation $C_p^1 - C_v^1 = R$, the gas constant, holds.

$$\therefore \quad S_e^{M^1} = \int_{\Delta T \to 0}^{T} \frac{R dT^1}{N_a T^1} + \int_{\Delta T \to 0}^{T} \frac{\gamma}{N_a} dT^1$$

$$= (R \ln T + \gamma T)/Na \qquad \ldots\ldots \quad (II.31)$$

Substituting the appropriate values in Equation (II.31) it is found that $\frac{S_e^{M^1}}{e}$ at 1000°K is 0.328 mV/°K.

II.4.2 THE ELECTRONIC ENTROPY IN ALKALI HALIDES

The Fermi level of the alkali-halides can be obtained from a simple model of an insulator [see e.g. Dekker (42)].

The alkali halides are very poor electronic conductors. This means that the valence band is completely full and the conduction band is practically empty. The number of electrons in the conduction per unit volume, n_c, band is given by

$$n_c = \int_{E_{c,b}}^{E_{c,t}} Z(E)R(E)dE \qquad \ldots\ (II.32)$$

where $E_{c,b}$ and $E_{c,t}$ are the energies at the bottom and the top of the conduction band and F(E) is the Fermi-Dirac distribution function and is given by

$$F(E) = \frac{1}{[1 + e^{(E-\epsilon_F)/kT}]} \qquad \ldots\ (II.33)$$

ϵ_F is the Fermi level.

Z(E) is the number of states per unit volume. As the energy, E, increases the probability of these states being occupied decreases extremely rapidly as can be seen in Equation (II.33). It is therefore only necessary to evaluate Z(E) at the bottom of the conduction band. At the bottom of the conduction band

$$Z(E) = \left(\frac{4\pi}{h_p^3}\right) (2m_e^*)^{3/2} (E-E_c)^{1/2} \qquad \ldots\ (II.34)$$

where h_p is the Planck's constant and m_e^* is the effective mass of the electrons.

Equation (II.34) is obtained as a consequence of the periodicity of the lattice. The periodicity of the lattice causes the density of states in $\underline{k}$-space to be uniform ($\underline{k}$ is the wave vector of the electron). At the bottom of the conduction band the electrons are nearly free and relation between

E and $\underline{k}$ is found by solving the Schrödinger Equation.

Putting Equations (II.33) and (II.34) into the integrand in (II.32), and assuming that $E_{c,b} - \epsilon_F \geq 4kT$,

$$n_c = 2(2\pi m_e^{*} kT/h^2)^{3/2} e^{(\epsilon_F - E_c)/kT} \quad \ldots\ldots \quad (II.35)$$

Similarly, the number of holes per unit volume in the valence band, n_h, is given by

$$n_h = 2(2\pi m_h^{*} kT/h^2)^{3/2} e^{(E_{v,t} - \epsilon_F)/kT} \quad \ldots\ldots \quad (II.36)$$

Since $n_e = n_h$

$$\epsilon_F = (E_c + E_{v,t})/2 + 3/4\ kT \ln (m_h^{*}/m_e^{*}) \quad \ldots\ldots \quad (II.37)$$

The electronic entropy of the alkali halides S_e^{MX}, is therefore $-3/4\ k \ln (m_h^{*}/m_e^{*})$.

The effective masses of the holes and electrons are not known exactly, but it can be readily seen that S_e^{MX}/e is negligible.

II.5 DISCUSSIONS.

Neither the Allnatt and Jacobs's (14) F-centre theory nor Jacobs and Maycock's (11) surface charge theory have been successful in explaining the irreversible electrode-crystal thermopower. When these two theories are used to analyse the experimental results, they have not been able to produce a plausible value of the heat of transport. [See Allnatt and Chadwick (12)].

Howard's (13) theory assumes that the electrons are

caught in traps the moment they enter the crystal at the crystal-electrode boundary. The model presented in Section (II.4) discusses the effect on the heterogeneous thermopower should the electrons not be trapped when it gets into the crystal.

These two models will be used to analyse the experimental results in Chapter (VII). The success, or otherwise, of these two theories to produce a plausible value of the heat of transport will determine whether or not the assumptions inherent in the respective theories are valid.

CHAPTER III

THE HEATS OF TRANSPORT (I)

III.1 INTRODUCTION

The heat of transport, Q^*, of a species has been defined in Chapter (II). It is the heat carried by a unit flux of the specie when there is no thermal gradient in the system.

Normally the heat of transport that is discussed in the literatures is the reduced heat of transport [See Chapter (II)]. The relationship between the heat of transport, Q^* and its reduced form Q^{*1} is given by [c.f. Equation (II.9)]

$$Q^{*1} = Q^* - h$$

where h is the enthalphy of the atom.

Hereafter the term the "heat of transport" will be taken to mean the reduced heat of transport and it will be referred to simply by the symbol Q^*.

III.2 LITERATURE REVIEW.

The theories of the heat of transport can be divided into two parts. The first computes the energy flux accompanying the atom flux under isothermal condition (transition state theory) and the second under non-isothermal condition (kinetic theory).

III.2 1: THE TRANSITION STATE OR ACTIVATED COMPLEX THEORY

Consider a reaction process, such as the jumping of an atom to a neighbouring vacant site in a lattice. In the

transition state theory, it is assumed that in the transit between the initial and final states of the jump, there exists a transition state whose life-time is long enough for its chemical potential to be defined explicitly. While the atom is at the saddle point which defines the transition state, the number passing through it in one direction under isothermal condition can be calculated by the use of statistical mechanics. Wert (24) suggests that the flux of atoms is determined by the fraction of time that the atom has sufficient energy to be in the activated state. He obtains the rate of jumping, Γ, in terms of the thermodynamic functions, namely

$$\Gamma = n^1 \nu \exp\left[-\Delta G/kT\right] \qquad \ldots. \quad (III.1)$$

where n^1 is the number of diffusive paths, ν is the frequency of vibration of the atom at the lattice site, and ΔG is the work done when an atom is moved isothermally from the lattice site to the transition state.

Using Wert's formulation, Haga (25) calculates the energy flux accompanying the ion flux. Physically when the ion moves from one lattice site to another, it is given an energy ΔH at the initial site to surmount the potential barrier. The heat transported is this energy plus the entropy contribution of the surrounding atoms when the atom comes down from the saddle point to the final site. Thus

$$Q^{*} = \Delta H - T\Delta S(x^{1})$$
$$= \Delta G \qquad \ldots\ (III.2)$$

where ΔS is the entropy contribution at the final site x^{1}.

In the Haga-Wert approach, the jumping process is thought of essentially as a one-body process. Strictly speaking, this is not correct. The jumping of an atom involves the corporate motions of the surrounding atoms. It is essentially a many-bodies problem since the moving atom interacts with all the surrounding atoms. In the transition-state approach of Vineyard[26], the flux of atoms across the saddle point is evaluated in the 3N configuration space of the crystal. Using Vineyard's approach, the energy flux accompanying the matter flux can be evaluated. However, the heat of transport is again found to be just the activation energy.

The transition-state approach has not been very successful experimentally. There are several objections to the theory. Rice [27] questions the assumption underlying the theory, that the life-time of the activated state is long-lived enough for its thermodynamic properties to be well-defined. It is generally thought that the atom spends most of its time on either side of the potential barrier. The theory also assumes that the properties of the activated state is the same as the unactivated state. However, in Equation (III.1), ΔG does not represent work in any simple

process. It is actually a ratio of the partition functions with different degrees of freedom.

Lidiard (43) draws attention to a serious limitation of the transition state approach. This approach depends on the probability of occurrence of the saddle-point configuration, but it says nothing about the correlated motions of the surrounding atoms. To work out the heat of transport, a knowledge of the energy which flows in and out of the region before and after the transition state is achieved is necessary. It is not within the transition state theory to evaluate this energy.

III.2 2 THE KINETIC THEORY

To evaluate the heat of transport under non-isothermal conditions, the so-called kinetic theory is used. First, the expression of the atom flux, j, under a thermal gradient is written down. This is given by

$$j = D\left[\text{Grad } n - \frac{Q^{*}n}{kT^{2}} \text{Grad } T\right] \qquad \ldots\ (III.3)$$

where D is the diffusion co-efficient, and n is the vacancy (or interstitial) concentration. [cf Equation (I.1)]

Following Le Claire (17) and Brinkman (18), consider the flow of atoms, via the vacancy mechanism, between plane 1 at temperature T, and plane 2, at temperature T + ΔT. The flux of atoms between planes 1 and 2 are given by

$$j12 = (n + \Delta n)\, \upsilon e^{-\Delta Gm/kT} \quad \ldots\ (III.4)$$

where υ is the frequency factor and Gm is the free energy of motion of the atom.

Similarly, the reverse flux is

$$j21 = n\upsilon e^{-\Delta Gm/h(T+\Delta T)} \quad \ldots\ (III.5)$$

The net flux, therefore, is

$$j = j12 - j21$$

$$= D\left[\text{Grad } n - \frac{n\Delta hm}{kT^2}\ \text{Grad } T\right] \quad \ldots\ (III.6)$$

where $D = (\Delta x)^2\, \upsilon e^{-\Delta Gm/hT}$, a result from the random walk theory. Δx is the distance between planes 1 and 2, and Δhm is the enthalphy part of ΔGm.

Comparing Equation (III.3) with Equation (III.6), the heat of transport, Q^*, is equal to the activation energy, Δhm.

In contrast, Wirtz [15], divides the energy necessary for the motion, into three parts, $\Delta g1$, $\Delta g2$ and $\Delta g3$, localized at planes 1, 2 and 3, which are at temperatures T, $T + \frac{\Delta T}{2}$ and $T + \Delta T$. Using the same procedure as outlined above Wirtz obtains

$$Q^* = -\Delta h_3 + \Delta h_1 \quad \ldots\ (III.7)$$

where Δh_1 and Δh_3 are the enthalphy parts of $\Delta g1$ and $\Delta g3$ respectively.

The failure of the kinetic approach lies in several factors. First it assumes that the interaction energies of the jumping atom is localized in the plane which the atom is at.

However, the motion of one atom involves the interactions of many bodies, both perpendicular to, and along, the thermal gradient. Secondly, the criticisms of the transition state approach with regard to the life-time of the activated state still apply to the kinetic approach. This is seen in using the results of the absolute rate theory implicit in Equation (III.4).

A number of authors have attempted to break away from some of the limitations implicit in both the transition state approach and the kinetic approach.

Orani [44] defines a "co-ordination sphere" of matter around the atom-vacancy pair. A diffusive jump is accomplished when an excess energy wave packet sweeps across the co-ordination sphere. Any energy flow across the reference flux plane, which divides the atom-vacancy pair, is part of the heat of transport.

Girifalco [45] attempts to define a temperature gradient by using the jump frequencies of the two isothermal systems. This temperature gradient defines a distance coordinate x_c, which is the distance between the peak of the excess energy wave and the reference flux plane. The distance coordinate, x_c, therefore, indicates where the maximum energy is located during a jump.

The Rice-Schottky approach [Rice (27), Schottky (30)] relate the role of the lattice dynamics to the diffusion process. It deduces an expression for Q^{*} in terms of the known fundamental parameters of the lattice. This can be used to analyse the experimental results of the thermoelectric power measurements.

III.3 LATTICE DYNAMICAL CONCEPTS OF A JUMPING PROCESS.

Consider an atom jumping into a vacancy in the crystal lattice. For this to happen, the amplitudes of the vibrations of the atom in the general direction of the vacancy must be large enough. At the same time the atoms surrounding the vacancy must be undergoing an out-of-phase motion so that the jumping atom can be accommodated. The vacancy must happen to be next to the atom.

The first condition immediately implies that anharmonic forces are important in a diffusive jump. However, anharmonic forces make the problem very complex, and a reasonably simple solution might not be possible. On the other hand, the use of harmonic forces often gives results which are of the right order of magnitude.

The second condition imposes only a small effect in any subsequent calculation as the following argument of Rice (27) shows. The frequency that a jumping atom acquires enough energy to make the jump is much smaller than the frequency

that the out-of-phase motions of the surrounding atoms would occur. The latter motions will require much smaller amplitude. Therefore the probability that a diffusive jump occurs depends very much on the probability that the jumping atom has enough energy.

III.3.1 THE RICE-SLATER MODEL (27)

Consider a microscopically large sphere of matter surrounding the vacancy, in a large crystal with a low density of vacancies, so that the rest of the crystal acts as a heat bath for the sphere.

The displacement of the atom next to the vacancy is given by

$$q1 = \sum_i \alpha_{1i} \epsilon_i^{\frac{1}{2}} \cos\left[2\pi(\nu_i t + \delta_i)\right] \quad \ldots\ldots \text{(III.8)}$$

where ν_i, ϵ_i and δ_i are the frequency, energy and phase of the $i^{\underline{th}}$ normal co-ordinate. ϵ_i's and δ_i's only change when there is an interaction between the heat bath and the volume element.

The total energy of the atom is $u = \sum_i \epsilon_i$ .... (III.9)

The atom will only jump if its amplitude exceeds q_o, that is

$$\sum_i |\alpha_{1i}| \epsilon_i^{\frac{1}{2}} > q_o$$

The minimum energy, U_o, required for this to happen is

$$U_o = q_o^2 / \sum_i^n \alpha_{1i}^2 \quad \ldots\ldots \text{(III.10)}$$

The frequency of jump is the ensemble average of a configuration such that $q_1 - q_o = 0$ which is achieved from the direction of $q_1 - q_o < 0$. It is assumed that the frequency of fluctuations in energy between the volume element and the heat bath is large compared with the frequency of a jump. This implies that as far as the jumping process is concerned the volume element is in thermal equilibrium. Thus the ensemble average can be replaced by the long term average. The long term average of the frequency of up-zeros of the function $q_1 - q_o$ is found by Kac's (46) method to be

$$M = \frac{1}{4\pi^2}\int_{-\infty}^{\infty}\int_{-\infty}^{\infty}\frac{\cos(q_o x)}{y^2}\prod_{i=1}^{n}\left\{J_o(\alpha_{1i}\epsilon_i^{\frac{1}{2}}x) - J_o(\alpha_{1i}[\epsilon_i(x^2+ 4\pi^2y^2\upsilon_i^2)]^{\frac{1}{2}})\right\}dxdy \quad .... \quad (III.11)$$

where $J_o(x)$ is the Bessel function of zero order, and M is automatically zero when $U < U_o$.

Under the condition that n is large and that the energies of each mode ϵ_i's are roughly the same, Slater (29) shows that, by taking

$$J_o(x) = \exp(-\tfrac{1}{4}x^2)\left\{1 - x^4/64\right\},$$

and neglecting $x^4/64$, Equation (III.11) reduces to

$$M = \upsilon^1 \exp(-q_o^2/\Sigma\alpha_i^2\epsilon_i) \quad .... \quad (III.12)$$

$$\text{where } \upsilon^{1\,2} = \Sigma\alpha_i^2\upsilon_i^2/\Sigma\alpha_i^2 \quad .... \quad (III.13)$$

Using Slater's approximation Rice obtains the rate at which the atom reaches the critical amplitude, Γ, as the product of the probability that the system has a total energy equal to or exceeding U_0, and the long term average of zeros corresponding to that total energy. Thus

$$\Gamma_1 = \int_{U>U_0} M \exp\left(-\frac{1}{kT}\sum_1^n \epsilon_i\right) \frac{d\epsilon_i \ldots d\epsilon_n}{(kT)^n} \quad \ldots\ldots \text{(III.14)}$$

$$= \nu^1 \exp - U_0/kT$$

Slater's approximation holds at high temperatures. It is a good enough approximation as most of the diffusion experiments are carried out at relatively high temperatures.

III.3 2 SCHOTTKY'S APPLICATIONS

Schottky (30) applies the Rice-Slater's concept of an atomic jump to a linear chain. A very big simplification is immediately introduced by the linear chain model. There are no surrounding atoms to either hinder or encourage a diffusive jump. Therefore in this model, U_0 becomes the energy of activation for the motion of the atom via the vacancy mechanism.

Schottky introduces a further simplification. He assumes that the jump frequency is just the long term average of zeros and that the system always have energy exceeding the activation energy. This is reasonable if the number of atoms in the chain is large and if the temperature

is high. In this model, then, the jump frequency is

$$\Gamma = \nu^1 \exp\left[-q_0^2 / \sum_i^n \alpha_i^2 \epsilon_i\right] \quad \ldots\ldots \text{(III.15)}$$

In a temperature gradient the energy of each mode is

$$\epsilon_i = k_B T - k_B t f_i \text{Grad } T \quad \ldots\ldots \text{(III.16)}$$

where $f_i = 2\pi \frac{d\omega_i}{dk_n}$, k_n is the wave-number and t is the relaxation time.

Equation (III.16) is obtained by solving the Boltzman's equation. By putting Equation (III.16) into Equation (III.15) the jump frequency is

$$\Gamma = \nu \exp -E/kT \left\{1 - \frac{t}{T}\left[\left(\frac{E}{kT} - \frac{1}{2}\right) w_1 + \tfrac{1}{2} w_2\right] \text{Grad } T\right\} \quad \ldots\ldots \text{(III.17)}$$

where

$$\alpha^2 = \sum_i \alpha^2 \qquad w^2 = \Sigma \alpha_i^2 w_i^2 / \alpha^2$$

$$w_1 = \sum_i \alpha_i^2 f_i / \alpha^2 \qquad w_2 = \sum_i \alpha_i^2 w_i^2 f_i / (\alpha^2 w^2)$$

$$w = 2\pi\nu \qquad E = q_0^2 / \alpha^2.$$

By evaluating the atomic fluxes up and down the temperature gradient, and comparing the resultant flux with (III.3), as in Section (III.2.2), the heat of transport, Q^*, is found to be given by the expression

$$Q^*/E = 2 - 2tw_1/a \quad \ldots\ldots \text{(III.18)}$$

Equation (III.18) expresses the heat of transport in terms of the activation energy, the phonon-phonon interaction relaxation time, the interatomic distance and a factor w_1, which can be evaluated from lattice dynamical calculations of a specific model of a vacancy in a linear chain. w_1 is expected to be temperature-independent, and any temperature-dependence of the heat of transport lies in the phonon-phonon interaction relaxation time.

CHAPTER IV

MODEL OF A VACANCY IN A LINEAR CHAIN LATTICE AND ITS DYNAMICS.

A comprehensive discussion on the dynamics of lattice vibrations is given by Maradudin, Montroll and Weiss [47].

In the following account, the lattice dynamics of a perfect one dimensional lattice are assumed to be known.

IV.1 GENERAL METHOD OF SOLVING THE PROBLEM OF A DEFECT IN THE LATTICE.

The effects of the introduction of a defect into the lattice can be studied in the following way. Let $\underline{M}_0(w)$ be a matrix such that the solution of the determinantal equation, $|\underline{M}_0(w)| = 0$, are the vibrational modes of the perfect lattice. When a defect is introduced into the lattice, it perturbs the motions of the other atoms. The corresponding matrix, $\underline{M}(w)$, will then represent the perturbed motions. The matrix can be represented by

$$\begin{aligned} \underline{M}(w) &= \underline{M}_0(w) + \underline{\Delta}M_0(w) \\ &= \underline{M}_0(w)\,[\underline{I} + \underline{M}_0^{-1}(w)\,\Delta\,\underline{M}_0(w)] \\ &= \underline{M}_0(w)\,\underline{\Delta}(w) \end{aligned} \qquad \ldots\ (IV.1)$$

where $\underline{\Delta}(w)$ characterises the defect.

In this formulation, the elements of $\underline{M}_0(w)$ represent the coefficients of $\underline{u}$'s, the vibrational displacements of the atoms in the perfect chain, in the time-independent equations

of motions. The elements of the inverse matrix $\underline{M}_0^{-1}(w)$ are the Green's functions g(m) where m is the number of atomic spacings from the origin. In the case of the scattering of waves whose frequencies lie between zero and the maximum "allowed" frequency (the maximum frequency which can be transmitted along the chain unattenuated) g(m) can be expressed in a closed and explicit form [see(47)]. This is given by

$$g(m) = -\frac{i}{2\gamma}\frac{\exp(i|m|\phi)}{\sin\phi} \qquad \ldots\ (III.2)$$

where γ is the force constant, $\phi = |ka|$ where k is the quasimomentum and 'a' is the lattice spacing. The waves are assumed to originate from atom '1'. Equation (IV.2) applies in the situation in which the forces are restricted to nearest neighbours only.

When the defect is introduced at the position '0' the vibrations of the $m^{\underline{th}}$ atom caused by this defect can be shown to be given by

$$u(m) = D\, g(m)\, \Delta \qquad \ldots\ (IV.3)$$

where Δ characterises the defect as in Equation (IV.1), and D is a factor depending on the lattice dynamics.

IV.2 THE VACANCY MODEL

From the point of view of the vibrations, the simplest model of a lattice is one in which the forces between the atoms are central and are between nearest neighbours only.

Only harmonic forces are considered. Therefore, in this model, the atoms are coupled to their nearest neighbours by springs of force constant δ.

In the next chapter on lattice calculations, the ions are attracted to each other by the Coloumbic and Van der Waal forces and repelled by the short range hard core repulsion. This is a very much more realistic model than the one in which the atoms are joined together by springs. When an atom is removed so that a vacancy is formed, the hard core repulsive and the Van der Waal attractive forces are removed. However the Coloumbic attraction between the vacancy and the other atoms still remains. There are no additional forces between atoms on either side of the vacancy.

In Schottky's [30] model of the vacancy in the linear chain the atoms are coupled to their nearest neighbours with a force constant δ, and to their lattice positions with a force constant g. The two atoms neighbouring the vacancy are coupled to each other by a force constant δ^1. The final expression with $\delta^1 \neq 0$ is extremely complicated, and it only reduces to a simple form when δ^1 is put equal to zero. Putting $\delta^1 = 0$ implies that the two parts of the chain are independent of each other. The removal of the atom so forming a vacancy removes the total coupling between the atom and its neighbours instead of removing a partial, albeit major, portion of the force.

Figure 2 Defect in the linear chain. The perfect linear chain consists of atoms of mass M coupled to each other with force constants γ. A defect of mass M^1 is introduced into the chain. It is coupled to its neighbours by force constants γ^1.

Figure 3 Scattering of lattice phonons by defect. A perfect lattice-phonon 'ϕ' travels from left to right. It is unperturbed by the normal atom at '-1'. However it is perturbed by the defect at position '0'. The phonon 'ϕ'' then emerges to be scattered by atom at position '1'.

Figure. 2.

DEFECT AT 'O' IN THE LINEAR CHAIN.

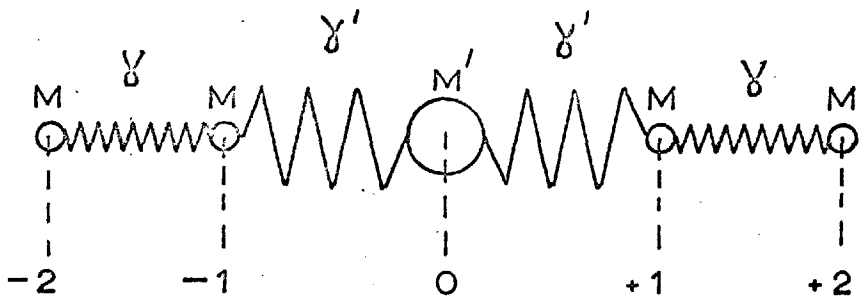

Figure. 3.

SCATTERING OF LATTICE PHONON BY DEFECT.

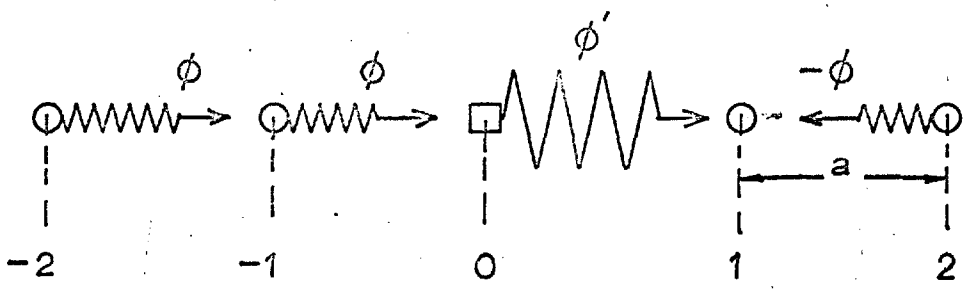

In view of the more elaborate lattice calculations, a model in which the atoms are coupled to each other with a force constant γ, and the vacancy is coupled to its nearest neighbours with a force constant γ^1, seems adequate. The dynamics of such a model are discussed below.

IV.3 THE EQUATIONS OF MOTIONS.

Introduce a single defect into the linear chain at position '0' as in Figure (2). Let the defect be of mass M^1, and the coupling constant between the defect and the two neighbouring atoms be γ^1.

Put $M^1 = (1-\epsilon)M$, and $\gamma - \gamma^1 = \epsilon^1 \gamma$, where M is the mass of the atoms and γ the coupling constant between the atoms. In the case of the defect being a vacancy ϵ will eventually be put equal to unity.

The time independent equation of motions for the atoms in the linear chain is

$$Mw^2U_n + \gamma \Delta^2 U_n = (M-M^1)w^2U_n\,\delta_{n,o} + (\gamma-\gamma^1)(U_{n+1}-U_n)(\delta_{n,o}+\delta_{n,-1}) - (\gamma-\gamma^1)(U_n-U_{n-1})(\delta_{n,o}+\delta_{n,1}) \quad \ldots\ (IV.4)$$

where n is the position of the atom, $\Delta^2 U_n = U_{n+1}+U_{n-1}-2U_n$, and $\delta_{n,m}$ is the delta function. When the R.H.S. of Equation (IV.4) is put equal to zero, the equation is the equation of motion of the normal perfect lattice. The R.H.S. of the Equation characterise the defect. For example when n = 0,

the Equation becomes

$$M^1 w^2 U_0 + \gamma^1 \Delta^2 U_0 = 0.$$

IV.4 THE SCATTERING OF LATTICE PHONONS.

Let a lattice phonon, travelling from left to right in Figure (3), be scattered by the defect at position '0'. From the general conclusion of Section (IV.1) [c.f Equation (IV.3)], the solution to Equation (IV.4) is of the general form:

$$U_n = e^{in\phi} + Cg(n) \quad \ldots\ldots (IV.5)$$

where $\phi > 0$ [The phonon in the positive direction, from left to right].

$e^{in\phi}$ represents a perfect lattice phonon and is the solution of Equation (IV.4) when the R.H.S. is put equal to zero. C is a constant to be evaluated.

To evaluate C, substitute Equation (IV.5) into Equation (IV.4) and put n = 0. Thus,

$$(1-\epsilon)Mw^2[1 + Cg(0)] + (1-\epsilon^1)\gamma[e^{i\phi}+e^{-i\phi}-2+C\{g(1)+g(-1)+2g(0)\}] = 0 \quad \ldots\ldots (IV.6)$$

From Equation (IV.2)

$$g(-1) = g(1) = \exp(i\phi) \cdot \left(\frac{-i}{2\gamma}\right) \frac{1}{\sin\phi}$$

$$= \exp(i\phi)\, g(0) \quad \ldots\ldots (IV.7)$$

Equation (IV.7) expresses the symmetry of the distribution of phonon round the defect. Also from the result of the equations of motions of a perfect lattice,

$$Mw^2 = 4\gamma \sin^2\phi/2 \quad \ldots\ (IV.8)$$

Thus Equation (IV.6) can be further reduced to

$$4\gamma\sin^2\phi/2(\epsilon^1 - \epsilon) + Cg(o)[4\gamma(\epsilon^1 - \epsilon)\sin^2\phi/2 + 2i(1-\epsilon^1)\gamma\sin\phi = 0$$

$$C = \frac{-[4\gamma\sin^2\phi/2\ (\epsilon^1-1)]}{(\epsilon^1-1)g(0)[4\gamma\sin^2\phi/2 - 2i\gamma\sin\phi]}$$

$$= \frac{4i\gamma\sin^2\phi/2\ \cos\phi/2}{[-\sin\phi/2 + i\cos\phi/2]}$$

$$= 4\gamma\sin^2\phi/2\ \cos\phi/2.\ \exp[-i\phi/2] \quad \ldots\ (IV.9)$$

where $\epsilon = 1$, in the case of a vacancy, and $g(0) = \left(\frac{-1}{2\gamma}\right)\frac{1}{\sin\phi}$ have been substituted.

The displacements of the atoms are therefore completely determined in terms of the quasimomentum, $k = \phi/a = \frac{2\pi}{\lambda}$, and the force constant, γ.

From Equation (IV.5) the displacements are given by

$$U_n = e^{in\phi} + 4\gamma\sin^2\phi/2\ \cos\phi/2\ \exp[-i\phi/2]\ g(n)$$

For $n \geq 0$, the displacement of an atom, to the right of the vacancy, due to a perfect lattice phonon, travelling from left to right, and scattered at the vacancy at position '0', is

$$U_n = e^{in\phi} - i\sin\phi/2\ \exp[i(n - \tfrac{1}{2})\phi]$$

$$= \{1 - i\sin\phi/2\ \exp(-\tfrac{i\phi}{2})\}\ \exp(in\phi) \quad \ldots\ (IV.10)$$

For $n \geq 0$, and $\phi' < a$, it is

$$U_n = [1 + i\sin\phi/2\ \exp\{-i(2n-\tfrac{1}{2})\phi\}]\ \exp(in\phi) \quad \ldots\ (IV.11)$$

Equation (IV.11) can be alternatively interpreted as follows. It is the displacements of the atoms to the right of the vacancy ($n \geq 0$) due to the phonons travelling from right to left ($\phi \leq 0$).

Specifically the displacement of the atom '1' [See Figure (3)] due to the scattering of all the phonons is

$$U_1 = \sum_{k=-\pi/a}^{\pi/a} A_{k\pm} \exp(ikx) \exp -i(w^{+}+\delta_k) \quad .... \quad (IV.12)$$

where from Equations (III.10) and (III.11)

$$\left.\begin{aligned} A_{k+} &= 1 - iSin\frac{ka}{2} \exp\left(\frac{-ika}{2}\right) \\ A_{k-} &= 1 + iSin\frac{ka}{2} \exp\left(\frac{-i3ka}{2}\right) \end{aligned}\right\} \quad .... \quad (IV.13)$$

IV.5 APPLICATIONS TO SCHOTTKY'S ATOMISTIC THEORY.

From Chapter III the heat of transport is expressed in terms of a lattice dynamical factor w_1, which is defined as

$$w_1 = \sum_k \alpha_k^2 f_k/\alpha^2, \quad f_k = dw/dk, \alpha^2 = \sum \alpha_k^2$$

and α_k is defined in the expression for the displacement of the atom next to the vacancy:

$$U_1 = \sum_{k=-\pi/a}^{\pi/a} \alpha_k \sqrt{\epsilon_k} \, Cos\,(w_k t + \delta_k) \quad .... \quad (IV.14)$$

where ϵ_k is the energy of the k^{th} vibrational mode, and is $\frac{1}{2}NMw_k^2$ where N is the number of atoms in the chain.

Comparing Equations (IV.12) and (IV.14),

$$\alpha_k = \sqrt{\frac{2}{NM}} \quad \frac{1}{w_k} |A_{k\pm}|$$

In view of Equation (IV.8),

$$w_k = 2\sqrt{\gamma/M}\ \mathrm{Sin}\ ka/2\ , \quad f_k = a\sqrt{\frac{\gamma}{M}}\ \mathrm{Cos}\ \frac{ka}{2}$$

Therefore

$$\alpha^2 = \frac{1}{2N\gamma} \quad \sum_k |A_{k\pm}|^2 / \mathrm{Sin}^2\ \frac{ka}{2}$$

$$= \frac{1}{2N\gamma} \quad S_1$$

$$\sum \alpha_k^2\ f_k = \frac{a}{2N\sqrt{\gamma M}} \quad \sum_k \frac{\mathrm{Cos}\ \frac{ka}{2}}{\mathrm{Sin}^2\ \frac{ka}{2}} \quad |A_{k\pm}|^2$$

$$= \frac{a}{2N\sqrt{\gamma M}} \quad S_2$$

From Equation (IV.13):

$$|A_{k+}|^2 = \left[1 - \mathrm{Sin}^2\left(\frac{ka}{2}\right)\right]^2 + \mathrm{Sin}^2\left(\frac{ka}{2}\right)\ \mathrm{Cos}^2\ \frac{ka}{2}$$

$$|A_{k-}|^2 = \left[1 + \mathrm{Sin}\left(\frac{ka}{2}\right)\mathrm{Sin}\left(\frac{3ka}{2}\right)\right]^2 + \mathrm{Sin}^2\left(\frac{ka}{2}\right)\mathrm{Cos}^2\left(\frac{3ka}{2}\right)$$

As the number of atoms in the chain becomes very large, the number of normal modes becomes correspondingly large, and the interval between the discrete modes becomes small. In the limit the sums S_1 and S_2 can be expressed as integrals. From the results of the dynamics of the perfect lattice, the density of modes of the linear chain is Na.

Thus S_1 and S_2 becomes

$$S_1 = Na \int_{k=\frac{1}{Na}}^{k=\pi/a} \frac{|A_{k+}|^2}{\sin^2 \frac{ka}{2}}\, dk + Na \int_{k=\frac{-\pi}{a}}^{k=\frac{-1}{Na}} \frac{|A_{k-}|^2}{\sin=\frac{ka}{2}}\, dk$$

$$S_2 = Na \int_{k=\frac{1}{Na}}^{k=\pi/a} \frac{|A_{k+}|^2 \cos\frac{ka}{2}}{\sin^2 \frac{ka}{2}}\, dk + Na \int_{k=-\pi/a}^{k=\frac{-1}{Na}} \frac{|A_{k-}|^2 \cos\frac{ka}{2}\, dk}{\sin^2 \frac{ka}{2}} \quad \Big\} \ldots (IV.15)$$

S_1 and S_2 are evaluated in Appendix (1) and the results are

$$S_1 = N\pi \ , \qquad S_2 = 4N/3$$

Therefore $w_1 = a\sqrt{\gamma/M} \cdot S_2/S_1$

$$= -a\sqrt{\gamma/M}\ \ 4/3\pi$$

From Equation (II.27) the heat of transport is given by

$$Q^* = \left[2 - \frac{8.t}{3\pi}\ \sqrt{\gamma/M}\right] E \qquad \ldots\ (IV.16)$$

This is a very lucid expression. For most alkali-halides everything on the R.H.S. is known experimentally except for γ, the force constant. In this model, the force constant cannot be related in any simple way to the bulk properties of the crystal. For example, bulk properties like the elastic constants depend on certain average sums of the various force constants of the ions. However, the jump process of the ion is very sensitive to the local strains around the vacancy. In this model the force constant, γ, can

be taken to be that which binds the vacancy's neighbour to the next ion on the other side to the vacancy along the chain. See Figure [(2)].

To evaluate γ, the forces acting between the ions in the alkali-halides will have to be known. To arrive at a realistic model of the forces, the procedure adopted here is as follows. First a plausible model of a vacancy is chosen. Then a form of the potential of the ion in the lattice is postulated. From then onwards, the sublimation energy of a pair of ions and the formation energy of a Schottky pair are calculated. These last two can be directly compared with the corresponding experimental values. The agreement between the theoretical and experimental values of the sublimation energy and the formation energy will be taken as the justification for both the model and the form of the potential chosen. With the form of the potential energy established, the force constants can then be determined.

Figure 4 <110> type linear chain in the NaCl lattice. The Na^+ vacancy is at 0,0,0 and a typical <110> type linear chain is shown.

Figure. 4.

<110> TYPE LINEAR CHAIN IN THE Na Cℓ. LATTICE.

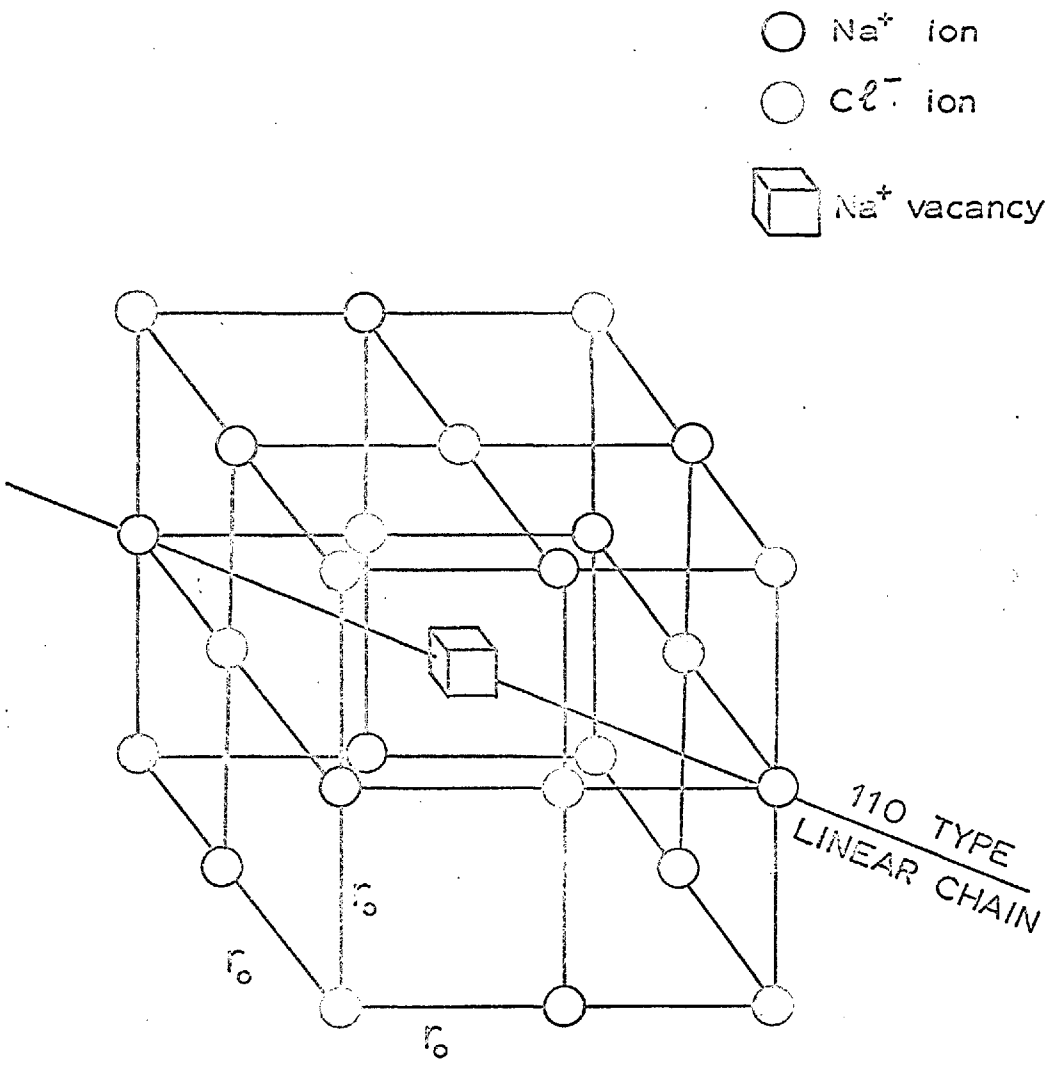

CHAPTER V

LATTICE CALCULATIONS.

V.1 INTRODUCTION

In the early Born theory of the ionic crystals, the ions are assumed to be point charges and the lattice is assumed to be static. The early models of the Frenkel and Schottky defects [Frenkel (48); Schottky and Wagner (49)] meet a theoretical difficulty in that the calculated formation energy is too high. Jost (50) shows that, letting the lattice relax, and the ions polarise round the point defect, the formation energies are brought down to reasonable values. For example, the Madelung energy required to remove a Na^+ ion from its normal lattice site in the NaCl lattice is around 4 eV. The polarisation energy gained, however, is around 3 eV, and therefore the formation energy of the defect is around 1 eV, which is roughly the experimental value.

V.2 THE SHORT RANGE FORCES

Schottky (51) introduces the short range closed shell repulsion of the ions and he gives an interaction of $1/r^n$ for the ions with $n \sim 9$.

However, by Xray methods, it is known that on the periphery of the ions, the electron density decreases exponentially with increasing distance from the centre. Therefore, it is plausible that the potential should have an exponential form.

The form of the repulsive potential adopted in this work is basically the Born-Mayer form [hereafter referred to as BM form; Born and Mayer (52), also see Tosi and Fumi(53),] and it has an inverse exponential form, i.e.

$$\phi(r) = A_{12} \exp(-r/p) \quad \ldots\ (V.1)$$

A_{12} depends on the interacting ion and p depends on the crystal. When only the nearest neighbour interactions are considered, A_{12} is eliminated in the subsequent analysis. However, in the present work, both the nearest neighbour and the next nearest neighbours are considered.

An expression for A_{12} is given by Born and Mayer (52)

$$A_{12} = b\, C_{12} \exp[(r_1 + r_2)/p] \quad \ldots\ (V.2)$$

where r_1 and r_2 are the Goldschmidt radii, and Pauling (63) gives the formula for C_{12} as

$$C_{12} = 1 + Z_1/n_1 + Z_2/n_2 \quad \ldots\ (V.3)$$

where Z_1 and Z_2 are the valencies, and n_1 and n_2 are the number of electrons in the outer shell of the ions.

Certain authors [Rittner (54), Versani (55), Baughan(56)] find that when the ions move much closer than the interatomic distance, a much harder potential is needed, namely the Verwey potential. This has the form

$\phi(r) = A + B/r^{12}$ where $r < r_0$, the interionic distance.

$$\ldots\ (V.4)$$

When the constants A and B are fixed by imposing the condition that the potential and its first derivative are continuous at $r = r_0$ with the BM. form, then the combined potential is called the Born-Mayer-Verwey form (hereafter known as the BMV potential). This potential has been used by Guccione, Tosi and Asdente (57), Tharmalingam (58) and (59) and Boswarva and Lidiard (60).

In addition to the short range hard core repulsive forces, there exist short range Van der Waal forces. The Van der Waal forces arise from the correlated movements of the electrons in the ions, which induce dipoles and quadrupoles in the other ions. The dipole-dipole and quadrupole-dipole interactions are attractive and are represented by the expression

$$- [C_{12}/r^6 + D_{12}/r^8] \qquad \ldots\ (V.4)$$

where C_{12} and D_{12} depend on the interacting ions.

The ions in the lattice are then described by their positions, their electrostatic interactions, their polarisibilities and their short range forces.

V.3. THE MOTT-LITTLETON APPROXIMATIONS.

In principle the energy of a point defect can be calculated to any degree of accuracy. Scholz (61) has calculated the energy of a small crystallite of 256 ions.

However, since the Coloumbic forces are long-range, even this amount of ions is not sufficient. What is more commonly done is to arbitrarily consider the neighbours of the defect in the first shell, second shell, third shell and so on, as lying in a discrete lattice; the rest of the crystal is taken as a continuum. This method is called the Mott-Littleton (64) approximation. The Mott-Littleton approximation, and various modifications of it, has been used by various authors [Brauer (62), Boswarva and Lidiard (60)].

In the zero approximation, the discrete part of the lattice consists of the ions to be removed; all the other ions are assumed to lie in a continuum. This approximation, in itself, is not of interest to the aim of this work, as it does not reveal the force constant binding the vacancy to the second nearest neighbour. The second nearest neighbour is the next element in the linear chain in the <110> direction.

The first order approximation takes the central ion, which is to be removed, and the nearest neighbour as the discrete part of the lattice.

The second order approximation takes, in addition to this the second nearest neighbour as the discrete part of the lattice. With the second order approximation, the binding on either side of the second nearest neighbour along the <110> direction can be studied in sufficient detail.

The Mott-Littleton description of the continuum part of the lattice (regionII) goes as follows.

In ionic crystals, when the vacancy is created in region I (the discrete part) it acts as a charge singularity. At a distance r away, the polarisation is given by

$$\underline{P} = \frac{1}{4\pi}\left(1 - \frac{1}{\epsilon}\right) \frac{q}{r^3} \underline{r}$$

where ϵ is the dielectric constant.

The displacement dipole moments, η, and the electronic dipole moments, μ, are then given by

$$\left.\begin{aligned} \eta \pm &\left(\frac{\alpha}{\alpha_+ + \alpha_- + 2\alpha}\right) \times 2r_o^3 \times \underline{P} \\ \mu \pm &\left(\frac{\alpha \pm}{\alpha_+ + \alpha_- + 2\alpha}\right) \times 2r_o^3 \times \underline{P} \end{aligned}\right\} \quad \ldots\ldots \quad (V.5)$$

where $\alpha_\pm$ are the electronic polarisibilities, and α is the displacement polarisibility.

α is given by the expression

$\alpha = e^2/f$, where f is the force constant.

V.4. THE ELASTIC STRENGTH OF THE VACANCY

Brauer (62) points out that the vacancy is also an elastic as well as an electrical singularity. The displacement of an ion at a distance r from the singularity is given by

$\zeta = kr_o^3/r^2$ where k is a constant.

If the displacement of the nearest neighbour ion to the vacancy is λr_0, Brauer assumes that, in the first order Mott-Littleton approximation, k is given by the equation

$$k = \lambda$$

In the second order approximation, the corresponding Braur assumption will be

$$k = \tfrac{1}{2} (\lambda + 2\sqrt{2}\, v) \qquad \ldots\ (V.6)$$

where $\sqrt{2}vr_0$ is the displacement of the second nearest neighbour along the line joining the vacancy to the ion. Here the region II ions are affected by both the elastic strength of the first and second nearest neighbous ions.

Boswarva and Lidiard [60] suggests that the Brauer assumption overemphasises the importance of the elastic term in the displacement of the more distant ions. They therefore suggest that the elastic displacements of the region II ions should join smoothly with those of the region I ions at the boundaries. Thus, in the first order Mott-Littleton approximation,

$$k = \lambda - M^1$$

where $$M^1 = \frac{\eta_{\pm} \times r^2}{q}$$

In the second order approximation Boswarva [84] suggests that the elastic displacements should arise from an average effect of the first and second nearest neighbours, i.e.

Figure 5 Relaxations of first and second nearest neighbours of the vacancy. The figure shows a typical (100) plane containing the vacancy. The 1,0,0 type ions relax a distance λr_0 along the [100] direction. The 1,1,0 type ions relax a distance $r_0 v/2$ along the [110] direction.

Figure. 5.

RELAXATIONS OF FIRST AND SECOND NEAREST NEIGHBOURS OF THE VACANCY.

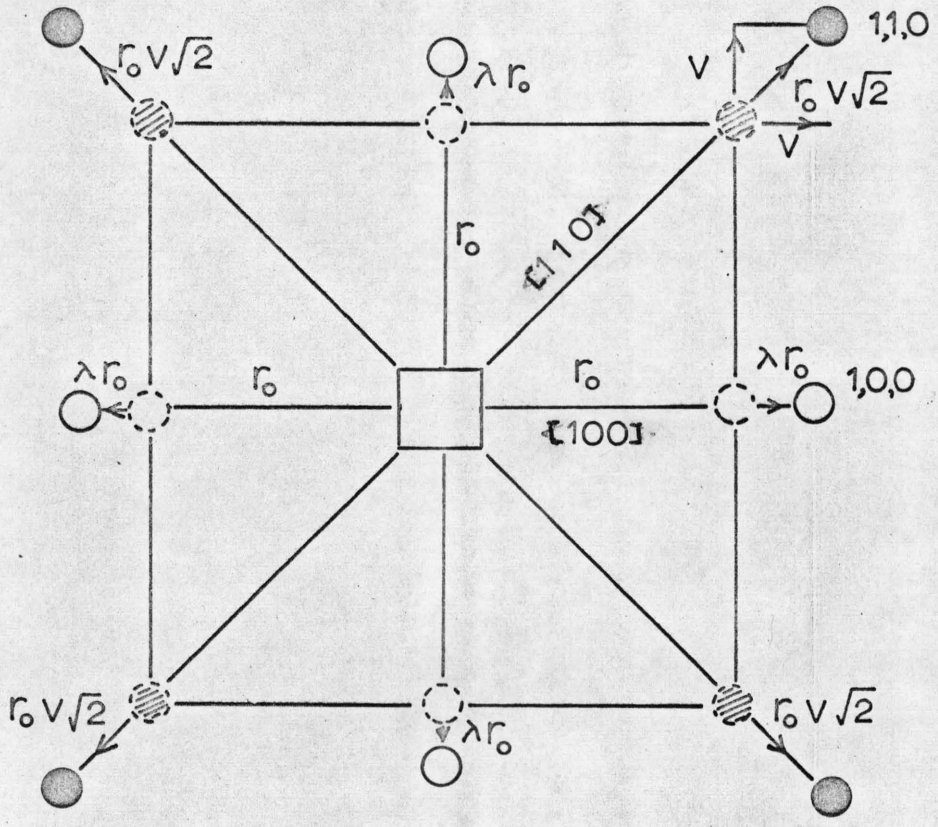

$$k = \tfrac{1}{2}(\lambda - M^1) + \tfrac{1}{2}(2\sqrt{2}v + M^1)$$

$$= \tfrac{1}{2}(\lambda + 2\sqrt{2}v) \qquad \ldots\ (V.7)$$

The Brauer and the Boswarva-Lidiard assumptions give identical results in the second order approximation. Boswarva and Lidiard [60] have made a systematic study of the alkali-halides, using the first order approximation. In particular they have developed a set of equations which is simple to work with, and which can be extended for any higher order approximation. The work in this line being undertaken here extends their approximation and, at the same time some of their conclusions are examined.

V.5 THE BASIC EQUATIONS.

When the ion is removed, its neighbours relax until the energy of that configuration is the minimum. Owing to the symmetry of the vacancy, the relaxations of the neighbours will be along the line joining the ions to the vacancy. For example, in the second order approximation, when the central ion is removed [as in Figure (5)], the 1,0,0 ions will all be displaced a distance λr_0, say, along the [100] direction, and the 1,1,0 ions a distance $\sqrt{2}vr_0$, say, along the [110] direction. All the other ions in the continuum will relax according to the Mott-Littleton approximations. The energy of the formation of a vacancy is then a function of λ, and γ.

It is then minimised with respect to these two parameters.

The energy needed to remove the ion from a normal lattice site to infinity is given by

$$W = W_1 + W_2(x;\ m) + W_3(x, m;\ \bar{3}\ ,\ \mu) + W_4\ (\bar{3},\ \mu) \quad .... \quad (V.8)$$

where x, $\bar{3}$ are the displacements of the ions in region I [the discrete lattice] and region II [the continuum] respectively.

m and μ are their respective electronic moments.

W_1 is the energy of the defect in a rigid, unpolarised lattice. The lattice is then allowed to relax. $W_2(x;\ m)$ is the relaxation energy in region I only. $W_3(x,\ m;\ \bar{3}\ ,\ \mu)$ is the interaction energy between regions I and II due to the relaxations. $W_4(\bar{3}\ ,\ \mu)$ is the relaxation energy of regions II only. The energy can be re-distributed between W_3 and W_4 so that W_4 represents the energy of a distorted polarised region II filled with a perfect region I. The perfect lattice is referred to as the lattice of zero energy.

By expanding the terms W_2, W_3 and W_4 in Equation (V.5) and imposing the equilibrium conditions

$$\frac{\partial W}{\partial m} = \frac{\partial W}{\partial \mu} = \frac{\partial W}{\partial \bar{3}} = 0$$

Equation (V.5) is reduced to

$$W = W_1 + W_2(x,0) - \tfrac{1}{2} \sum_{i}^{I} \bar{m}_i F_i^{(1)} - \tfrac{1}{2} \sum_{\nu}^{II} \bar{\mu}_\nu F_\nu^{(1)}$$

$$+ W_3(x,0;\ \bar{3},0) - \tfrac{1}{2}\sum_{\nu} \bar{3}_\nu \frac{\partial W_3}{\partial \bar{3}}\ (x,0;\ \bar{3}\ ,0)\Big|_{\bar{3}} \quad .... \quad (V.9)$$

i and ν refer to regions I and II respectively.

$\bar{m}_i$ and $\bar{\mu}_\nu$ are the equilibrium electronic moments.

$F_i^{(1)}$ and $F_\nu^{(1)}$ are the monopole fields due to the charges at the lattice points and the relaxed positions.

$\bar{\xi}_\nu$ are the equilibrium relaxations of region II.

Both $W_3(x,0;\bar{\xi},0)$ and $\frac{\partial W_3(x,0;\bar{\xi},0)}{\partial \xi}$ contain electrostatic as well as short-range force terms. Separating the two types of potentials and introducing $\bar{\eta}_\nu$ as the equilibrium displacement dipoles, i.e. $\bar{\eta}_\nu = q_\nu \bar{\xi}_\nu$, the energy expression becomes

$$W = W_1 + W_2(x,0) - \tfrac{1}{2}\sum^{I} \bar{m}_i F_i^{(1)} - \tfrac{1}{2}\sum^{II}_{\nu} (\bar{\mu}_\nu + \bar{\eta}_\nu) F_\nu^{(1)}$$

$$+ W_{3,R}(x,0;\bar{\xi},0) - \tfrac{1}{2}\sum^{I}_{\nu} \bar{\xi}_\nu \frac{\partial}{\partial \xi_\nu} W_{3,R}(x,0;\xi,0)\Big|_{\bar{\xi}} \quad \ldots\ldots (V.10)$$

where $W_{3,R}$ is the energy due to short range potential part of W_R. The derivation of Equation (V.7) was first done by Boswarva and Lidiard [60].

V.6. APPLICATIONS TO THE IONIC MODEL.

The simplest ionic model is one in which the central, two bodies forces consist of only the long range electrostatic monopole and dipole interactions and the short range hard core and Van der Waal interactions only. Thus the potential, ϕ, can be divided into the Coloumb potential, ϕ_C, and the short range forces, ϕ_R. The explicit expressions for

W_1, W_2, W_3 and W_4 can then be written explicitly as follows:

$$W_1 = - \sum_j^{I\prime} \phi\,(r_j^{\,o}) - \sum_s^{II} \phi\,(r_s^{\,o}) \qquad \ldots\ (V.11)$$

which is the work needed to create a vacancy in a rigid non-polarisable lattice. r^o and r are respectively the perfect lattice and the relaxed positions.

$$W_2 = \tfrac{1}{2} \sum_{j\neq k}^{I\prime}\sum^{I\prime} \left\{\phi_R(r_j - r_k) - \phi_R\,(r_j^{\,o} - r_k^{\,o})\right\}$$

$$+ \tfrac{1}{2} \sum_{j\neq k}^{I\prime}\sum^{I\prime} \left\{\phi_c(r_j - r_k) - \phi_c\,(r_j - r_k^{\,o}) - \phi_c(r_j^{\,o} - r_k) + \phi_c(r_j^{\,o} - r_k^{\,o})\right\}$$

$$- \sum_j^{I\prime} \left\{\phi_c(r_j) - \phi_c(r_j^{\,o})\right\} - \sum_j^{I\prime} \chi\,(-r_j; m_j) + \tfrac{1}{2} \sum_{j\neq k}^{I\prime}\sum^{I\prime} w(r_j - r_k; m_j, m_k)$$

$$\ldots\ (V.12)$$

which is the change in the energies of the region I ions when they relax. The region II lattice is assumed for the time being to be rigid and unpolarisable. The first term is the short range interactions. The second and third term are the electrostatic monopole interactions. The fourth and fifth terms are respectively the monopole-dipole and the dipole-dipole interactions. All other terms which are negligible in magnitude, e.g. the dipole self-interaction or the change in the Madelung energy as the ions relax, are ignored. This will be the case for the following two expressions.

W_3 is the interaction energy of the region I and II ions, their effective charges and their dipoles, plus the interaction energy of the effective charge of the vacancy with the monopoles and dipoles of region II.

$$
\begin{aligned}
W_3 = & \sum_{j}^{I'} \sum_{\nu}^{II} \left\{ \phi_R(r_j - r_\nu) - \phi_R(r_j^0 - r_\nu) \right\} \\
& + \sum_{j}^{I'} \sum_{\nu}^{II} \left\{ \phi_c(r_j - r_\nu) - \phi_c(r_j - r_\nu^0) - \phi_c(r_j^0 - r_\nu) \right. \\
& \qquad \left. + \phi_c(r_j^0 - r_\nu^0) \right\} \\
& - \sum_{\nu}^{II} \left\{ \phi(r_\nu) - \phi(r_\nu^0) \right. - \left. \sum_{\nu}^{II} \chi(-r_\nu; \mu_\nu) \right. \\
& + \sum_{j}^{I'} \sum_{\nu}^{II} \left\{ \chi(r_j - r_\nu; \mu_\nu) - \chi(r_j^0 - r_\nu; \mu_\nu) \right\} \\
& + \sum_{j}^{I'} \sum_{\nu}^{II} \left\{ \chi(r_\nu - r_j; m_j) - \chi(r_\nu^0 - r_j; m_j) \right\}
\end{aligned}
$$

.... (V.13)

The first term represents the change in the short range potential when the region I ions relax and the region II ions are in their relaxed position. The second term is the interactions of the real and effective changes of the regions I and II. The third and fourth terms are respectively the interactions of the vacancy and the monopoles and dipoles of region II. The fifth and sixth terms are respectively the

interactions of monopoles of region I and the dipoles of region II and the interactions of the dipoles of region I and the monopoles of region II.

W_4 is the energy of a relaxed and polarised region II when region I has no defect and the ions are in their perfect lattice position and they are not polarised.

$$W_4 = \sum_j^I \sum_\nu^{II} \left\{\phi(r_j^o - r_\nu) - \phi(r_j^o - r_\nu^o)\right\}$$

$$+ \tfrac{1}{2} \sum_\nu^{II} \sum_\pi^{II} \left\{\phi(r_\nu - r_\pi) - \phi(r_\nu^o - r_\pi^o)\right\}$$

$$+ \sum_{\nu \neq}^{II} \sum_\pi^{II} \left\{\chi(r_\nu - r_\pi ; \mu_\pi) - \chi(r_\nu^o - r_\pi ; \mu_\pi)\right\} \quad \ldots\ldots \quad (V.14)$$

The energy of formation of a Schottky pair is defined as the energy required to take a pair of positive and negative ions to the surface of the crystal. Thus the Schottky formation energy is

$$W_S = W_+ + W_- - \tfrac{1}{2}(W_{1+} + W_{1-})$$

and $W_\pm = W_{1\pm} + W_{2\pm} + W_{3\pm} + W_{4\pm}$

V.7. THE CALCULATIONS

On the basis of Equations (V.11) to (V.14), the energy needed to extract an ion from the NaCl lattice to infinity,

Tables 1 and 2 Calculated Schottky pair formation energies of NaCl. Mayer's (66) data of Van der Waal co-efficients are used in Table 1 and Haff's (67) in Table 2. The notations λ, ν .... $E_{T\pm}$, W_S are as in Appendix (II).

Tables 3 and 4 Calculated formation energies of nine other alkali-halide. Mayer's data are used throughout. Table 3 uses the Accurate Field terms (see SectionIV1) and Table 4 the Approximate Field terms.

Table 5 Comparisons of Calculated and Experimental values. All the calculated values are from Table (1) and Table (3) where Mayer's data and Accurate Field terms are used. The calculated sublimation energies for all salts and the calculated formation pair energy for NaBr, NaCl, KCl, RbCl and LiI are excellent.

TABLE 1. NaCl FORMATION ENERGIES (MAYER)

BM M^1=0.042 A12=0.04972 ρ=0.324 Å E_{1+}=7.9125 eV E_{4+}=-2.1186 eV

BMV M^1=0.038 B12=0.13129 σ=0.159 eV E_{1-}=8.0518 eV E_{4-}=-1.1899 eV

ELASTIC	FORCE FIELD		VACANCY	λ	V	E_3eV	E_4eV	E_5eV	$E_{T\pm}$eV	W_seV
Non Elastic	BMV	Accurate Field	+ ion	0.04324	-0.02231	-0.9221	-1.2201	1.2998	4.952	2.41
			- ion	0.05072	-0.02922	-1.4422	-1.1278	1.1577	5.343	
		Approxi-mate Field	+ ion	0.04724	-0.02440	-0.9440	-1.2116	1.4261	5.064	2.58
			- ion	0.05419	-0.03056	-1.4608	-1.1254	1.2379	5.506	
Non Elastic	BM	Accurate Field	+ ion	0.05933	-0.02521	-1.0825	-1.1936	1.3086	4.820	2.06
			- ion	0.06979	-0.03328	-1.7273	-1.1265	1.2283	5.230	
		Approxi-mate Field	+ ion	0.06468	-0.02737	-1.1012	-1.1912	1.4002	4.902	2.17
			- ion	0.07403	-0.03459	-1.7424	-1.1240	1.2759	5.265	
Elastic Bos/Lid	BMV	Accurate Field	+ ion	0.04014	-0.02381	-0.9519	-1.1986	1.3054	4.949	2.40
			- ion	0.04877	-0.03038	-1.4600	-1.1055	1.1549	5.445	
		Approxi-mate Field	+ ion	0.04452	-0.02631	-0.9797	-1.1887	1.4338	5.059	2.58
			- ion	0.05230	-0.03168	-1.4778	-1.1044	1.2354	5.509	
Elastic Bos/Lid	BM	Accurate Field	+ ion	0.05363	-0.02889	-1.1492	-1.17518	1.3447	4.814	2.04
			- ion	0.06475	-0.03662	-1.7703	-1.1036	1.2416	5.223	
		Approxi-mate Field	+ ion	0.05793	-0.03186	-1.1789	-1.1641	1.4421	4.893	2.16
			- ion	0.06933	-0.03768	-1.7824	-1.1037	1.2897	5.259	

TABLE 2 NaCl FORMATION ENERGIES (HAFF)

BM M^1=0.042 A12=0.04972 ρ=0.324 Å E_{1+}=7.923 E_{4+}=-2.1186

BMV M^1=0.038 B12=0.13129 σ=0.159eV E_{1-}=7.9530 E_{4-}=-1.1899

ELASTIC	FORCE	FIELD	VACANCY	λ	V	E_3eV	E_4eV	E_5eV	$E_{T\pm}$eV	W_seV
Non Elastic	BMV	Accurate Field	+ ion	0.04413	-0.02208	-0.9407	-1.2202	1.2950	4.94	2.34
			- ion	0.05058	-0.02923	-1.4498	-1.1278	1.1576	5.34	
		Approximate Field	+ ion	0.04889	-0.02423	-0.9636	-1.2116	1.4198	5.05	2.52
			- ion	0.05419	-0.03065	-1.4693	-1.1253	1.2379	5.41	
Non Elastic	BM	Accurate Field	+ ion	0.06199	-0.02479	-1.1051	-1.2002	1.3000	4.80	1.99
			- ion	0.06966	-0.03329	-1.7352	-1.1265	1.2282	5.13	
		Approximate Field	+ ion	0.06730	-0.02685	-1.1225	-1.1921	1.3883	4.88	2.10
			- ion	0.07413	-0.03454	-1.7499	-1.1242	1.2756	5.16	
Elastic Bos/Lid	BMV	Accurate Field	+ ion	0.04246	-0.02333	-0.9648	-1.2019	1.2991	4.94	2.34
			- ion	0.04852	-0.03054	-1.4695	-1.1048	1.1556	5.34	
		Approximate Field	+ ion	0.04651	-0.02586	-0.9936	-1.1916	1.4260	5.04	2.51
			- ion	0.05226	-0.02182	-1.4872	-1.1039	1.2363	5.41	
Elastic Bos/Lid	BM	Accurate Field	+ ion	0.05760	-0.02769	-1.1561	-1.1818	1.3288	4.79	1.97
			- ion	0.06473	-0.03649	-1.7770	-1.1040	1.2406	5.12	
		Approximate Field	+ ion	0.06152	-0.03080	-1.1884	-1.1697	1.4258	4.87	2.09
			- ion	0.06930	-0.03769	-1.7907	-1.1037	1.2897	5.16	

TABLE 3 FORMATION ENERGIES (ACCURATE FIELD)

Crystal	ρ Å	σ eV	M^1	Elastic	Vacancy	λ	V	E_1 eV	E_2 eV	E_3 eV	E_4 eV	E_5 eV	$E_{T\pm}$ eV	W_s eV
LiF	0.291	0.150	0.056	Non Elastic	+ ion	0.07157	-0.03213	10.7021	-20309	-20142	-1.7550	1.2400	6.142	1.88
					- ion	0.07833	-0.03967	10.7545	-10726	-2.7325	-1.6852	1.1998	6.464	
				Elastic Bos/Lid	+ ion	0.05999	-0.03977	10.7021	-20309	-21653	-1.6970	1.3135	6.122	1.93
					- ion	0.06578	-0.04747	10.7545	-10726	-28476	-1.6304	1.2328	6.437	
NaBr	0.333	0.156	0.041	Non Elastic	+ ion	0.07242	-0.03201	7.7100	-12556	-16679	-1.0677	1.3152	5.0339	1.97
					- ion	0.06053	-0.02352	7.5538	-23042	-09564	-1.1448	1.4184	4.5669	
				Elastic Bos/Lid	+ ion	0.06947	-0.03408	7.7100	-12556	-16933	-1.0533	1.3238	5.0314	1.96
					- ion	0.05616	-0.02645	7.5538	-23042	-10091	-1.2786	1.4513	4.5639	
KCl	0.337	0.159	0.040	Non Elastic	+ ion	0.06410	-0.02637	7.2398	-15743	-11105	-1.0035	1.0492	4.601	2.12
					- ion	0.07042	-0.03011	7.3513	-11839	-14013	-0.9730	1.0262	4.819	
				Elastic Bos/Lid	+ ion	0.06118	-0.02827	7.2398	-15743	-11374	-0.9914	1.06.5	4.599	2.12
					- ion	0.06821	-0.03168	7.3512	-11839	-14197	-0.9618	1.0324	4.818	
KBr	0.346	0.155	0.038	Non Elastic	+ ion	0.06232	-0.02484	6.9480	-17273	-09815	-0.9714	1.1198	4.388	2.04
					- ion	0.07073	-0.02988	7.0740	-11926	-13621	-0.9305	1.0816	4.670	
				Elastic Bos/Lid	+ ion	0.05995	-0.02664	6.9484	-17273	-10073	-0.9608	1.1333	4.386	2.05
					- ion	0.06887	-0.03114	7.0740	-11926	-13765	-0.9211	61.0862	4.670	
RbCl	0.339	0.161	0.034	Non Elastic	+ ion	0.06392	-0.02650	6.9918	-14261	-10940	-0.8456	0.9913	4.617	2.33
					- ion	0.06826	-0.02876	7.0783	-12094	-12663	-0.8296	0.9791	4.752	
				Elastic Bos/Lid	+ ion	0.06182	-0.02797	6.9918	-14261	-11128	-0.8357	0.9989	4.616	2.28
					- ion	0.06681	-0.0297	7.0782	-12094	-12776	-0.8215	0.9819	4.752	

TABLE 3 CONTINUED

Crystal	ρ Å	ϵ eV	M^1	Elastic	Vacancy	λ	V	E_1 eV	E_2 eV	E_3 eV	E_4 eV	E_5 eV	$E_{T\pm}$ eV	W eV
RbBr	0.354	0.160	0.034	Non Elastic	+ ion	0.06386	-0.02546	6.7047	-1.5422	-0.9909	-0.32941	.30424	4.376	2.20
					- ion	0.06985	-0.02899	6.8045	-1.1845	-1.2529	-0.30421	.01081	.574	
				Elastic Bos/Lid	+ ion	0.06168	-0.02679	6.7047	-1.5422	-1.0083	-0.32131	.01254	4.375	2.20
					- ion	0.06834	-0.03002	6.8045	-1.1845	-1.2640	-0.79671	.01434	4.574	
LiCl	0.330	0.144	0.049	Non Elastic	+ ion	0.07990	-0.02177	8.7809	-2.9593	-1.1874	-1.+505	1.73024	4.9218	1.48
					- ion	0.08834	-0.03438	8.8486	-1.5012	-2.3015	-1.35451	.69205	.3834	
				Elastic Bos/Lid	+ ion	0.07873	-0.02248	8.7809	-2.9593	-1.2013	-1.4555	1.73604	4.9248	1.49
					- ion	0.08543	-0.03613	8.8486	-1.5012	-2.3238	-1.34121	.70255	.3819	
LiBr	0.344	0.142	0.048	Non Elastic	+ ion	0.08421	-0.01903	8.2910	-3.1257	-1.0037	-1.3774	1.31414	4.5980	1.35
					- ion	0.09292	-0.03291	8.3807	-1.5794	-2.2141	-1.27971	.77775	.0853	
				Elastic Bos/Lid	+ ion	0.08593	-0.01760	8.2910	-3.1259	-0.9766	-1.39881	.81154	.6017	1.35
					- ion	0.09267	-0.03312	8.3807	-1.5794	-2.2165	-1.27881	.77935	.0853	
LiI	0.372	0.127	0.048	Non Elastic	+ ion	0.09613	-0.01406	7.7258	-3.3138	-0.7650	-1.2650	1.84704	.230	1.17
					- ion	0.10595	-0.03056	7.8958	-1.6685	-2.1735	-1.17121	.87344	4.7561	
				Elastic Bos/Lid	+ ion	0.10541	-0.00747	7.7258	-3.3138	-0.6436	1.31991	.77974	.2282	1.17
					- ion	0.11142	-0.02728	7.8958	-1.6685	-2.1383	-1.18681	.85014	4.7324	

TABLE 4 FORMATION ENERGIES (APPROXIMATE FIELD)

Crystal	ρ Å	b eV	M^1	Elastic	Vacancy	λ	V	E_1 eV	E_2 eV	E_3 eV	E_4 eV	E_5 eV	E_T eV	Ws eV
LiF	0.291	0.150	0.056	Non Elastic	+ ion	0.07354	-0.03275	10.7021	-2.0309	-2.0211	-1.7515	1.2722	6.171	1.92
					- ion	0.08041	-0.0400	10.7545	-1.0726	-2.7373	-1.6841	1.2162	6.477	
				Elastic Bos/Lid	+ ion	0.06033	-0.04136	10.7021	-2.0309	-2.1873	-1.6889	1.3519	6.147	1.87
					- ion	0.06846	-0.04759	10.7545	-1.0726	-2.8495	-1.6325	1.2506	6.451	
NaBr	0.333	0.156	0.041	Non Elastic	+ ion	0.07773	-0.03362	7.7100	-1.2556	-1.6862	-1.0651	1.3677	5.071	2.11
					- ion	0.06744	-0.02645	7.5538	-2.3042	-0.9780	-1.1337	1.5290	4.667	
				Elastic Bos/Lid	+ ion	0.07511	-0.03522	7.7110	-1.2556	-1.7067	-1.0536	1.3751	5.069	2.10
					- ion	0.06169	-0.03032	7.5538	-2.3042	-1.0444	-1.1132	1.5697	4.662	
KCl	0.337	0.159	0.040	Non Elastic	+ ion	0.06850	-0.02827	7.2398	-1.5743	-1.1254	-0.9980	1.1247	4.667	2.24
					- ion	0.07422	-0.03171	7.3513	-1.1839	-1.4145	-0.9696	1.0793	4.863	
				Elastic Bos/Lid	+ ion	0.06483	-0.03065	7.2398	-1.5743	-1.1577	-0.9841	1.1400	4.664	2.24
					- ion	0.07206	-0.03327	7.3513	-1.1839	-1.4326	-0.9590	1.0854	4.861	
KBr	0.346	0.155	0.038	Non Elastic	+ ion	0.06806	-0.02728	6.9484	-1.7273	-0.9991	-0.9642	1.2106	4.468	2.17
					- ion	0.07518	-0.03172	7.0740	-1.1926	-1.3772	-0.9270	1.1384	4.716	
				Elastic Bos/Lid	+ ion	0.06463	-0.02955	6.9484	-1.7373	-1.0305	-0.9520	1.2271	4.466	2.17
					- ion	0.07341	-0.03284	7.0740	-1.1926	-1.3904	-0.9186	1.1427	4.715	
RbCl	0.339	0.161	0.034	Non Elastic	+ ion	0.06827	-0.02831	6.9918	-1.4261	-1.1073	-0.8413	1.0633	4.680	2.42
					- ion	0.07210	-0.03028	7.0782	-1.2094	-1.2779	-0.8267	1.0368	4.801	
				Elastic Bos/Lid	+ ion	0.06564	-0.03009	6.9918	-1.4261	-1.1291	-0.8307	1.0724	4.678	2.42
					- ion	0.07038	-0.03163	7.0782	-1.2094	-1.2926	-0.8178	1.0417	4.800	

TABLE 4 CONTINUED

Crystal	ρ Å	ϵ eV	M^1	Elastic	Vacancy		λ	V	E_1 eV	E_2 eV	E_3 eV	E_4 eV	E_5 eV	$E_{T\pm}$ eV	W_S eV
RbBr	0.354	0.160	0.034	Non	+	ion	0.06883	-0.02766	6.7047	-1.5422	-1.0060	-0.82421	1.1160	4.448	2.32
				Elastic	-	ion	0.07398	-0.03089	6.8045	-1.1845	-1.2671	-0.80091	1.0698	4.622	
				Elastic	+	ion	0.06614	-0.02948	6.7047	-1.5422	-1.0284	-0.81461	1.1271	4.447	2.32
				Bos/Lid	-	ion	0.07267	-0.03184	6.8045	-1.1845	-1.2775	-0.79381	1.0728	4.6216	
LiCl	0.330	0.144	0.049	Non	+	ion	0.08558	-0.02556	8.7810	-2.9593	-1.2265	-1.43381	1.8589	5.020	1.60
				Elastic	-	ion	0.09325	-0.03562	8.8486	-1.5012	-2.3167	-1.35191	1.7205	5.399	
				Elastic	+	ion	0.08068	-0.02893	8.7810	-2.9593	-1.2903	-1.42201	1.9134	5.023	1.61
				Bos/Lid	-	ion	0.09214	-0.03625	8.8486	-1.5012	-2.3260	-1.34741	1.7250	5.399	
LiBr	0.344	0.142	0.042	Non	+	ion	0.09067	-0.02420	8.2911	-3.1259	-1.0549	-1.35601	1.9622	4.716	1.48
				Elastic	-	ion	0.09835	-0.03427	8.3807	-1.5794	-2.2300	-1.27721	1.8032	5.097	
				Elastic	+	ion	0.08775	-0.02625	8.2911	-3.1259	-1.0936	-1.35432	2.004	4.721	1.48
				Bos/Lid	-	ion	0.10015	-0.03309	8.3807	-1.5794	-2.2163	-1.28201	1.7941	5.097	
LiI	0.372	0.127	0.048	Non	+	ion	0.10233	-0.02185	7.7258	-3.3138	-0.8452	-1.23692	2.0363	4.366	1.31
				Elastic	-	ion	0.11061	-0.0320	7.8958	-1.6685	-2.188	-1.16861	1.886	4.756	
				Elastic	+	ion	0.10297	-0.02140	7.7258	-3.3138	-0.8417	-1.25082	2.0533	4.373	1.31
				Bos/Lid	-	ion	0.11905	-0.02687	7.8958	-1.6685	-2.1324	-1.18941	1.8413	4.747	

TABLE 5

COMPARISONS OF CALCULATED AND EXPERIMENTAL VALUES

		Sublimation Energy		Schottky Pair Energy	
Crystal	Elastic	Calculated	Experimental	Calculated	Experimental
LiF	Non Elastic	10.729		1.88	2.42
	Elastic Bos/Lid			1.93	(85)
NaBr	Non Elastic	7.632	7.627	1.97	1.68
	Elastic Bos/Lid		(90)	1.96	(86)
NaCl	Non Elastic	7.983	8.009	2.06	2.12
	Elastic Bos/Lid		(90)	2.17	(70)
KCl	Non Elastic	7.296	7.276	2.12	2.22
	Elastic Bos/Lid		(90)	2.12	(70)
KBr	Non Elastic	7.011	6.990	2.04	2.53
	Elastic Bos/Lid		(90)	2.05	(87)
RbCl	Non Elastic	7.035	7.094	2.33	2.25
	Elastic Bos/Lid		(90)	2.28	(88)

TABLE 5 Continued.

		Sublimation Energy		Schottky Pair Energy	
Crystal	Elastic	Calculated	Experimental	Calculated	Experimental
RbBr	Non Elastic	6.755	6.851	2.20	
	Elastic Bos/Lid		(90)	2.20	
LiCl	Non Elastic	8.815	8.737	1.48	2.12
	Elastic Bos/Lid		(90)	1.49	(89)
LiBr	Non Elastic	8.336	8.303	1.35	1.80
	Elastic Bos/Lid		(90)	1.35	(89)
LiI	Non Elastic	7.811	7.805	1.17	1.34
	Elastic Bos/Lid		(90)	1.17	(89)

W, is expressed in terms of the two unknowns, namely the relaxations of the nearest ion to the vacancy, λr_0, and the next nearest neighbour $\sqrt{2}\, v r_0$. [See Figure (5)]. The energy W is minimised with regard to these two variables using computational methods. The I.B.M. 7090/7094 computer is used.

The BM and BMV potentials are used. The constants b and p are deduced from lattice stability and compressibility of each individual alkali halide crystal.

The Mott-Littleton approximation and the Brauer and Boswarva-Lidiard modifications are used. The non-elastic form is the form where the elastic constant, k, equals zero; the Boswarva-Lidiard modification is when k equals $\frac{1}{2}(\lambda + 2\sqrt{2}\, v)$.

The Van der Waal potentials are used explicitly.

The lattice calculations are done for various alkali halide crystals namely, LiF, NaCl, NaBr, KCl, KBr, RbCl and RbBr, LiCl, LiBr and LiI.

The calculated energy of the Schottky defect and the sublimation energy of each crystal are compared with the experimental values. The agreement in the comparison justifies the use of the form of the potential and the Mott-Littleton approximation or its modification.

After these calculations the equations for the force constant of the motion of the next nearest neighbour

constrained to move in the <110> direction is written down. This is done by first separating out one ion, say the 1,1,0, from all the eleven other next nearest neighbours. Its displacement is represented by v^1 whereas the displacements of the other eleven ions is represented by v. The energy, W, written in this new form, is differentiated with respect to v^1. When $v^1 = v$ the force acting on the particular 1,1,0 ion should vanish. The force constants are then obtained. This method makes the plausible assumption that the form of the potential is produced by the surrounding ions in their relaxed equilibrium position. The actual jump of the ion is fast enough so that the surrounding ions have no time to rearrange their positions in an energetically more favourable position.

By an extension of the method outlined above the saddle-point configuration in the transition state theory of the heat of transport can be obtained.

V.7. 1 DATA USED IN THE CALCULATIONS.

The interatomic distances, ionic radii and the compressibility are from Fumi and Tosi (65). The Van der Waal coefficients are from Mayer (66) and Haff (67). The electronic polarisibilities are from Tessman, Khan and Shockley (68) and the static dielectric constants are from Haiissuhl (69).

IV.8 RESULTS AND DISCUSSIONS.

The results of the lattice calculations are given in Tables (1) to (5). The Pauling (63) form of the pre-exponential term in the repulsive potential is used throughout. (c.f V.3). In the results of NaCl in Tables 1 and 2 both the BM and the BMV potentials are used. As expected, with the harder BMV potential the relaxations of the ions are more restricted, and the Schottky pair formation energies are higher. For NaCl, the BM potential gives excellent agreement with the experimental value [2.12 eV (70)] whereas the BMV potential gives markedly higher values ($\sim$0.3 to 0.4 eV more). The inclusion of the elastic term makes very little difference in the final results. Table 1 shows the results with the use of Mayer's (66) data on the Van der Waal co-efficients and Table 2 with Haff's (67) more recent data. There is very little difference in the sublimation and formation energies although the Mayer's version gives slightly higher values ($\sim$0.05 eV in the sublimation energy and $\sim$0.06 eV in the formation energy).

From the evidence of the NaCl results, there is no justification in resorting to the use of the BMV potential. The subsequent calculations for the nine salts, i.e. LiF, LiCl, LiBr, LiI, NaBr, KCl, KBr, RbCl and RbBr, involve the use of only the BM potential. The inclusion of the elastic

strength is again found to have little effect on the formation energy (Tables 3 and 4). The calculated sublimation energies compare favourably with the experimental data in all cases (Table 5), and in NaBr, RbCl, NaCl, KCl and LiI the agreement between the experimental and calculated values of the formation energies is excellent. The reason why the LiF, LiBr and LiCl results should be in poor agreement with experiment, has been attributed by Boswarva and Lidiard (60) to the breakdown of the point dipole approximation. The breakdown occurs when the small Li^+ ion approaches close to the Cl^- ion and when this happens it is no longer valid to assume that the electronic dipoles of the ions are point dipoles. [Note the LiI exception].

The relaxations of the second nearest neighbours towards the vacancy (i.e. v is negative) is as expected. The removal of the ion removes both the repulsive Coloumb interactions [++ or -- interactions] and the repulsive short range interactions of the second nearest neighbours and itself. This causes the second nearest neighbour to relax towards the vacancy. The relaxations outwards of the first nearest neighbours are due to the removal of the attractive Coloumb force.

In all cases the extraction of a negative ion from the lattice requires more energy than that of a positive ion.

Also the relaxations of the neighbour due to the extraction of the negative ion is more pronounced than the relaxations due to a positive ion vacancy. These two related effects are obviously caused by the fact that generally the radii of the negative ions are larger than that of the positive ions.

V.8 1 CONCLUSIONS.

The objects of undertaking the lattice calculations hav been to produce a suitable model of the lattice around the vacancy and to find a suitable form of short range potential between the ions. From there on, the force constant of the second nearest neighbours at their equilibrium relaxed positions is determined realistically.

From the comparisons which are made between the lattice calculations and experimental data, it is found that the vacancy model chosen, with the use of the BM and the explicit Van der Waal short range potentials, is sound.

It is then concluded that the force constant of the second nearest neighbour obtained from the use of this model and the form of the short range potential is realistic.

CHAPTER VI

THE HEAT OF TRANSPORT (II)

VI. 1. THE ANALYSIS AND CALCULATIONS:

The equilibrium relaxations of the nearest neighbour, λr_o, and the next nearest neighbour, $\sqrt{2}$ v r_o, to the vacancy has been found in Chapter (V).

Let the relaxation of the ion at 1,1,0 be $\sqrt{2}\ v^1 r_o$ and the relaxations of the other eleven 1,1,0 type ions remain at $\sqrt{2}vr_o$. By differentiating the vacancy formation energy expression, $E(\lambda, v, v^1)$, with respect to v^1, as is shown in Appendix III, the force on the 1,1,0 ion is found. By computing the change of this force with respect to a change in v^1 around equilibrium value v, the force constant is found. This is done with the help of the IBM 7090/7094 computer and the results for NaCl and KCl are summarised in the Graphs in Figures (6) and (7). The Born-Mayer potential and the unmodified Mott-Littleton Approximation are used.

From Equation (A III.12), it can be seen that the exact solution for the dipole fields, F_I's, involves the solution of a 8 x 8 x 3 matrix equation. This is an extremely difficult problem to solve. However, by putting the FI terms in the RHS of Equation (A III.12) to be zero, the solution becomes simple. Correspondingly, the FI terms in Equations (A II.10) and (A II.11) have to be put equal to zero. The Schottky pair

formation energy found by the use of this approximation [the Approximate Field approximation] are shown in Table (4) and included in Tables (1) and (2) for comparison with the energy found without resorting to this approximation. [Note that the FI fields can be solved exactly when they appear in the expression for the formation energy in Appendix (II) since their solution, as is seen in Equations (A II.10) and (A II.11), only involves the solution of a 2 x 2 matrix equation]. It is seen that neither the formation energies, nor the relaxations, differ drastically between those found with, and those found without, the use of the field approximation. This justifies the use of the field approximation.

From Equation (IV.16) the heat of transport

$$Q^* = [2 + q/T]E \qquad \ldots\ (VI.1)$$

where $q = \frac{T}{3\pi}\frac{8t}{}\sqrt{\gamma_M}$; t is expected to vary inversely proportionally with T, and therefore q is independent of temperature.

t can be expressed in terms of the thermal conductivity, x,

i.e.

$$t = \frac{r_o^3}{k_B v_s^2}\chi \qquad \ldots\ (VI.2)$$

[See Klemens (71)]

where r_o is the interionic distance of the crystal k_B is

Figures 6 and 7 Graphs of the force exerted on the second nearest neighbour against the distance. (v^1-v) is in units of fractions of the interionic distance r_o. The force constant γ = -gradient/$r_o\sqrt{2}$ eV/Å^2.

γ is used to calculate the heats of transports Q^* and the results are summarised in Table 6.

Figure. 6.

FORCE IN THE NaCℓ CRYSTAL

POSITIVE ION VACANCY

GRADIENT = − 11 eV/Å

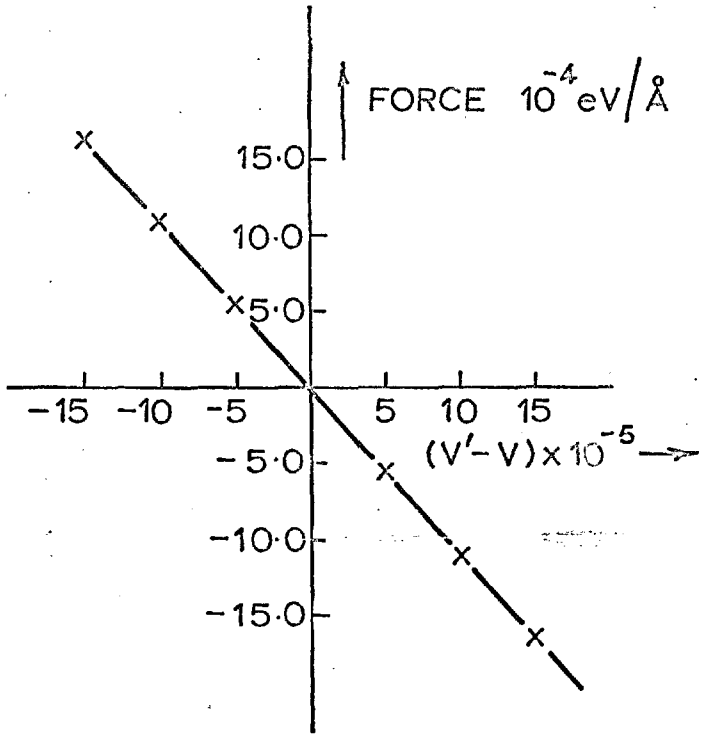

NEGATIVE ION VACANCY

GRADIENT = −12 eV/Å

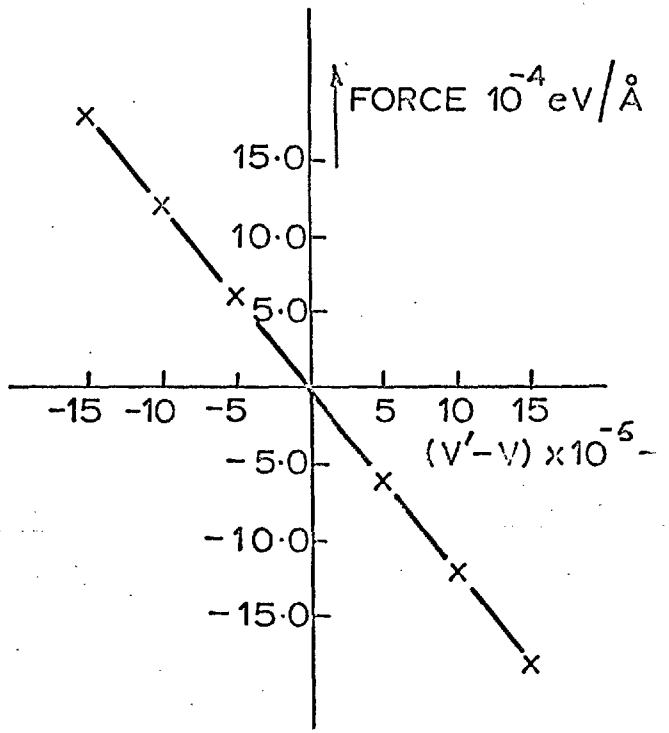

Figure. 7.

FORCE IN THE KCℓ CRYSTAL

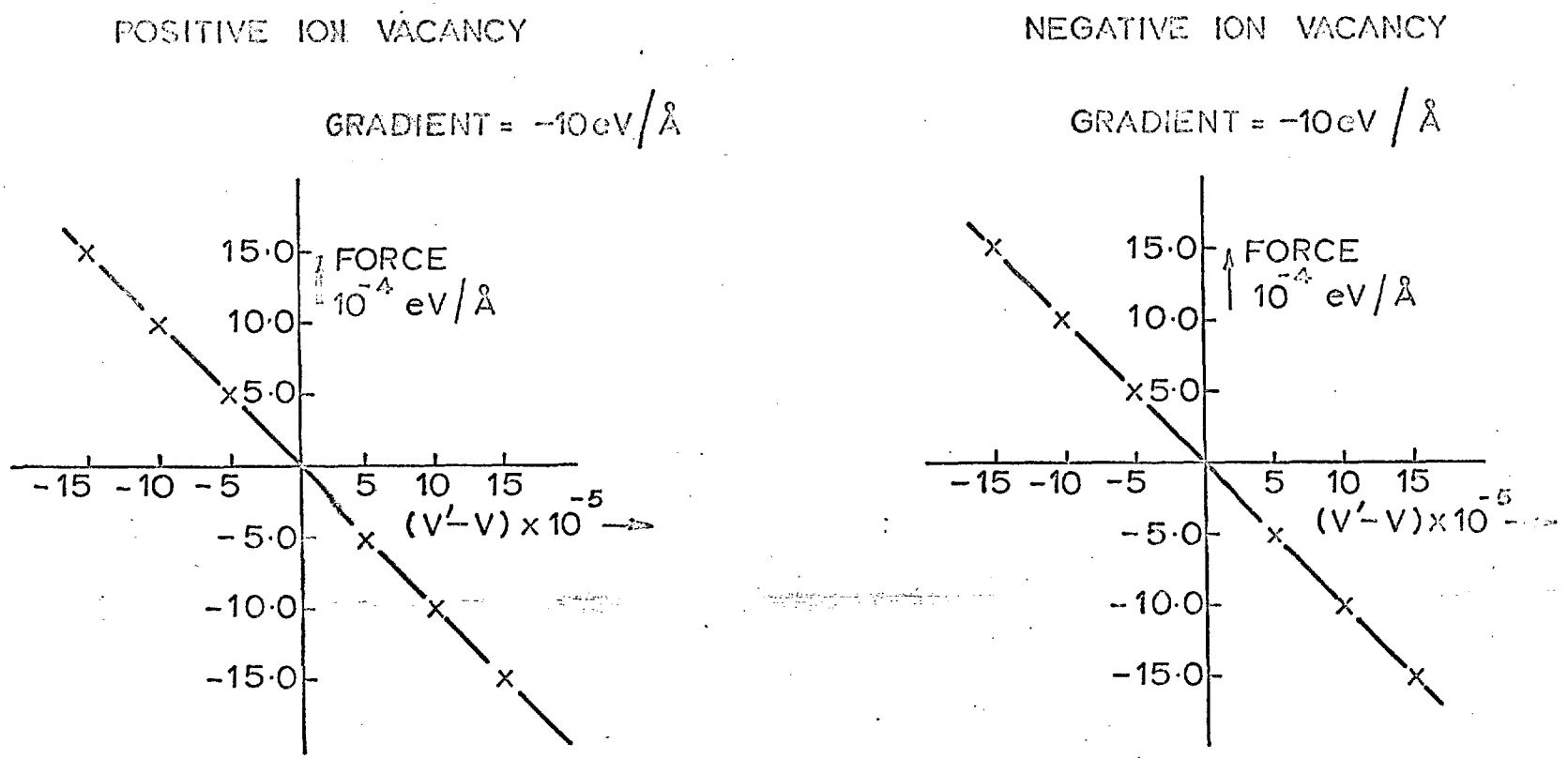

Table 6 The Calculated Heats of Transport of NaCl and KCl. The heats of transport are calculated for 1000°K. The force constants, γ , are obtained from the graphs in Figures (6) and (7). w is the frequency of vibrations of the lattice in the <110> direction.

TABLE 6. THE CALCULATED HEATS OF TRANSPORT

Crystal	λ (72) cal/cm/sec/^{o}C	λ^{c} cal/cm/sec	$\theta_{D}(90)$ ^{o}K	f_{c} ^{o}K sec	t sec at 1000^{o}K		γ eV/A^{o2}	$w=\sqrt{\gamma/M}$ sec^{-1}	q^{o}K	Q^{*} eV at 1000^{o}K
NaCl	1.47×10^{-2} at 308^{o}K	4.494	281	8.37×10^{-10}	8.37×10^{-13}	+	1.95	2.86×10^{13}	-25.7	1.36
	1.30×10^{-2} at 343^{o}K					-	2.15	2.44×10^{13}	-21.7	1.80
KCl	1.56×10^{-2} at 343^{o}K	5.097	230	15.87×10^{-10}	15.87×10^{-13}	+	1.59	1.98×10^{13}	-32.5	1.48 *
	1.53×10^{-2} at 345^{o}K					-	1.58	2.08×10^{13}	-35.2	3.54 *

* Activation Energy from (82)

the Boltzman's Constant and v_S is the velocity of sound in the crystal. v_S is related to the Debye temperature, θ_D, i.e.

$$v_S = \frac{k_B \theta_D}{\hbar k_m} \cdot 2\pi$$

where $\hbar$ is the Planck's Constant, k_m is the maximum value of the wave vector $|\underline{k}|$, and for the alkali halides it is $\frac{\pi\sqrt{3}}{a_o}$.

$$\gamma = \lambda c/T \qquad \text{[See Klemens (71)]}$$

and the experimental values for λ for NaCl and KCl are tabulated in Table (6), and they are from data obtained by Ballard, MacCathy, Davis (72).

Therefore from Equation (IV.2)

$$t = fc/T$$

where $$fc = \frac{3\hbar^2 a_o}{4 k_B^3 \theta_D^2} \lambda c$$

VI. 6 RESULTS AND DISCUSSIONS.

The results of the computer calculations [See Figures (6) and (7)] show that the force constant γ^1 binding the vacancy to its neighbouring ion is practically the same as the force constant, γ, binding that ion to the other neighbouring ion in the linear chain [See Figure (2)]

Table (6) summarises the results of the heats of transport

calculations. For the temperatures at which diffusion experiments are generally carried out, that is about 900°K to about 1100°K for NaCl and KCl, the heats of transport for each type of ion (Na^+, Cl^-, or K^+) are about one and a half to two times the corresponding activation energy for diffusion. So far, the experimental values of the heats of transport for the alkali halides are not known. This is due to a lack of knowledge of the irreversible electrode-crystal thermopower. However the thermopower of AgCl and AgBr with Ag electrodes have been found [see Christy (6), Susuki, Endo and Haga (73)] and the heat of transport plus an entropy term for the Ag vacancies in both crystals are known. At 623°K $Q^*_v + Ts_v$, where s_v is the entropy of formation of a Ag vacancy, is -0.39 eV for AgCl and -0.40 eV for AgBr (6). The activation energy for the diffusion of Ag vacancy is 0.36 eV for both crystals. [(74) and (75)]. The contribution from the entropy term is not known exactly, but it can be readily seen that the heat of transport is more than the corresponding activation energy.

Some of the assumptions which are implicit in the linear chain model are quite drastic [See Section (III.3)] . The most notable being:-

(i) The harmonic potential approximation is used.

(ii) The assumption that the area surrounding the vacancy

is always in thermal equilibrium.

(iii) The interaction potentials of the surrounding ions with the jumping ion is assumed to be directed not from the surrounding ions themselves, but from the vacancy.

When the actual jump process occurs, the vibrational amplitude of the jumping ion is necessarily large. However Assumption (i) stipulates that the amplitude should be small.

For the jump to occur the jumping ion must collect the extra energy from the surrounding. This causes an imbalance of energy distribution, contrary to Assumption (ii).

In view of the drastic nature of these assumptions, the agreement between the general results of the calculations and the experiments on AgBr and AgCl are surprisingly good.

CHAPTER VII

THE EXPERIMENTS.

VII.1 LITERATURE REVIEW.

Thermoelectric power measurements in ionic crystals have been most thoroughly and successfully carried out in systems where reversible electrodes can be used, e.g. Christy, Fukushima and Li (5) on AgBr, Christy (6) on AgBr and AgCl, Susuki, Endo and Haga (73) on AgCl and Hsueh and Christy (76) on CuCl. The results are successfully analysed using Howard and Lidiard's formula [Equation (II.17)].

However, in the alkali halides the experiments that are done [Nikitinskaya and Murin (7) on NaCl and KCl, Allnatt and Jacobs (8) on KCl, Christy Hsueh and Mueller (9) on polycrystalline NaCl, Jacobs and Maycock (11) on KCl, Hoshimo and Shimoji (10) on NaBr, and Allnatt and Chadwick (4) on single crystal NaCl; all the authors use platinum electrodes] suggest that the experimental difficulties involved are quite considerable, and that all the phenomena observed are by no means easily explained.

VII.1.1 Nikitinskaya and Murin

Nikitinskaya and Murin's (7) results are very scattered, and their reproducibility is poor. They observe a potential of uncertain magnitude when the temperature is uniform.

VII. 1.2 Allnatt and Jacobs.

Allnatt and Jacobs's [8] results are much more reproducible. They measure the thermoelectric power of pure KCl and KCl containing 107 x 10^{-5} mole fraction of $SrCl_2$ with platinum electrodes in the temperature range 834°K to 966°K.

They observe large fluctuating voltages across the crystals when they are annealed at temperatures less than about 670°C. Their crystals are under mild compression for good electrode contact and they attribute this spurious potential to some form of plastic deformation of the crystal.

VII. 1.3 Christy, Hseuh and Mueller

Christy, Hsueh and Mueller's [9] results on the measurements on pure and doped polycrystalline NaCl are very scattered. They also see the spurious potentials which Allnatt and Jacobs reported. They attribute this potential to the presence of HOH contamination in the salt. In their individual plots of the voltage differences, ΔV, caused by the temperature differences, ΔT, there is a maximum intercept of about 30 mV on the ΔV axis. In their analysis they give a thermopower of pure NaCl as -0.95 mV/°C from 550°C to 780°C.

VII. 1.4 Jacobs and Maycock

Jacobs and Maycock[11], measure the thermopower of pure

KCl and KCl doped with $SrCl_2$ and AgCl in the temperature range between 600°K and 950°K. At about 820°K they observe a so-called inverted $\wedge$ point in their plot of θ against T. Their results for the thermopower of pure KCl are that it varies between -1.35 mV/°C and -1.93 mV/°C at high temperatures, and for KCl with 100 x 10^{-5} mole fraction of $SrCl_2$ it is -1.40 mV/°C.

VII. 1.5 Hoshino and Shimoji

Hoshino and Shimoji's[10] measurements on NaBr, both pure and doped with 28.8 x 10^{-5} mole fraction of $BaBr_2$, are done between 580°C and 720°C. They attribute the time-dependent spurious potential to the influence of the Frenkel-Lehovec[40] space charge at the surface of the crystal.

VII. 1.6 Allnatt and Chadwick

Allnatt and Chadwick [4] measure the thermopower of the pure and $SrCl_2$-doped single crystals of NaCl in the temperature range of 550°C to 755°C. They find that the reproducibility on different crystals vary as much as 30%. In contrast to Jacobs and Maycock [11] and in agreement with Christy et al [9], they find that the intercepts on the ΔV axis in the individual plots of ΔV against ΔT are finite. In addition they plot a straight line graph of the intercepts against the temperatures. Their results are summarised in Figure (12).

Allnatt and Chadwick see the fluctuating voltages even though they take most care to avoid water contamination. They suggest that the cause of the fluctuating voltages is due to the mechanical state of the crystal.

CHAPTER VII

THE EXPERIMENTS

THERMOELECTRIC POWER

VII. 1. SPECIMEN PREPARATIONS

A modified version of Czochralski's method (77) for the growing of single crystals is used. The jig and the actual operations have been extensively described by Newey (78).

The starting material is the Hopkins and Williams analar grade NaCl. This is held molten in a fused silica beaker for approximately fourteen hours. A single crystal seed is then lowered into the molten surface and slowly withdrawn at an approximate speed of about 1 inch per three hours. The boule so obtained varies in diameter as the temperature of the molten surface, the lower the temperature, the larger the diameter. A typical boule is about $1\frac{1}{2}$ inches in diameter and 4 inches long. The crystal grows in the $\langle 100 \rangle$ axis, and immediately after growth, it is transferred to the annealing furnace. This furnace is held at about 650°C for sixteen hours, after which the temperature is brought down to room temperatures over a period of thirty-six to forty hours.

NaCl single crystal cleaves along the $\{100\}$ plane. Each specimen is carefully cleaved by sharp razor blades into rectangular cubes of linear dimensions of between 0.5 to 1.0 cm. The specimens are then examined under the microscope to

Figure 8 The tube furnaces. The outer tube is wound uniformly to provide a uniform temperature. The bottom is closed for temperature stability. The inner tube is wound uniformly in two sections. When the current is passed through E and D the top end of the crystal is at a higher temperature. The temperature gradient is reversed when the current passes between E and C.

Figure 9 The crystal in position in the silica jig. The silica jig is air-tight. It is first evacuated and then filled with high purity argon. The crystal sits between the platinum electrodes at the bottom of the tube. The middle stem is made of silica, and it can slide up and down through the rubber bung. The whole of the middle stem including the platinum electrodes and the crystal can be taken out in one piece.

Figure. 8.

THE TUBE FURNACES.

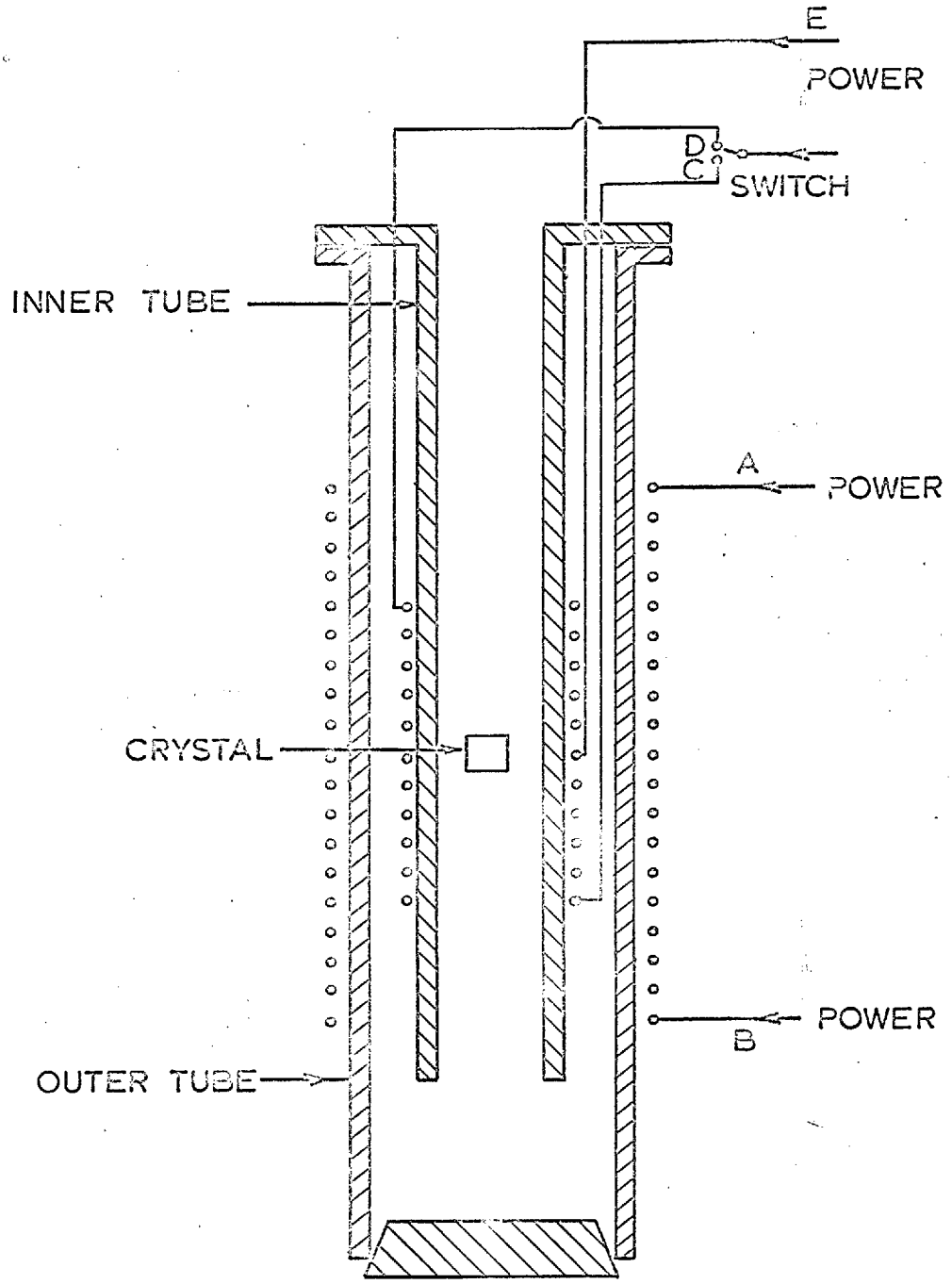

Figure. 9.

THE CRYSTAL IN POSITION IN THE SILICA JIG.

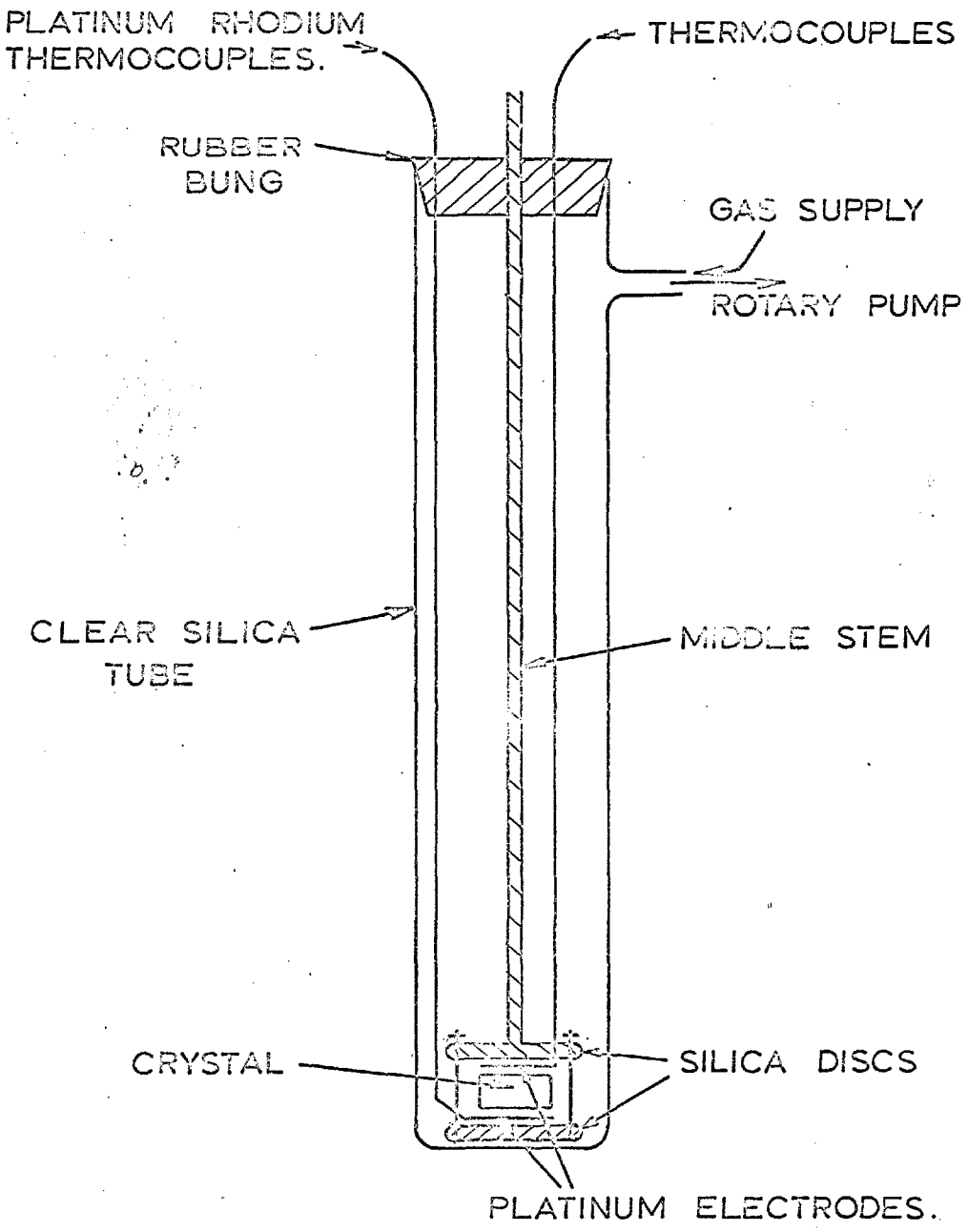

detect surface damage. With good specimens damage is done only at the corner where the razor blade has been in contact. The satisfactory specimen is then transferred to the jig ready for the experiment.

VII. 2 THE APPARATUS

A vertical tube furnace is used. The outer tube is of fused alumina, and it is about 70 inches long with an inside diameter of 3 inches. About 55 inches of the middle section i wound by gauge 20 michrome wires. The total resistance of the heating element is about 60 Ω. Within this tube is an inner tube of fused alumina. The inner tube is wound in two equal sections, as is shown in Figure (8). Each section has a resistance of about 40 Ω. The crystal sits in between these two sections and it is found by trial and error that the separation between the ends of the two sections should not be more than 1 inch apart to produce the required maximum temperature gradient of 10^{o}C per cm. By passing a current through either the top or the bottom windings, a thermal gradient can be established in one direction or its reverse. The maximum current allowed through the sections is about 1 ampere. This is to ensure that the thermal gradient can be altered fast enough.

The outer tube is surrounded by laggings contained in a box 40 inches square and 60 inches high. This large amount of

laggings is needed to maintain temperature stability, especially as the experiments have to be carried out through the night and the temperature drop in the room is quite significant.

Both alternating currents and direct currents are used to drive the furnace. The over-all temperature is controlled by an "Ether" type anticipator controller, which only controls the current of the outer tube. An additional circuit is introduced in parallel to the windings for better control. The average fluctuation is controlled to $\pm\frac{1}{2}^{o}C$ in a period of half an hour. The current passing through this outer tube varies from 2 amperes to 4 amperes when the temperature is between $600^{o}C$ to $800^{o}C$.

The jig is made of clear silica and is constructed as shown in Figure (9). The middle stem holds the crystal and it can be slid in and out of the silica tube. The electrodes are platinum foils of roughly 1 mm. thick. They are backed onto silica discs. Platinum-platinum 13% rhodium thermocouples are used both to measure both ends of the crystal and to act as leads to measure the potential developed across the crystal.

The silica tube is surrounded by an earthed stainless-steel pipe. All the leads outside are screened.

Temperatures are taken with respect to a water-ice mixture at $0^{o}C$. A high impedance digital valve-voltmeter is used. The input impedance of the voltmeter is more than 50 MΩ,

and it is capable of reading to within ± 0.0025 mV.

The Tinsley potentiometer is used to measure the voltage developed across the crystal. It is capable of detecting a voltage of 0.1 uV. It has a reversing switch which eliminates the thermal potentials of the measuring instrument. The potential difference set up in the potentiometer wire is maintained by an A.C. mains-operated device which employs a Zener diode to maintain voltage stability.

The current from the crystal to offset the null detector must necessarily be small. Therefore a Tinsley-made D.C. amplifier is used to amplify the current going through the galvanometer.

VII. 3 EXPERIMENTAL PROCEDURES AND OBSERVATIONS.

The pure NaCl single crystal is placed in between the electrodes, and they are lowered into the silica jig. The air in the jig is evacuated with a rotary pump. The pressure in the jig is reduced to about 10^{-2}mm Hg, or lower. It is then filled with high purity, water vapour-free argon. This procedure is carried out on the average six times.

The temperature of the crystal is brought up over a period of four or five hours from room temperatures to 600°C. It is then maintained at this temperature for twelve to fifteen hours. After this time it is raised to over 730°C and maintained at this temperature for four or five hours.

Then it is brought down to about 620°C at a rate of about 5°C per minute and maintained at this temperature for two to three hours before readings are taken.

The digital valve voltmeter is used to give an indication of the voltage developed across the crystal. The approximate position on the potentiometer is then set, and the actual readings are taken. It is ensured that no currents flow from the crystal.

If the temperature of the specimen is brought up from room temperature to 600°C and readings are immediately taken, it is found that, without any thermal gradient on, the potential difference between the ends of the crystal varies between 20 to 80 mV. This potential fluctuates violently. After annealing at about 600°C for about twelve to fifteen hours, the thermopower is found to have an unsteady value of between 2 to 3 mV/°C. This drops fairly rapidly at a rate of about 0.03 mV/°C/minute. After about twenty-four hours at 600°C, the thermopower is between 0.6 to 0.8 mV/°C; the readings still fluctuate. All this time, there is a potential at zero gradient.

Consistent reproducible readings are obtained by the following procedure. After an overnight anneal at 600°C the temperature is brought up to about 730°C and held for four or five hours. It is then brought down rapidly to about 620°C, and readings are taken after two or three hours.

At each temperature, the thermal gradient is varied from $0^{o}C/cm$ to $\pm 6^{o}C/cm$. The potential differences are then plotted against the temperature differences. Within this range of thermal gradients the plot of the potential differences against the temperature differences are extremely good linear plot. Only four points are needed for each plot. [See Figure (10)]. At more than about $\pm 10^{o}C/cm$ the linearity of the plots is lost. After a large gradient has been imposed on to the crystal, there is no deviation from linearity when small gradients are once again used.

As reported by Christy et al [9] and Allnatt and Chadwick [4], there is a finite [illegible] intercept on the individual plots of potential difference against temperature difference. [See Figure (10)]. However, unlike Allnatt and Chadwick [4] the plot of the intercept against the temperatures does not correspond to any good straight line.

Below about $600^{o}C$ the pure NaCl specimen has a resistance of about 10^{5} [illegible]. This resistance is too high for the potential to be measured with the use of the potentiometer. Below a temperature of about $620^{o}C$ the readings are not considered seriously for the final analysis. Readings are taken at an interval of between $10^{o}C$ to $15^{o}C$ from about $600^{o}C$ to about $790^{o}C$. Altogether about seven runs are done to complete the whole temperature range.

Figure 10 Graph of ΔV against ΔT. This is a typical plot of the measured potential difference against the temperature difference across the NaCl crystal. Only five points are needed. The points lie on a very good straight line. Note that the straight line does not pass through the origin. The total thermopower is equal to the gradient.

Figure 11 Graph of thermopower of pure NaCl vs temperature. The specimens for different runs are different, although they are all cleaved from the same boule. The low values at between 870°K to 900°K are probably due to the difficulties encountered in the measurements since at these temperatures the resistance of the crystal becomes very large. The size of the points indicate the error in the values of the thermopower.

Figure 12 Graph of thermopower of NaCl against temperature. The measurements of the pure NaCl is done by the author. The two dotted straight line graphs are from Allnatt and Chadwick (4).

Figure. 10.

GRAPH OF ΔV AGAINST ΔT

TEMPERATURE 771°C.

POWER −1·14 mV/°C.

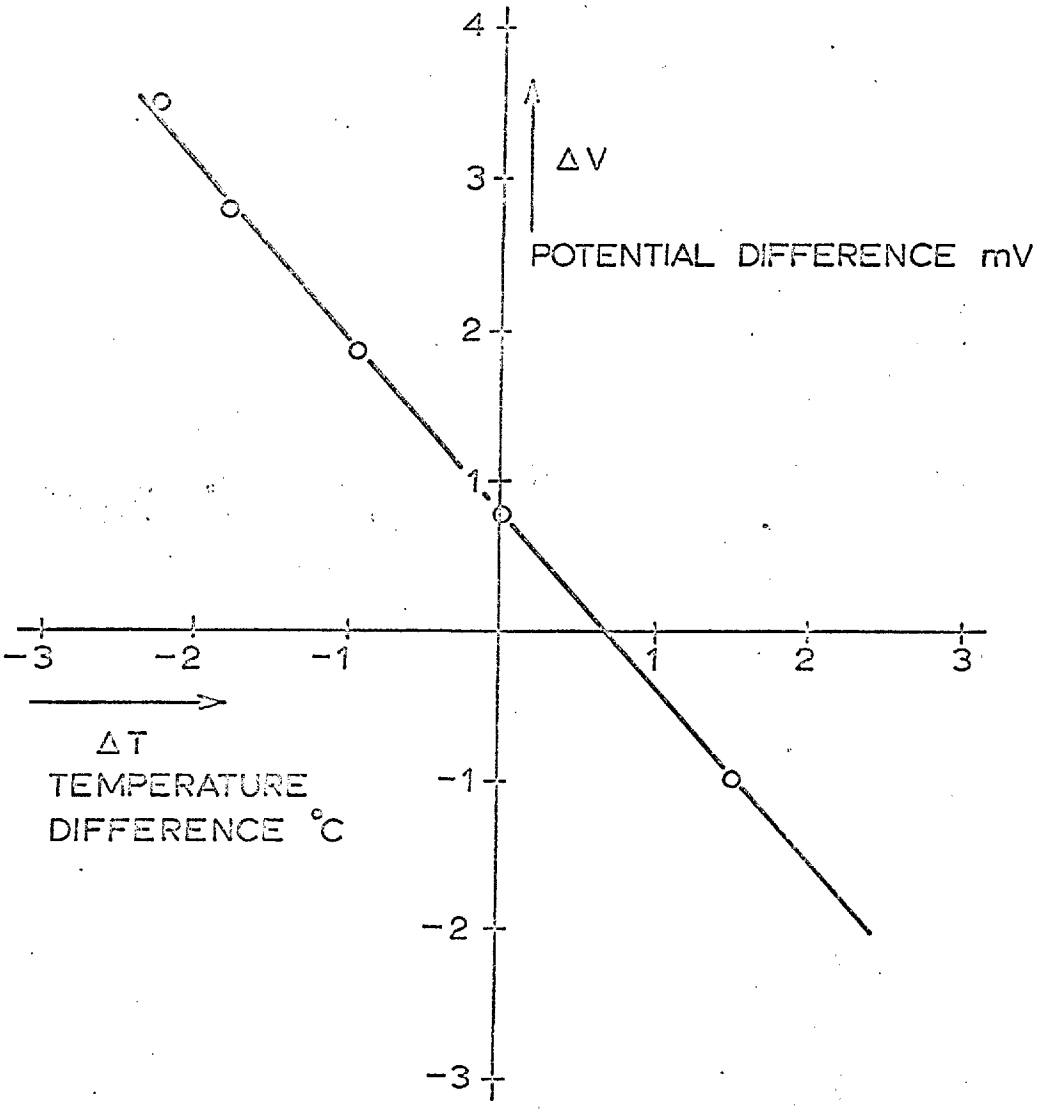

Figure. 11.

GRAPH OF THERMOPOWER OF PURE Na Cℓ AGAINST TEMPERATURE.

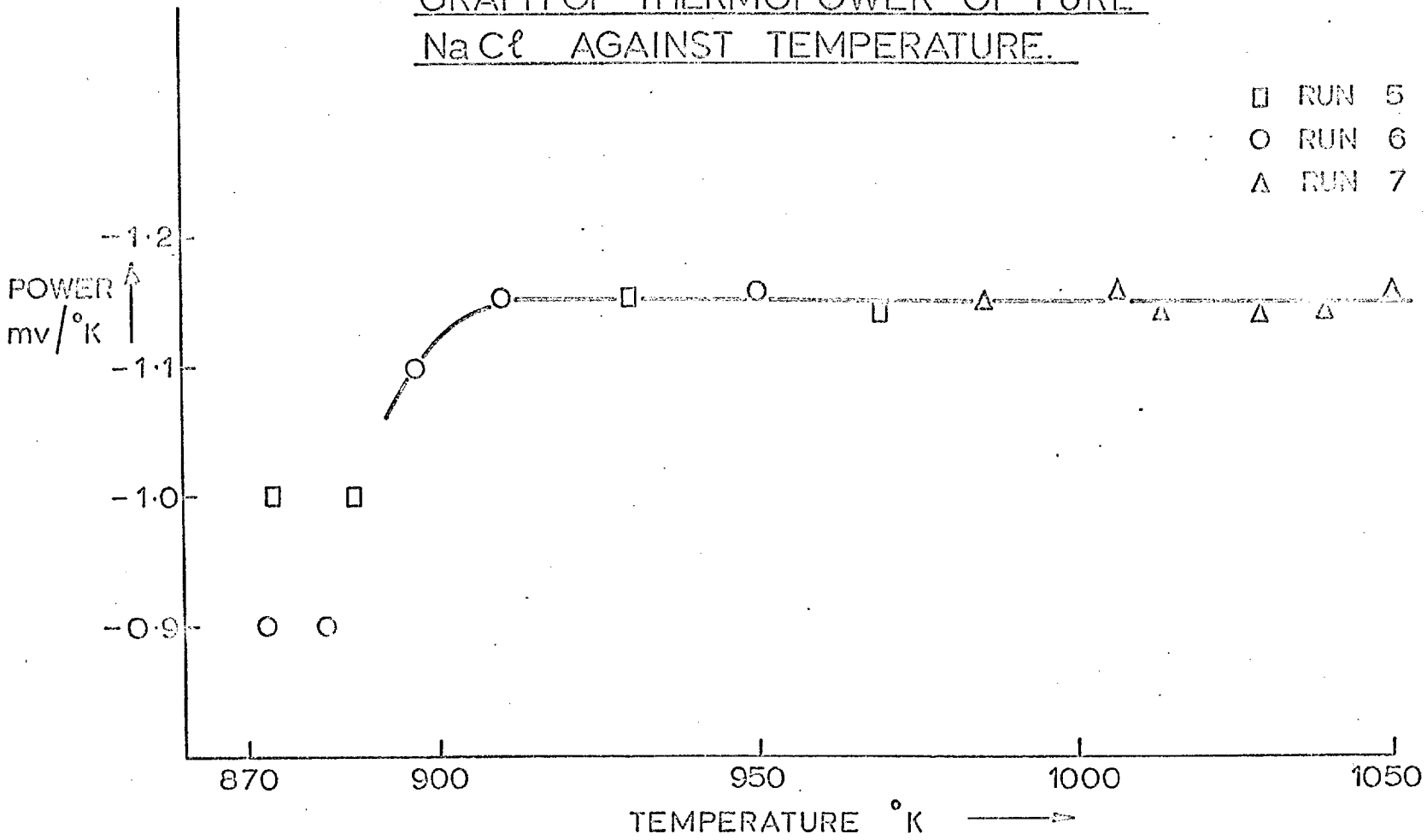

Figure. 12.

GRAPH OF THERMOPOWER OF NaCℓ AGAINST TEMPERATURE

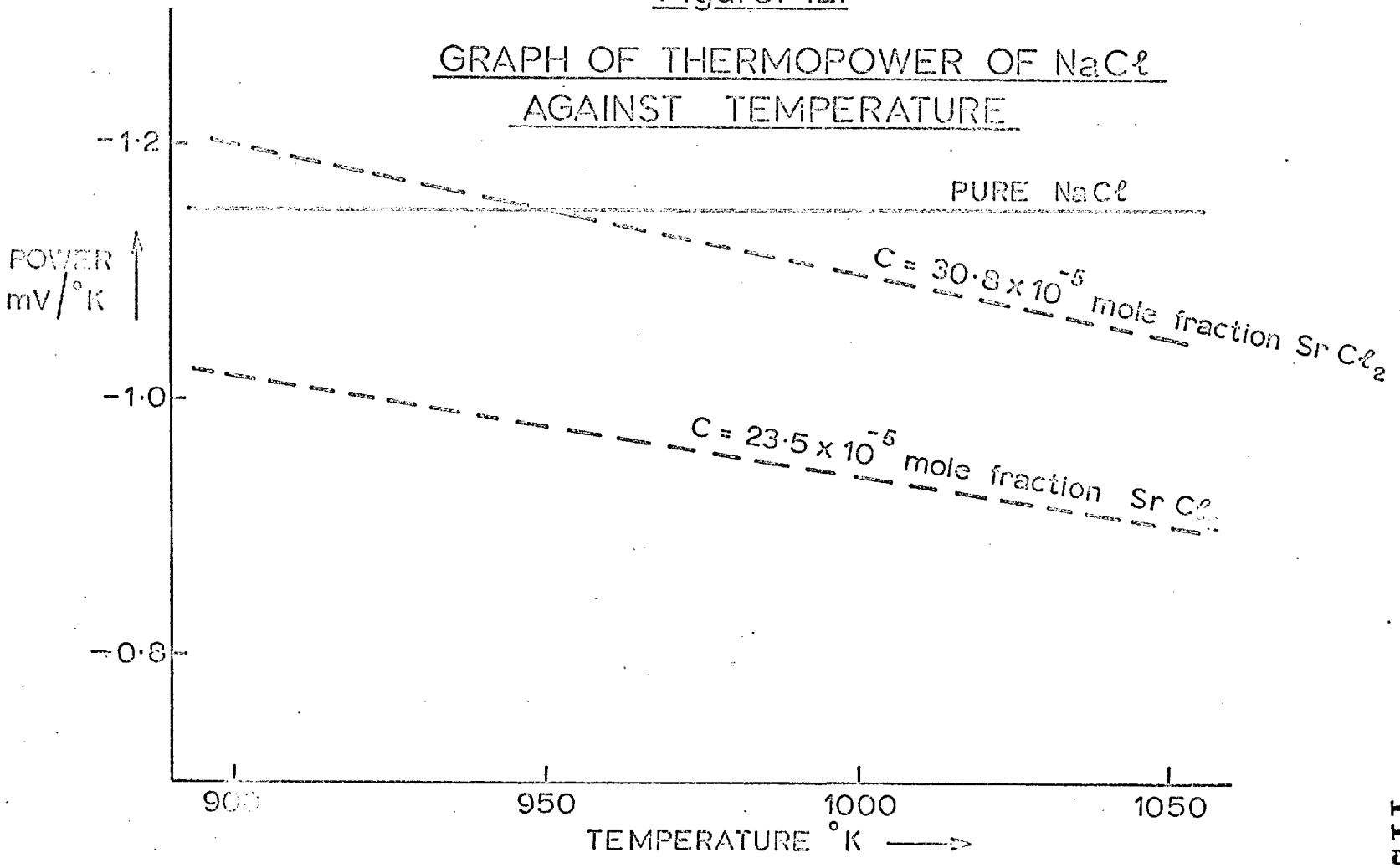

VII.4 RESULTS AND ANALYSIS.

The thermoelectric power of pure NaCl crystal in the temperature range of about 870°K and 1060°K is summarised in the graph in Figure (11). Between 900°K and 1060°K the measured thermopower is -1.15 ± 0.05 mV/°K.

VII.4.1 THE NO-TRAP MODEL ANALYSIS.

The no-trap model of Section (II.4) predicts that the heterogeneous thermopower is zero and therefore the measured thermopower is just the homogeneous thermopower, which is, from Equation (II.14), for a pure crystal:

$$e\Theta = -\frac{h_s}{2T} + \frac{\{(h_s - Q_+^{\ddagger}) + \phi\, Q_-^{\ddagger}\}}{(1+\phi)\,T} - S_e^{M^1} \qquad \ldots\ (VII.1)$$

where for a pure crystal $n_{(+)} = n_{(-)}$ and $\frac{\text{Grad } n(-)}{n_{(-)}} = + \frac{h_s}{2kT^2}\,\text{Grad } T$ has been substituted, and $S_e^{M^1}$ is defined in Equation (II.31).

From the results of Chapter (VI) the heats of transport are given by

$$Q_{\pm}^{\ddagger} = (2 + {}^{q_{\pm}}/_{T})\, E_{(\pm)} \qquad \ldots\ (VII.2)$$

Substituting Equation (VII.2) into Equation (VII.1) and re-arranging the resultant equation, q+ and q- are found to be given by:

$$q- = \frac{[F(T_1)-F(T_2)]}{\{[\phi(T_1)-\phi(T_2)] \quad E_{(-)}\}}$$

$$q+ = \phi(T_1)\ q-E_{(-)} - F(T_1) \qquad \text{.... (VII.3)}$$

where T_1 and T_2 are the temperatures,

$\phi \equiv \phi(T)$, the mobilities of the anion vacancy over the cation vacancy,

$$F(T) = T\left\{(e\theta_0 T + h_s/2)\cdot[1+\phi(T)] + [2E_{(+)}-2E_{(-)}\phi(T)-h_s]\right\},$$

and $\theta_0 = \theta + S_e^{M^1}/e$

Analysing the experimental results, as summarised in the graph in Figure (12), and using the following data:

$\phi(T)$ is obtained from Tubandt's[79] measurements of the transport numbers and is given by

$$\phi(T) = 4.275 - 6.76 \times 10^3/T + 2.68 \times 10^6/T^2$$

h_s = 2.12 eV from Dreyfus and Nowick [70]

$E_{(+)}$, the cation activation energy = 0.69 eV from Kirk and Pratt [80]

$E_{(-)}$ = 0.91 eV from Barr and Morrison [81].

The results of the analysis are summarised in Table (7).

VII.4.2 HOWARD'S MODEL ANALYSIS

The results of the measurements of the thermopower of pure NaCl conducted by the author compare favourably with those of Allnatt and Chadwick [4]. However, Allnatt and Chadwick also measure the thermopower of NaCl doped with

2.35×10^{-4} and 3.08×10^{-4} mole fraction of $SrCl_2$. Using their results of the doped specimens and the author's pure specimens, an analysis is carried out using Howard's model of the irreversible electrode-crystal thermopower. Howard's model predicts that the difference between the thermopower of the doped and pure crystal, $\Delta\theta(\eta)$, is given by [from Equation (II.21)]

$$\Delta\theta(\eta) = \frac{1}{eT}\frac{\phi}{(1+\phi)}\frac{(\eta^2-1)}{(\eta^2+\phi)}\left[h-Q_+^{*}-Q_-^{*}\right] + \frac{kT}{e}\cdot\frac{1}{\eta}\frac{\partial}{\partial T}\eta \quad \ldots\ldots \text{(VII.4)}$$

where ΔS_R of Equation (II.21) has been put equal to zero as suggested by Lidiard and Howard (38).

Substituting Equation (VII.2) into Equation (VII.4), and rearranging the terms, the following equation is obtained

$$E_{(+)}\, q+ + E_{(-)}\, q- = T\left[(h_s - 2E_{(+)} - 2E_{(-)}) - W\right] \ldots\ldots \text{(VII.4)}$$

where $W = \frac{eT(1+\phi)}{\phi}\frac{(\eta^2+\phi)}{(\eta^2-1)}\left[\Delta\theta(\eta) - \frac{kT}{e}\frac{1}{\eta}\frac{\partial n}{\partial T}\right]$

At high temperatures, when the anion vacancy-cation vacancy association can be neglected,

$$\eta = \frac{C}{2C_o} \pm \sqrt{1+(C/2C_o)^2} \qquad \text{[See Lidiard (1)]}$$

C is the impurity concentration

and $C_o = e^{-\Delta g/2kT} = e^{\Delta S/2k}\, e^{-h_s/2kT}$

For NaCl $\Delta S/k$ is 6.20 $^{o}K^{-1}$ [From Dreyfus and Nowick (70)]

Table 7 The No-Trap Analysis. Using the No-Trap theory, the graph in Figure (11) is analysed to produce the heats of transport, $Q^{*} = (2 + q/T)E$. The values of q+ and q- are shown.

Table 8 Howard's Model Analysis. Using Howard's theory, the graph in Figure (12) is analysed.

TABLE 7

THE NO TRAP ANALYSIS

T_1 °K	T_2 °K	q_+ °K	q_- °K
900	920	-72.1	-2029.7
920	940	-120.8	-1845.2
940	960	-185.4	-1629.6
960	980	-256.6	-2107.9
980	1000	-319.7	-1636.5
1000	1020	-399.5	-1751.2
1020	1040	-486.5	-2152.2
1040	1060	-548.2	-2369.9

TABLE 8

HOWARD'S MODEL ANALYSIS.

	23.5×10^{-5} Mole-fraction of $SrCl_2$		30.8×10^{-5} Mole-fraction of $SrCl_2$	
T^oK	$mV/^oK$	$\frac{q_+E_{(+)}+q_-E_{(-)}}{eV^oK}$	$mV/^oK$	$\frac{q_+E_{(+)}+q_-E_{(-)}}{eV^oK}$
900	0.13	-16.5×10^3	-0.050	-14.4×10^3
940	0.17	-10.4×10^3	-0.005	-10.3×10^3
980	0.21	-9.3×10^3	0.04	-8.3×10^3
1000	0.21	-8.5×10^3	0.05	-7.5×10^3
1040	0.26	-7.8×10^3	0.09	-6.6×10^3

VII.4.3 DISCUSSIONS

The results of the analysis using the No Trap theory are summarised in Table (7). The analysis covers the measurements of pure NaCl between 900°K and 1050°K. At each temperature, a temperature range, $(T_2 - T_1)$°K, of 20°K is used.

Both q+ and q- are negative in agreement with both the prediction of the heat of transport theory of Chapter (VI), and the results of the measurements on AgBr and AgCl [(6) and See Chapter (VI)]. However both q+ and q- show a strong temperature-dependence.

Table (8) summarises the results of the analysis using Howard's Model. Howard's Model only predicts the value of $E_{(+)}$ q+ + $E_{(-)}$ q-. No further breakdown of the quantity is possible. Table (8) shows that $E_{(+)}$ q+ + $E_{(-)}$ q- is negative, agreeing with the results of Chapter (VI). It is also temperature- and impurity concentration-dependent.

On the basis that the theory of the heats of transport developed in Chapters (III), (IV) and (VI) is correct, the analyses summarised in Tables (7) and (8) suggest that the irreversible electrode-crystal thermopower is both temperature- and impurity concentration-dependent. The failure of the No-Trap analysis suggests further that should the electrons be actually transferred across the electrode-crystal interface, they will be captured by some form of traps in the crystal.

CHAPTER VIII

DISCUSSIONS, CONCLUSIONS AND SUGGESTIONS FOR FUTURE WORK

VIII.1 DISCUSSIONS

VIII.1.1 THE THERMOELECTRIC POWER

The successful analysis of the alkali-halides' thermopower measurements depends on both an adequate knowledge of the irreversible electrode-crystal thermopower, and an adequate theory of the heats of transport.

All the theories of the irreversible electrode-crystal thermopower assume that the electrons are responsible for the heterogeneous thermopower. Jacobs and Maycock (11) suggest that the electrons wander about the crystal-electrode interface, Howard (13) suggests that the electrons are trapped at the crystal surface by the formation of the metal phase. Allnatt and Jacobs (14) assume that the electrons are trapped by the anion vacancies in the crystal to form F-centres. The No Trap theory studied in Chapter (II) explores the possibility that the electrons may enter into the crystal and not fall into any traps at all. All these theories have been found to be unsatisfactory.

It is not possible, at present to explain definitely the behaviour of the electrical potential developed across the

crystal when a temperature difference is first imposed. This is because it is not known whether the phenomenon observed is a crystal-electrode, or a purely crystal, effect.

VII.1.2 THE HEATS OF TRANSPORT

The work on the heats of transport done here uses a vastly different approach from that used by Wirtz (16) in his original kinetic theory. A simple linear chain model is used, and by studying the jumping process in this model, the heats of transport are successfully related to the dynamics of the lattice. Quantitative values are obtained by studying the forces operating between the alkali halide ions.

The results of the lattice calculations are most satisfying in terms of the agreement between the calculated and the experimental sublimation energies and the Schottky pair formation energies. From the lattice calculations, the forces operating between the ions and some of the physical properties of the vacancy, e.g. the relaxations of the surrounding ions, are known.

By an extension of the lattice calculations, the force constants binding the ion to its neighbours in the linear chain, is found. This is done specifically for NaCl and KCl. Subsequently, quantitative values for the anion and cation heats of transport of these two crystals are found. Unfortunately, these values cannot be compared with the results of

the alkali halide thermopower measurements as it is not possible to analyse these results since no adequate irreversible electrode-crystal theory is available. However, comparing the predicted relationship between the heats of transport and the activation energies of the alkali halides, and the experimental values of the Ag vacancies in AgCl and AgBr, the general agreement is good. But it is not possible to make a detailed direct comparison as in the final analysis of the experiments on AgCl and AgBr, an entropy term is present which cannot be eliminated since there is no data on the entropy of formation of a vacancy.

VIII.2 CONCLUSIONS

The total thermopower of single crystal, pure NaCl is -1.15 ± 0.05 mV/°C in the temperature range of 900°K and 1060°K.

No adequate theory of the irreversible electrode-crystal thermopower is known.

The theoretical heats of transport for an ion in the alkali-halide crystal is about one and a half to two times the corresponding activation energies at normal temperatures for which diffusion experiments are carried out.

For NaCl, the heat of transport is

$(2 - 25.7/T)E^{NaCl}_{Na^+}$ for Na^+ ions,

and $(2 - 21.7/T)\ E^{NaCl}_{Cl^-}$ for Cl^- ions.

For KCl, it is

$(2 - 32.5/T)\ E^{KCl}_{K^+}$ for K^+ ions,

and $(2 - 35.2/T)\ E^{KCl}_{Cl^-}$ for Cl^- ions,

where the E's are the respective activation energies for diffusion.

VIII.3 SUGGESTIONS FOR FUTURE WORKS.

An adequate theory for the irreversible electrode-crystal thermopower need to be developed. It might be possible to develop a reversible electrode for the alkali-halides, e.g. a chlorine electrode for NaCl. This might be done by saturating a porous carbon electrode with a stream of chlorine gas.

Quantitative values for the heats of transport for Ag^+ vacancy in AgCl and AgBr can be calculated. Lattice calculations for these two salts will have to be done. It is then possible to find the entropy of vacancy formation quantitatively from a study of the vibrational modes of the crystals.

From the knowledge of the relaxations of the ions surrounding the vacancies, it should be possible to compare the theoretical values with that found by density measurements.

It is interesting to investigate whether the saddle-point configuration of the transition state theory exists. If so, it should be possible to determine the life-time of the jumping ion in this configuration. This can be done by an extension of the method used for calculating the force constant.

APPENDIX I

EVALUATION OF THE INTEGRALS S_1 AND S_2

$$S_1 = N\int_{0}^{\pi/2}\{\operatorname{Cosec}^2\phi - 1\}\,d\phi + N\int_{-\pi/2}^{0}\{\operatorname{Cosec}^2\phi + 2\sin 3\phi \operatorname{Cosec}\phi + 1\}\,d\phi$$

$$= 2N\int_{-\pi/2}^{0}\frac{\sin 3\phi}{\sin\phi}\,d\phi$$

$$= N\pi$$

$$S_2 = N\int_{0}^{\pi/2}\{\cos\phi\operatorname{Cosec}^2\phi - \cos\phi\}\,d\phi + \int_{-\pi/2}^{0}\{\operatorname{Cosec}^2\phi\cos\phi + \cos\phi + 2\cos\phi\sin 3\phi\operatorname{Cosec}\phi\}\,d\phi$$

$$= I_1 - 2N$$

$$I_1 = 2N\int_{-\pi/2}^{0}\{\cos\phi\cos 2\phi + \frac{\cos^2\phi\sin 2\phi}{\sin\phi}\}\,d\phi$$

$$= {}^{2N}/_{3} + {}^{8N}/_{3}$$

$$S_2 = {}^{4N}/_{3}$$

APPENDIX II

ENERGY OF A SCHOTTKY PAIR

The energy of a Schottky pair, E_S, is defined in the following equations as

$$E_S = E_{T\pm} - \tfrac{1}{2}\,(E_{1\pm} + E_{1\mp})$$

where $E_{T\pm} = \sum_{i=1}^{S} E_{i\pm}$

and $E_{i\pm}$ are defined as follows.

$E_{1\pm}$ This is the energy needed to extract the ion from the rigid non-polarisable lattice. This term comes from Equation (V.11)

$$E_{1\pm} = \frac{\alpha_m (A_e)^2}{r_o} - 6\,\phi^R_{+-}(r_o) - 12\,\phi^R_{+-}(r_o\sqrt{2}) \qquad \ldots\ (A.II.1)$$

where for the BM form

$$\phi^R_{+-}(r) = b(1 + {}^{A}/_{n_+} - {}^{A}/_{n_-}) \exp\left[{}^{(r_+ + r_-)}/_{p}\right] \exp\left({}^{-r}/_{p}\right) - {}^{C_{+-}}/_{r^6} - {}^{D_{+-}}/_{r^8} \qquad \ldots\ (A.II.2)$$

Similar expressions exist for $\phi^R_{+-}(r)$ and $\phi^R_{--}(r)$.

For the BMV form Equation (A.II.2) holds only for $r > r_o$; for $r < r_o$ it becomes

$$\phi^R_{+-}(r) = B_1 + {}^{B_2}/_{r^{12}} - {}^{C_{+-}}/_{r^6} - {}^{D_{+-}}/_{r^8}$$

α_m is the Madelung Constant and is 1.7476 for the NaCl structure.

$E_{2\pm}$

This is the polarisation energy of region I due to the effective charge on the vacancy. It comes from the third term of Equation (V.10).

$$E_{2\pm} = -\frac{6\,(A_e)^2}{2r_o{}^4}\,\alpha_{\mp} - \frac{12\,(A_e)^2}{2(\sqrt{2}\,r_o)^4}\,\alpha_{\pm} \qquad \ldots\ldots \quad (A.II.3)$$

where the α's are the polarisabilities.

$E_{3\pm}$

This term can be divided into three parts, i.e.

$$E_3 = E_{3C} + E_{3R} + E_{3P}$$

where $E_{3C} = W_{2C}(x,0)$. It is the Coloumb interactions of the real and effective charges and the vacancy of region I comes from the second and third term in Equation (V.12).

$$E_{3,C} = \frac{6(A_e)^2}{r_o}\left[\frac{(\sqrt{2}+5/4)}{(1+\lambda)} - \frac{4}{[1-(1+\lambda)^2]^{\frac{1}{2}}} - \frac{1}{(2+\lambda)}\right.$$

$$\left. + \frac{4}{(1+\lambda^2)^{\frac{1}{2}}} + \frac{4}{[2+(1+\lambda)^2]^{\frac{1}{2}}} + \frac{4}{[1+(2+\lambda)^2]^{\frac{1}{2}}} + \frac{5\sqrt{2}/4+1+4/\sqrt{6}}{(1+V)}\right.$$

$$\left. - \frac{8}{[1+V^2+(1+V)^2]^{\frac{1}{2}}} - \frac{4}{[V^2+(2+V)^2]^{\frac{1}{2}}}\right]$$

$$- \frac{8}{\left[1+(1+V)^2+(2+V)^2\right]^{\frac{1}{2}}} - \frac{\sqrt{2}}{(2+V)} + \frac{4}{\left[V^2+(1+V)^2\right]^{\frac{1}{2}}} + \frac{4}{\left[1+2(1+V)^2\right]^{\frac{1}{2}}}$$

$$+ \frac{4}{\left[(1+V)^2+(2+V)^2\right]^{\frac{1}{2}}} - \frac{4}{\left[(1+V)^2+(\lambda-V)^2\right]^{\frac{1}{2}}} \frac{-4}{\left[(1+\lambda)^2+2(1+V)^2\right]^{\frac{1}{2}}}$$

$$- \frac{4}{\left[(2+\lambda+V)^2+(1+V)^2\right]^{\frac{1}{2}}} + 8.5/\sqrt{2} - 3.75 - 4/\sqrt{3} - 4/\sqrt{5} + 4/\sqrt{6} \Big] \quad \ldots\ldots (A.II.4)$$

$$E_{3,R} = W_{2R}(x,0) + W_{3R}(x,0;\bar{3},0) - \frac{1}{2}\sum_S \left\{ \bar{3}_S \left[\frac{\partial W_{3R}(x,0;\bar{3},0)}{\partial \bar{3}} \right]_{\bar{3}=\bar{3}_S} \right\}$$

$W_{2R}(x,0)$ comes from the first term of Equation (V.12) and $W_{3R}(x,0;\bar{},0)$ represents the short range interactions of regions I and II and is given by the first term of Equation (V.13).

$$W_2R = 12\, \phi_{\substack{--\\++}} \left[(1+\lambda)\sqrt{2}\right] - 12\, \phi_{\substack{--\\++}} \left[\sqrt{2}\right]$$

$$+ 24\, \phi_{\substack{++\\--}} \left[(1+V)\sqrt{2}\right] - 24\, \phi_{\substack{++\\--}} \left[\sqrt{2}\right]$$

$$+ 24\, \phi_{+-} \left[\sqrt{(\lambda-V)^2+(1+V)^2}\right] - 24\, \phi_{+-} [1] \qquad \ldots\ldots (A.II.5)$$

$$W_{3R}(x,0;\bar{\bar{3}},0) = 6\,\phi_{+-}\,[1+\bar{\bar{3}}_4-\lambda] - 6\,\phi_{+-}\,[1+\bar{\bar{3}}_1]$$

$$+24\,\phi_{\substack{--\\++}}\left[\sqrt{(\bar{\bar{3}}3/\sqrt{3}-\lambda)^2+2(1+\bar{\bar{3}}3/\sqrt{3})^2}\right] - 24\phi_{\substack{--\\++}}\left[\sqrt{\bar{\bar{3}}3^2/3+2(1+\bar{\bar{3}}3/\sqrt{3})^2}\right]$$

$$+24\phi_{+-}\left[\sqrt{(1+\frac{2\bar{\bar{3}}5}{\sqrt{5}}-\lambda)^2+(1+\bar{\bar{3}}5/\sqrt{5})^2}\right] - 24\phi_{+-}\left[\sqrt{(1+\frac{2\bar{\bar{3}}5}{\sqrt{5}})^2+(1+\bar{\bar{3}}5/\sqrt{5})^2}\right]$$

$$+24\phi_{+-}\left[\sqrt{2(\bar{\bar{3}}3/\sqrt{3}-V)^2+(1+\bar{\bar{3}}3/\sqrt{3})^2}\right] - 24\phi_{+-}\left[\sqrt{\frac{2\bar{\bar{3}}3^2}{3}+(1+\frac{\bar{\bar{3}}3}{\sqrt{3}})^2}\right]$$

$$+24\phi_{\substack{+-\\-+}}\left[\sqrt{(1+\bar{\bar{3}}_4-V)^2+(1+V)^2}\right] - 24\phi_{\substack{+-\\-+}}\left[\sqrt{(1+\bar{\bar{3}}_4)^2+1}\right]$$

$$+12\phi_{\substack{+-\\-+}}\left[(1+\bar{\bar{3}}8/\sqrt{2}-V)\sqrt{2}\right] - 12\phi_{\substack{+-\\-+}}\left[(1+\bar{\bar{3}}8/\sqrt{2})\ V2\right]$$

$$+48\phi_{\substack{+-\\-+}}\left[\sqrt{(1+\frac{2\bar{\bar{3}}6}{\sqrt{6}}-V)^2+(\frac{\bar{\bar{3}}6}{\sqrt{6}}-V)^2+(1+\bar{\bar{3}}6/\sqrt{6})^2}\right]$$

$$-48\phi_{\substack{+-\\-+}}\left[\sqrt{(1+2\bar{\bar{3}}6/\sqrt{6})^2+\frac{\bar{\bar{3}}^2 6}{6}+(1+\bar{\bar{3}}6/\sqrt{6})^2}\right]$$

$$+12\phi_{+-}\left[\sqrt{(1+\frac{2\bar{\bar{3}}5}{\sqrt{5}}-V)^2+(\bar{\bar{3}}5/\sqrt{5}-V)^2}\right] - 12\phi_{+-}\left[\sqrt{(1+\frac{2\bar{\bar{3}}5}{\sqrt{5}})^2+\bar{\bar{3}}5^2/5}\right]$$

..... (A.II.6)

where $\bar{\bar{3}}_3 = M^1/3$, $\bar{\bar{3}}_4 = -M^1/4$, $\bar{\bar{3}}_5 = M^1/5$

$\bar{\bar{3}}_6 = -M^1/6$, $\bar{\bar{3}}_8 = -M^1/8$.

$E_{3,P}$ is caused by the relaxation of the polarisable ions of region I due to the effective charge at the vacancy.

$$E_{3,P} = -3\alpha_{\mp} \left[\left| \underline{F}_V^{(1)}{}_{\pm}(\lambda) \right|^2 - \left| \underline{F}_{V\pm}^{(1)}(0) \right|^2 \right]$$
$$-6\alpha_{\pm} \left[\left| \underline{F}_{V\pm}^{(2)}(V) \right|^2 - \left| \underline{F}_{V\pm}^{(2)}(0) \right|^2 \right]$$

where the $\underline{F}_V$'s are the fields due to the vacancy.

$$\underline{F}_{V\pm}^{(1)}(\lambda) = \frac{\mp A_e}{r_o^2(1+\lambda)^2} \hat{\underline{x}}$$

$$\underline{F}_{V\pm}^{(2)}(V) = \frac{\mp A_e}{2r_o^2(1+V)^2} \frac{\hat{\underline{x}} + \hat{\underline{y}}}{\sqrt{2}}$$

where $\hat{\underline{x}}$ and $\hat{\underline{y}}$ are the unit vectors from the vacancy along the positive <100> and <010> respectively.

$\underline{E_{4\pm}}$

This term comes from the vacancy and the displacement dipoles of region I being in the fields caused by the electronic dipoles of region II. The fields at different positions have been calculated by Mott and Littleton(64).

$$E_{4\pm} = \frac{-(A_e)^2}{2r_o} \left[4.1977M_{\mp} + 3.3346M_{\pm} \right]$$
$$+ \frac{6(A_e)^2}{2r_o} \lambda \left[0.388M_{\mp} - 0.323M_{\pm} \right]$$
$$- \frac{12(A_e)^2}{2r_o} V\sqrt{2} \left[0.730M_{\mp} + 0.247M_{\pm} \right]$$

.... (A.II.7)

where $M_{\pm} = \mu_{\pm} \times r^2$, and $\mu_{\pm}$ is the electronic dipole caused by the effective charge of the vacancy.

$E_{5\pm}$

The electionic dipoles of region II and the real and effective charges and the vacancy of region I collectively produce a field at each lattice point in region I. The energy of the induced dipoles is given by $E_{5\pm}$. Some of these energy terms have already been dealt with in $E_{3,P}$, and $E_{5\pm}$ contains the remaining terms.

$$E_{5\pm} = -6 \times \tfrac{1}{2}\alpha_{\pm} \{ (F^{(1)}_{V\pm}(\lambda) + F^{(1)}_{D\pm}(\lambda, V) + F^{(1)}_{I\pm}(\lambda,V)) \times (F^{(1)}_{V\pm}(\lambda) + F^{(1)}_{D\pm}(\lambda,V)) - (F_{V\pm}(\lambda))^2 \}$$

$$-12 \times \tfrac{1}{2}\alpha_{\pm} \{ (F^{(2)}_{V\pm}(V) + F^{(2)}_{D\pm}(\lambda,V) + F^{(2)}_{I\pm}(\lambda,v)) \times (F^{(2)}_{V\pm}(V) + F^{(2)}_{D\pm}(2)) - (F^{(2)}_{V\pm}(V))^2 \}$$

$F^{(1)}_{D\pm}(\lambda,V)$ is the field at the relaxed 1,0,0 site in the $\langle 100 \rangle$ direction caused by the real and effective charges of region I.

$F^{(1)}_{I\pm}(\lambda,V)$ is the field at the relaxed 1,0,0 site in the $\langle 100 \rangle$ direction caused by the induced electronic dipoles regions I and II.

$\underline{F}^{(2)}_{D\pm}(\lambda,V)$ and $\underline{F}^{(2)}_{I\pm}(\lambda,V)$ are similarly defined as the field at the relaxed (110) position in the <110> direction.

The full expressions for the fields are

$$\underline{F}^{(1)}_{D\pm}(\lambda,V) = \mp \frac{Ae}{r_o^2}\left[\frac{1.6642}{(1+\lambda)^2} - \frac{1}{(2+\lambda)^2} - \frac{4(1+\lambda)}{[1+(1+\lambda)^2]^{3/2}}\right.$$

$$- \frac{4(\lambda-V)}{[(\lambda-V)^2+(1+V)^2]^{3/2}} + \frac{4\lambda}{[1+\lambda^2]^{3/2}} - \frac{4(1+\lambda)}{[(1+\lambda)^2+2(1+V)^2]^{3/2}}$$

$$\left. + \frac{4(1+\lambda)}{[2+(1+\lambda)^2]^{3/2}} - \frac{4(2+\lambda+V)}{[(2+\lambda+V)^2+(1+V)^2]^{3/2}} + \frac{4(2+\lambda)}{[(2+\lambda)^2+1]^{3/2}}\right]\hat{\underline{x}}$$

.... (A.II.8)

$$\underline{F}^{(2)}_{D\pm}(\lambda,V) = \mp \frac{Ae\sqrt{2}}{r_o^2}\left[\frac{1+2V-\lambda}{[(\lambda-V)^2+(1+V)^2]^{3/2}} - \frac{1+2V}{[V^2+(1+V)^2]^{3/2}}\right.$$

$$+ \frac{2(2V+1)}{[V^2+(1+V)^2+1]^{3/2}} + \frac{2(1+V)}{[V^2+(2+V)^2]^{3/2}} + \frac{3+2V+\lambda}{[(1+V)^2+(2+V+\lambda)^2]^{3/2}}$$

$$- \frac{3+2V}{[(1+V)^2+(2+V)^2]^{3/2}} + \frac{2(3+2V)}{[(2+V)^2+(1+V)^2+1]^{3/2}} + \frac{1}{2\sqrt{2}(2+V)^2} - \frac{1.4538}{(1+V)^2}$$

$$\left. + \frac{2(1+V)}{[2(1+V)^2+(1+\lambda)^2]^{3/2}} - \frac{2(1+V)}{[1+2(1+V)^2]^{3/2}}\right](\hat{\underline{x}}+\hat{\underline{y}})\frac{1}{\sqrt{2}} \quad \text{.... (A.II.9}$$

$$\underline{F}^{(1)}_{I\pm}(\lambda,V) = \left\{ -\frac{2\sqrt{2}}{r_o^3} \alpha_{\pm} f(\lambda,V) \left[\underline{F}^{(2)}_{V\pm}(\lambda) + \underline{F}^{(2)}_{D\pm}(\lambda,V) \right.\right.$$

$$\left. + \underline{F}^{(2)}_{I\pm}(\lambda,V) \right] - \frac{\alpha_{\mp}(1+6\sqrt{2})}{4r_o^3(1+\lambda)^3} \left[\underline{F}^{(1)}_{V\pm}(\lambda) + \underline{F}^{(1)}_{D\pm}(\lambda,V) + \underline{F}^{(1)}_{I\pm}(\lambda,V) \right]$$

$$\left. \pm \frac{A_e}{r_o^2} \left[0.388\ M_{\mp} - 0.323\ M_{\pm} \right] \right\} \hat{\underline{x}} \qquad \ldots\ (A.II.10)$$

$$\underline{F}^{(2)}_{I\pm}(\lambda,V) = \left\{ \frac{-\alpha_{\mp}\sqrt{2}}{r_o^3} f(\lambda,V) \left[\underline{F}^{(1)}_{V\pm}(\lambda) + \underline{F}^{(1)}_{D\pm}(\lambda,V) + \underline{F}^{(1)}_{I\pm}(\lambda,V) \right] \right.$$

$$- \frac{2.7071}{r_o^3(1+V)^3} \alpha_{\pm} \left[\underline{F}^{(2)}_{V\pm}(\lambda) + \underline{F}^{(2)}_{D\pm}(\lambda,V) + \underline{F}^{(2)}_{I\pm}(\lambda,V) \right] \pm \frac{A_e}{r_o^2}$$

$$\left. \left[0.730\ M_{\mp} + 0.247\ M_{\pm} \right] \right\} \qquad (\hat{\underline{x}} + \hat{\underline{y}}) \frac{1}{\sqrt{2}} \qquad \ldots\ (A.II.11)$$

where $f(\lambda,V) = \dfrac{6(1+V)(1+\lambda)}{\left[(1+\lambda)^2+2(1+V)^2\right]^{5/2}} + \dfrac{3(3+\lambda+2V)(2+\lambda+V) - (1+V)^2 - (2+\lambda+V)^2}{\left[(2+\lambda+V)^2 + (1+V)^2\right]^{5/2}}$

$$+ \frac{(1+V)^2+(\lambda-V)^2+3(1+2V-\lambda)(\lambda-V)}{\left[(\lambda-V)^2 + (1+V)^2\right]^{5/2}}$$

THE ELASTIC CONTRIBUTIONS.

The elastic strength of the vacancy modifies the displacement dipoles of region II as follows:

(a) In $E_{3,R}$ the displacements $\vec{3}$'s are modified so that

$$\vec{3}_3 = \frac{M^1+k}{3} \ , \ \vec{3}_4 = \frac{k-M^1}{4} \ , \vec{3}_5 = \frac{k+M^1}{5} \ , \ \vec{3}_6 = \frac{k-M^1}{6} \ ,$$

$$\vec{3}_8 = \frac{k-M^1}{8} \ .$$

(b) In E_4, the electronic dipoles are modified so that M_- becomes M_-+k and M_+ becomes M_+-k.

(c) In E_5, the dipole fields, $\underline{F}_{I\pm}$'s, which contains M_+ and M_- are similarly modified.

APPENDIX III

FORCE ON THE NEXT NEAREST NEIGHBOUR.

Take the ion at 1,1,0 as the specimen ion. Let its displacement from 1,1,0 in the <110> direction be $\sqrt{2}\, V^1 r_0$. The other eleven second neighbour ions have displacements $\sqrt{2}\, V\, r_0$. As usual, the six first neighbour ions are displaced a distance λr_0. The energy, E, of the vacancy is then

$$E = E(\lambda, v, V^1).$$

Then $-\frac{1}{r_0\sqrt{2}} \frac{\partial E}{\partial V^1}$ is the force on the 1,1,0 ion in the positive <110> direction [from the vacancy to the 1,1,0 ion].

The relevant energy terms [i.e. those which are functions of V^1] corresponding to those of Appendix (II) are given below. E_1 and E_2 [of Appendix II] contain no terms of present interest.

E_3

$$E_{3,c} = -\frac{A_e}{r_0^2}\left[\frac{2}{[(\lambda-V^1)^2+(1+V^1)^2]^{\frac{1}{2}}} - \frac{2}{[V^{1\,2}+(1+V^1)^2]^{\frac{1}{2}}}\right.$$

$$+\frac{2}{[(1+\lambda)^2+(1+V^1)^2]^{\frac{1}{2}}} - \frac{2}{\sqrt{1+2(1+V^1)^2}} + \frac{2}{\sqrt{2+V^1+\lambda)^2+(1+V^1)^2}}$$

$$\left. - \frac{2}{[(1+V^1)^2+(2+V^1)^2]^{\frac{1}{2}}} - \frac{4}{[(V^1-V)^2+(1+V^1)^2+(1+V\ )^2]^{\frac{1}{2}}}\right.$$

$$+\frac{4}{[v^{12}+(1+v^1)^2+1]^{\frac{1}{2}}}-\frac{2}{[(v^1-v)^2+(2+v^1+v)^2]^{\frac{1}{2}}}+\frac{2}{[v^{12}+(2+v^1)^2]^{\frac{1}{2}}}$$

$$-\frac{4}{[(1+v^1)^2+(2+v^1+v)^2+(1+v)^2]^{\frac{1}{2}}}+\frac{4}{[(1+v^1)^2+(2+v^1)^2+1]^{\frac{1}{2}}}$$

$$-\frac{1}{(2+v+v^1)/2}+\frac{1}{(2+v^1)/2}+\frac{1}{(1+v^1)/2}\Big]$$

$$W_{2,R}=2\phi_{+-}\left[\sqrt{(\lambda-v^1)^2+(1+v^1)^2}\right]+4\phi_{\underline{++}}\left[\sqrt{(v^1-v)^2+(1+v^1)^2+(1+v)^2}\right]$$

$$W_{3,R}=2\phi_{+-}\left[\sqrt{2(v^1-\sqrt[3]{3}/\sqrt{3})^2+(1+\sqrt[3]{3}/\sqrt{3})^2}\right]$$

$$+2\phi_{\pm\pm}\left[\sqrt{1+\sqrt[3]{4}-v^1)^2+(1+v^1)^2}\right]+2\phi_{+-}\left[\sqrt{(1+\frac{2\sqrt[3]{5}}{\sqrt{5}}-v^1)^2+(v^1-\sqrt[3]{5}/\sqrt{5})^2}\right]$$

$$+\phi_{\pm\pm}\left[(1+\sqrt[3]{8}/\sqrt{2}-v^1)\sqrt{2}\right]+4\phi_{\underline{++}}\left[\sqrt{(1+\frac{2}{\sqrt{6}}\sqrt[3]{6}-v^1)^2+(\sqrt[3]{6}/\sqrt{6}-v^1)^2+(1+\sqrt[3]{6}/\sqrt{6})^2}\right]$$

.... (A.III.1)

where $\bar{3}_3=M^1/3$, $\bar{3}_4=-M^1/4$, $\bar{3}_5=M^1/5$, $\bar{3}_6=-M^1/6$, $\bar{3}_8=-M^1/8$

$$E_{3,P}=-\tfrac{1}{2}\alpha\pm\;|\;\underline{F}_{V1\pm}|^2$$

where $\underline{F}_{V1\pm}=-\dfrac{A_e}{2r_o^2(1+v^1)^2}\;\dfrac{(\hat{\underline{x}}+\hat{\underline{y}})}{\sqrt{2}}$ .... (A.III.2)

$\underline{E_4}$

$$E_{4\pm}=-\frac{(A_e)^2}{\sqrt{2}\;r_o}\;\left[0.730\;M_{\mp}+0.247\;M_{\pm}\right]$$ .... (A.III.3)

E_5

Owing to the difference in the displacement of the 1,1,0 ion from the displacements of the other 1,1,0 type ions, the respective region I fields are no longer symmetric. For example, at the 1,0,0 ion site the field, $\underline{F}_{D\pm}(\lambda,V)$, which is caused by the real and effective charges of region I, is no longer effectively in the <100> direction. In the same way, the magnitude of the similar field at $\bar{1},0,0$ is different from that at 1,0,0. The asymmetry of the $\underline{F}_D$ fields are reflected in the $\underline{F}_{I\pm}$ fields. ($\underline{F}_I$ fields are caused by the induced dipoles of the region I ions).

The region I ions can be divided into eight groups such that within each group the equivalent fields bear some sort of simple relation at different ion sites. The ions in each group are:

Groups 1: 1,1,0 the specimen ion.

2: $1,0,1$, $1,0,\bar{1}$, $0,1,1$, $0,1,\bar{1}$

3: $1,\bar{1},0$, $\bar{1},1,0$

4: $0,\bar{1},\bar{1}$, $0,\bar{1},1$, $\bar{1},0,\bar{1}$, $\bar{1},0,1$

5: $\bar{1},\bar{1},0$

6: $1,0,0$, $0,1,0$

7: $0,0,1$, $0,0,\bar{1}$

8: $\bar{1},0,0$, $0,\bar{1},0$

See Figure (6) .... (A.III.4)

The fields at different ion sites are then represented by the following revised symbols:

$F_V(a,b,x)$, $F_D(a,b,x)$, $F_I(a,b,x)$

where 'a' represents the group which the ion belongs to, 'b' represents the particular ion in the group, and 'x' represent the directional component of the fields.

For example the y component of the F_D field at the (011) ion site [the third ion in group 2; see Expression (A.III.4)] is represented by $F_D\ (2,3,y)$.

The relationship between the F_D fields at different ion sites of group 2 is given by the following equations:

$$\underline{F}_D\ (2,2,x) = \underline{F}_D\ (2,1,x)$$

$$\underline{F}_D\ (2,2,y) = \underline{F}_D\ (2,1,y)$$

$$\underline{F}_D\ (2,2,z) = -\underline{F}_D\ (2,1,z);$$

$\underline{F}_D\ (2,3,x) = \underline{F}_D\ (2,1,y)$, $\underline{F}_D\ (2,3,y) = \underline{F}_D\ (2,1,x)$,
$\underline{F}_D\ (2,3,z) = \underline{F}_D\ (2,1,z)$; $\underline{F}_D\ (2,4,x) = \underline{F}_D\ (2,1,y)$,
$\underline{F}_D\ (2,4,y) = \underline{F}_D\ (2,1,x)$, $\underline{F}_D\ (2,4,2) = -\underline{F}_D(2,1,z)$.

.... (A.III.5)

Similar relationships hold between the F_V and F_I fields of the ions in the other groups.

The expressions for the fields are:

$$F_D(1,1,x) = F_D(1,1,y)$$

$$= -\frac{Ae}{r_o^2}\left[\frac{1+2V^1-\lambda}{[(\lambda-V^1)^2+(1+V^1)^2]^{3/2}} - \frac{1+2V^1}{[V^{1\,2}+(1+V^1)^2]^{3/2}}\right.$$

$$+\frac{2(1+V^1)}{[2(1+V^1)^2+(1+\lambda)^2]^{3/2}} - \frac{2(1+V^1)}{[1+2(1+V^1)^2]^{3/2}} + \frac{(3+2V^1+\lambda)}{[(1+V^1)^2+(2+V^1+\lambda)^2]^{3/2}}$$

$$+\frac{(3+2V^1)}{[(1+V^1)^2+(2+V^1)^2]^{3/2}} - \frac{2(1+2V^1-V)}{[(V^1-V)^2+(1+V^1)^2+(1+V)^2]^{3/2}} + \frac{2(1+2V^1)}{[1+V^{1\,2}+(1+V^1)^2]^{3/2}}$$

$$-\frac{2(1+V^1)}{[(V^1-V)^2+(2+V^1+V)^2]^{3/2}} + \frac{2(1+V^1)}{[V^{1\,2}+(2+V^1)^2]^{3/2}} - \frac{2(3+2V^1+V)}{[(1+V^1)^2+(2+V^1+V)^2+(1+V)^2]^{3/2}}$$

$$\left.+\frac{2(3+2V^1)}{[(1+V^1)^2+(2+V^1)^2+1]^{3/2}} - \frac{1/2\sqrt{2}}{[2+V^1+V]^2} + \frac{1/2\sqrt{2}}{[2+V^1]^2}\right] \quad \ldots\ldots (A.III.6)$$

$$F_D(1,1,2) = 0$$

Define FA as the expression within the large square brackets in Equation (A.III.6) with $V^1=V$. [c.f Equation (A.II..9)]. Define FA9 as the expression within the large square brackets in Equation (A.II .8).

$$F_D(2,1,x) = -\frac{A_e}{r_0^2}\left[FA - \frac{(V-V^1)}{\left[(V-V^1)^2+(1+V^1)^2+(1+V)^2\right]^{3/2}}\right]$$

$$F_D(2,1,y) = -\frac{A_e}{r_0^2}\left[\frac{(1+V^1)}{\left[(V-V^1)^2+(1+V^1)^2+(1+V)^2\right]^{3/2}} - \frac{1}{2\sqrt{2}(1+V)^2}\right]$$

$$F_D(2,1,z) = -\frac{A_e}{r_0^2}\left[FA + \frac{1}{2\sqrt{2}(1+V)^2} - \frac{(1+V)}{\left[(V-V^1)^2+(1+V^1)^2+(1+V)^2\right]^{3/2}}\right]$$

$$F_D(3,1,x) = -\frac{A_e}{r_0^2}\left[FA + \frac{(V^1-V)}{\left[(V-V^1)^2+(2+V+V^1)^2\right]^{3/2}}\right]$$

$$F_D(3,1,y) = -\frac{A_e}{r_0^2}\left[-FA - \frac{1}{4(1+V)^2} + \frac{(2+V+V^1)}{(V-V^1)^2+(2+V+V^1)^{2\,3/2}}\right]$$

$$F_D(3,1,2) = 0$$

$$F_D(4,1,x) = -\frac{A_e}{r_0^2}\left[\frac{(1+V^1)}{\left[(1+V^1)^2+(1+V)^2+(2+V+V^1)^2\right]^{\frac{3}{2}}} - \frac{1}{(1+V)^2 6\sqrt{6}}\right]$$

$$F_D(4,1,y) = -\frac{A_e}{r_0^2}\left[-FA - \frac{1}{(1+V)^2 3\sqrt{6}} + \frac{(2+V+V^1)}{\left[(1+V^1)^2+(1+V)^2+(2+V+V^1)^2\right]^{3/2}}\right]$$

$$F_D(4,1,z) = -\frac{A_e}{r_0^2}\left[-FA - \frac{1}{(1+V)^2 6\sqrt{6}} + \frac{(1+V)}{\left[(1+V)^2+(1+V^1)^2+(2+V+V^1)^2\right]^{3/2}}\right]$$

$$F_D(5,1,x) = FD(5,1,y)$$

$$= -\frac{A_e}{r_0^2}\left[-FA - \frac{1}{(1+V)^2 8\sqrt{2}} + \frac{1}{2(2+V+V^1)^2\sqrt{2}}\right]$$

$$F_D(5,1,z) = 0$$

$$F_D(6,1,x) = -\frac{A_e}{r_0^2}\left[FA9+\frac{(\lambda-V)}{[(\lambda-V)^2+(1+V)^2]}3/2 - \frac{(\lambda-V^1)}{[(\lambda-V^1)^2+(1+V^1)^2]}3/2\right]$$

$$F_D(6,1,y) = -\frac{A_e}{r_0^2}\left[\frac{(1+V^1)}{[(\lambda-V^1)^2+(1+V^1)^2]}3/2 - \frac{(1+V)}{[(\lambda-V)^2+(1+V)^2]}3/2\right]$$

$$F_D(6,1,z) = 0$$

$$F_D(7,1,x) = -\frac{A_e}{r_0^2}\left[\frac{(1+V^1)}{[(1+\lambda)^2+2(1+V^1)^2]}3/2 - \frac{(1+V)}{[(1+\lambda)^2+2(1+V)^2]}3/2\right]$$

$$F_D(7,1,y) = -\frac{A_e}{r_0^2}\left[\frac{(1+V^1)}{[(1+\lambda)^2+2(1+V^1)^2]}3/2 - \frac{(1+V)}{[(1+\lambda)+2(1+V)^2]}3/2\right]$$

$$F_D(7,1,z) = -\frac{A_e}{r_0^2}\left[FA9 + \frac{(1+\lambda)}{[(1+\lambda)^2+2(1+V)^2]}3/2 - \frac{(1+\lambda)}{(1+\lambda)^2+2(1+V^1)^2]}3/2\right]$$

$$F_D(8,1,x) = -\frac{A_e}{r_0^2}\left[-FA9- \frac{(2+\lambda+V)}{[(2+ +V)^2+(1+V)^2]}3/2 + \frac{(2+\lambda+V^1)}{[(2+\lambda+V)^2+(1+V^1)^2]}3/2\right]$$

$$F_D(8,1,y) = -\frac{A_e}{r_0^2}\left[\frac{(1+V^1)}{[(2+\lambda+V^1)^2+(1+V^1)^2]}3/2 - \frac{(1+V)}{[(2+\lambda+V)^2+(1+V)^2]}3/2\right]$$

$$F_D(8,1,z) = 0$$

.... (A.III.7)

The field produced by the dipole $\underline{m}_2$ at the dipole $\underline{m}_1$ is, in general, given by

$$\underline{F} = -(\underline{m}_2 \cdot \hat{\underline{m}}_1/d^3 - 3(\underline{m}_2 \cdot \underline{d})(\hat{\underline{n}}_1 \cdot \underline{d})/d^5)\hat{\underline{m}}_1 \quad \ldots(A.III.8)$$

where $\underline{d}$ is the line joining dipoles $\underline{m}_1$ and n_2, and $\hat{\underline{n}}_1$ is the unit dipole.

Define co-efficients C's such that the dipole fields $\underline{F}_{\pm}$'s are, in general, given by

$$\underline{F}_{\pm} = -\alpha_{\pm} C/r^3 \quad (\underline{F}_V + \underline{F}_D + \underline{F}_{\pm}) + W \quad \ldots(A.III.9)$$

where $\alpha_{\pm}$ is the ionic polarisibility and W is the field contribution from region II. Numerically for ions in Groups 1 to 5 W is $Ae/\sqrt{2}r_0^2$ $(0.730\ M_{\mp} + 0.247\ M_{\pm})$ and for ions in Groups 6 to 8 it is Ae/r_0^2 $(0.388\ M_{\mp} - 0.323\ M_{\pm})$.

From Equation (A.III.8) C is given by

$$C = (\hat{\underline{m}}_2 \cdot \hat{\underline{m}}_1/d^3 - 3(\hat{\underline{n}}_2 \cdot \underline{d})(\hat{\underline{n}}_1 \cdot \underline{d})/d^5) \quad \ldots(A.III.10)$$

Taking specifically the dipole $\underline{m}_1$ at 1,1,0 ,

$C = C(a,b,x,y)$

where 'a' specifies the Group which $\underline{m}_2$ belongs to,

'b' specifies the particular ion in the Group which $\underline{m}_2$ belongs to.

'x' specifies the component of $\hat{\underline{M}}_2$ which is producing the field

and 'y' specifies the direction of the field produced at $\hat{\underline{M}}_1$.

For example C(2,1,x,y) is the field co-efficient with $\hat{\underline{M}}_2$ at (101) [first ion in group 2] and $\hat{\underline{M}}_1$ at (110). This is the field coefficient produced by the '$\underline{x}$' component of $\hat{\underline{M}}_2$ in the 'y' direction at $\hat{\underline{M}}_1$.

The expressions for the C's are

$$C(2,1,x,x) = \frac{1}{d_2^3} - \frac{3(V^1-V)^2}{d_2^5}\ ,\quad C(2,1,y,y) = \frac{1}{d_2^3} - \frac{3(1+V^1)^2}{d_2^5}\ ,$$

$$C(2,1,z,z) = \frac{1}{d_2^3} - \frac{3(1+V)^2}{d_2^5}\ ,\quad C(2,1,x,y) = -\frac{3(V^1-V)(1+V^1)}{d_2^5}\ ,$$

$$C(2,1,y,z) = \frac{3(1+V^1)(1+V)}{d_2^5}\ ,\quad C(2,1,x,z) = \frac{3(V^1-V)(1+V)}{d_2^5}$$

and $d_2 = [(V^1-V)^2 + (1+V^1)^2 + (1+V)^2]^{\frac{1}{2}}$;

$$C(3,1,x,x) = \frac{1}{d_3^3} - \frac{3(V^1-V)^2}{d_3^5}\ ,\quad C(3,1,y,y) = \frac{1}{d_3^3} - \frac{3(2+V+V^1)^2}{d_3^5}\ ,$$

$$C(3,1,z,z) = \frac{1}{d_3^3}\ ,\quad C(3,1,x,y) = -\frac{3(V^1-V)(2+V+V^1)}{d_3^5}\ ,$$

$$C(3,1,x,z) = C(3,1,y,z) = 0\ ,$$

$$d = [(V^1-V)^2 + (2+V+V^1)^2]^{\frac{1}{2}}\ ;$$

$$C(4,1,x,x) = \frac{1}{d_4^3} - \frac{3(1+V^1)^2}{d_4^5}\ ,\ C(4,1,y,y) = \frac{1}{d_4^3} - \frac{3(2+V+V^1)^2}{d_4^5}$$

$$C(4,1,z,z) = \frac{1}{d_4^3} - \frac{3(1+V)^2}{d_4^5}\ ,\ C(4,1,x,y) = -\frac{3(2+V+V^1)(1+V^1)}{d_4^5}$$

$$C(4,1,x,z) = -\frac{3(1+V^1)(1+V)}{d_4^5}\ ,\ C(4,1,y,z) = -\frac{3(1+V)(2+V+V^1)}{d_4^5}$$

$$d_4 = \left[(1+V^1)^2 + (2+V+V^1)^2 + (1+V)^2\right]^{\frac{1}{2}}\ ;$$

$$C(5,1,x,x) = \frac{1}{d_5^3} - \frac{3(2+V+V^1)^2}{d_5^5}\ ,\ C(5,1,y,y) = \frac{1}{d_5^3} - \frac{3(2+V+V^1)^2}{d_5^5}$$

$$C(5,1,x,y) = -\frac{3(2+V+V^1)^2}{d_5^5}\ ,\ C(5,1,z,z) = \frac{1}{d_5^3}$$

$$C(5,1,x,z) = C(5,1,y,z) = 0$$

$$d_5 = [2+V+V^1]\sqrt{2}\ ;$$

$$C(6,1,x,x) = \frac{1}{d_6^3} - \frac{3(V^1-\lambda)^2}{d_6^5}\ ,\ C(6,1,y,y) = \frac{1}{d_6^3} - \frac{3(1+V^1)^2}{d_6^5}$$

$$C(6,1,z,z) = \frac{1}{d_6^3}\ ,\ C(6,1,x,y) = -\frac{3(V^1-\lambda)(1+V^1)}{d_6^5}$$

$$C(6,1,x,z) = C(6,1,y,z) = 0,$$

$$d_6 = \left[(V^1-\lambda)^2 + (1+V^1)^2\right]^{\frac{1}{2}}\ ;$$

$$C(7,1,x,x) = C(7,1,y,y) = \frac{1}{d_7^3} - \frac{3(1+V^1)^2}{d_7^5}\ ,$$

$$C(7,1,z,z) = \frac{1}{d_7^3} - \frac{3(1+\lambda)^2}{d_7^5}\ ,$$

$$C(7,1,x,y) = -\frac{3(1+V^1)^2}{d_7^5}, \quad C(7,1,x,z) = C(7,1,y,z) = \frac{3(1+V^1)(1+\lambda)}{d_7^5},$$

$$d_7 = \left[2(1+V^1)^2 + (1+\lambda)^2\right]^{\frac{1}{2}};$$

$$C(8,1,x,x) = \frac{1}{d_8^3} - \frac{3(2+\lambda+V^1)^2}{d_8^5}, \quad C(8,1,y,y) = \frac{1}{d_8^3} - \frac{3(1+V^1)^2}{d_8^5}, \quad C(8,1,z,z) = \frac{1}{d_8^3},$$

$$C(8,1,x,y) = -\frac{3(2+\lambda+V^1)(1+V^1)}{d_8^5}, \quad C(8,1,x,z) = C(8,1,y,z) = 0$$

$$d_8 = \left[(2+\lambda+V^1)^2 + (1+V^1)^2\right]^{\frac{1}{2}} \qquad \ldots\ (A.III.11)$$

Similarly $A(a,b,x,y)$ are defined as numerically equal to $C(a,b,x,y)$ with $V^1 = V$.

From Equation (A.III.9)

$$F_{\bar{I}}(1,1,x) = F_{\bar{I}}(1,1,y)$$

$$= \sum_{a=1}^{5} \sum_{b=1}^{4} \sum_{w=x,y,z} \frac{-\alpha_+}{r_0^3} \left\{C(a,b,w,y)\left[F_{\bar{V}}(a,b,w) + F_{\bar{D}}(a,b,w) + F_{\bar{I}}(a,b,w)\right] + W(a)\right\}$$

$$+ \sum_{a=6}^{8} \sum_{b=1}^{2} \sum_{w=x,y,z} \frac{\alpha_-}{r_0^3} \left\{C(a,b,w,y)\left[F_{\bar{V}}(a,b,w) + F_{\bar{D}}(a,b,w) + F_{\bar{I}}(a,b,w)\right] + W(a)\right\}$$

$$F_{\bar{I}}(1,1,z) = 0 \qquad \ldots\ (A.III.12)$$

The expressions for the $F_{\bar{I}}$ fields of the other groups are similarly given, with the co-efficeints A's substituted

for C's where appropriate. The energy, E_5, due to the field terms is then given by

$$\underline{E}_5 = -\tfrac{1}{2}\alpha \underline{+} \sum_{a=1,6}^{5,8} \sum_{b=1}^{4} \sum_{w=x,y,z} \{ (F_I(a,b,w)+F_D(a,b,w)+F_V(a,b,w)) \times$$

$$(F_D(a,b,w)+F_V(a,b,w)) - (F_V(a,b,w))^2 \}$$

$$-\tfrac{1}{2}\alpha \underline{+} \sum_{a=6,1}^{5,8} \sum_{b=1}^{4} \sum_{w=x,y,z} \{ (F_I(a,b,w)+F_D(a,b,w)+F_V(a,b,w)) \times$$

$$(F_D(a,b,w)+F_V(a,b,w)) - (F_V(a,b,w))^2 \}$$

.....(A.III.13)

References.

1. LIDIARD, A.B., 1957, Handbuk der Physik, 20 337
2. REINHOLD, H., 1929, Z Physik. Chem. A 141 137
3. REINHOLD, H. and SCHULZ, R., 1933, Z Physik. Chem. A 164 241
4. ALLNATT, A.R. and CHADWICK, A.V., 1967, Trans. Fara- Soc., 536 1929
5. CHRISTY, R.W., FUKUSHIMA, E. and LI, H.T., 1959 J. Chem. Phys. 30 136
6. CHRISTY, R.W., 1961, J. Chem. Phys., 34 4
7. NIKITINSKAYA, T.I. and MURIN, A.N., 1955, Zh. Tekhn. Fiz. 25 1198.
8. ALLNATT, A.R. and JACOBS, P.W.M., 1962, Proc. Roy. Soc. A 267 31
9. CHRISTY, R.W., HSUEH, Y.W., and MUELLER, R.C., 1963 38 1647
10. HOSHINO, H. and SHINOJI, M., 1967 J. Phy. Chem. Solids 28 1167
11. JACOBS, P.W.M. and MAYCOCK, J.N., 1966 Trans. Met. Soc. AIME 236 165
12. ALLNATT, A.R. and CHADWICK, A.V., 1967 J. Chem. Phys. 47 2372
13. HOWARD, R.E., 1958 Ph. D. Thesis, OXFORD.
14. ALLNATT, A.R. and JACOBS, P.W.M., 1961 Proc. Roy. Soc. A260 350

15. SHIMOJI, M. and HOSHINO, H., 1967,
J. Phys. Chem. Solids 28 1155

16. WIRTZ, K., 1943, Phys. Z., 44 221

17. LECLAIRE, A.D., 1954, Phy. Rev, 93 344

18. BRINKMAN, J.A., 1954, Phy. Rev. 93 345

19. SCHOCKLEY, W., 1954, Phy. Rev. 93 345

20. ALLNATT, A.R. and RICE, S.A., 1960, J. Chem. Phys.,
33 573.

21. HOWARD, R.E. and MANNING, J.R., 1962,
J. Chem. Phys. 36 910

22. JAFFE, D. and SHEWMON, P.G., 1964,
Acta Met. 12 515.

23. ALLNATT, A.R., 1965, J. Chem. Phys. 43 1855

24. WERT, C.A., 1950, Phy. Rev, 79 601

25. HAGA, E., 1960, J. Phy. Soc. Japan 15 1949.

26. VINEYARD, G.H., 1957, J. Phys. Chem. Solids
3 121.

27. RICE, S.A., 1958, Phy. Rev., 112 804

28. MANLEY, O.S. and RICE, S.A., 1960 Phy. Rev.,
117 634

29. SLATER, N.B., 1959, Theory of Unimolecular Reactions,
Cornell University Press, Ithaka, New York.

30. SCHOTTKY, G., 1965. Phys. Stat. Sol., 8 357

31. DE GROOT, S.R., 1951, Thermodynamics of Irreversible Processes, Amsterdam, North Holland Publishing House Co.

32. DE GROOT, S.R. and MAZUR, P., 1962 Non-Equilibrium Thermodynamics Amsterdam, North Holland Publishing House Co.

33. BARDEEN, J. and HERRING, C. 1952 Imperfections in Nearly Perfect Crystals, p. 261 New York, Wiley.

34. PATRICK, L and LAWSON, A.W. 1954 J. Chem. Phys. 22 1492

35. HOWARD, R.E. and LIDIARD, A.B., 1957 Phil. Mag. 2 1462

36. HAGA, E., 1958 J. Phys. Soc. Japan 13 1090

37. HOLTAN, H., MAZUR, P., and DE GROOT, S.R. 1953 Physica 19 1109

38. LIDIARD, A.B. and HOWARD, R.E. 1960 Tr. Vses. Kouf.

39. KROGER, F.A., 1964, The Chemistry of Imperfect Crystals, Amsterdam, North Holland Publishing Co.

40. LEHOVEC, K., 1953, J. Chem. Phys. 21 1123

41. DAUNT, J.G., 1955, Progress in Low Temperature Physics, Amsterdam, North Holland Publishing Co.

42. DEKKER, A.J., 1963, Solid State Physics Macmillan, London, p.308

43. LIDIARD, A.B., 1966, Thermodynamics, I.A.E.A. 2 3 Vienna.

44. ORANI, R.A., 1961, J. Chem. Phy. 34 1773

45. GIRIFALCO, L.A. 1962., Phys. Rev, 128 2630

46. KAC, M., 1943, Am. J. Math. 65 609

47. MARADUDIN, A.A., MONTROLL, A.W., and WEISS, G.H., 1963, Theory of Lattice Dynamics in the Harmonic Approximation, Solid State Physics, Supplement 3.

48. FRENKEL, J. 1926 Z. Phys. 35 652

49. SCHOTTKY, W. and WAGNER, C., 1930, Z. Phys. Chem. B11 163

50. JOST, W., 1933, J. Chem. Phys. 1 466

51. SCHOTTKY, W., 1935, Z. Phys. Chem. Abt B. 29 335

52. BORN, M., and MAYER, J., 1932, Z. Physik 75 1

53. TOSI, M.P. and FUMI, F.G., 1964, J. Phys. Chem. Solids, 25 45

54. RITTNER, E.S., 1951, J. Chem. Phys. 19 1030

55. VERSANI, Y.P., 1957, Trans. Faraday Soc., 53 132

56. BAUGHAN, E.C., 1959, Trans. Faraday Soc., 55 736

57. GUCCIONE, R. TOSI, M.P., and ASDENTE, M., 1959 J. Phys. Chem. Solids, 10 162

58. THARMALINGAM, K., 1963, J. Phys. Chem. Solids, 24, 1380.

59. THARMALINGAM, K., 1964, J. Phys. Chem. Solids, 25, 255.

60. BOSWARVA, I.M., and LIDIARD, A.B., 1967
Phil. Mag. 5 805.

61. SCHOLZ, A., 1964 Phys. Stat. Sol, 7 973

62. BRAUER, P., 1952, Z. Naturforsch, 7a 372

63. PAULING, L., 1928, Z. Krist, 67, 377

64. MOTT, N.F. and LITTLETON, M.J., 1938 Trans.
Faraday Soc., 34, 485

65. FUMI, F.G. and TOSI, M.P., 1964, J. Phys
Chem. Solids, 25 31

66. MAYER, J.E., 1933, J. Chem. Phys. 1 270

67. HAJJ, F., 1966, J. Chem. Phys. 44 4618

68. TESSMAN, J.R., KHAN, A.H., and SCHOCKLEY, W.,
1953 92 890.

69. HAUSSUHL, S., 1957, Z. Naturforsch, 12a 445

70. DREYFUS, R.W. and NOWICK, A.S., 1962
J. Appl. Phys. Suppl. 33 473

71. KLEMENS, P.G., 1958, Thermal Conductivity and
Lattice Vibrational Modes, Solid State Physics 7 1

72. BALLARD, S.S., MacCARTHY, K.A., and DAVIS, W.C.,
1950 Rev. Sc. Instru. 21 905

73. SUSUKI, Y., ENDO, S., and HAGA, E, 1959
J. Phys. Soc. Japan 14 729

74. EBERT, J. and TEITOW, J., 1950,
Ann. Phys. 5 63

75. COMPTON, W.D. and MAURER, R.J., 1956,
J. Phys. Chem Sol. 1 191

76. HSUEH, Y.W., and CHRISTY, R.W., 1963,
J. Chem. Phy. 39, 3519

77. CZOCHRALSKI, J., 1918, Z. Phys. Chem. 92 219

78. NEWEY, C.W.A. 1959, Ph. D. Thesis, Birmingham University.

79. TUBANDT, C. 1932, Handbuk der Experimentalphysik
12 (1) 383.

80. KIRK, D.L. and PRATT, P.L.
1967, Proc. Brit. Cer. Soc. 9 215

81. BARR, L. and MORRISON, 1965
J. Appl. Phys. 36 624

82. ALLNATT, A.R. and JACOBS, P.W.M., 1962,
Trans. Fara. Soc., 58, 116

83. HOWARD, R.E. and LIDIARD, A.B., 1964,
Rep. Prog. Phys. 27 161

84. BOSWARVA, I.M. PRIVATE COMMUNICATIONS.

85. STOEBE, T.G. and HUGGINS, R.A., 1966 J. Mat. Sci.,
1, 117

86. SCAMP, H.W. and KATZ, E., 1954, Phys. Rev. 94, 828

87. ROLFE, J., 1964, Can. J. Phys., 42 2195

88. ROTHMAN, S.J., PETERSON, N.L., and NOWICKI, L.J.,
1968, Bull. Am. Phys. Soc., 13 466

89. HAVEN, T., 1950, Rec. Trav. Chim. Pays-Bas,
69, 1259, 1471 and 1505.

90. BORN, M. and HUANG, K., 1956,

Dynamical Theory of Crystal Lattices p. 26.

Acknowledgement

I wish to thank my supervisor, Professor P.I. Pratt, for the constant help and encouragement in this work.

I wish to thank Professor J.G. Ball for providing the research facilities and the Atomic Energy Research Establishment for sponsoring the project.

Dr. I.M. Boswarva suggested this topic, and from the very beginning of the project, he has been a sympathetic, helpful and generous tutor and friend. I thank him most sincerely.

I wish to thank both my parents. My father has spared nothing as far as the education and well being of his children is concerned. We are all indebted to him.

FIGURE 13

GRAPH COMPARING THE PREDICTIONS OF THE 'NO TRAP' THEORY AND THE EXPERIMENTAL THERMOPOWER VS. TEMPERATURES OF PURE NaCl CRYSTALS

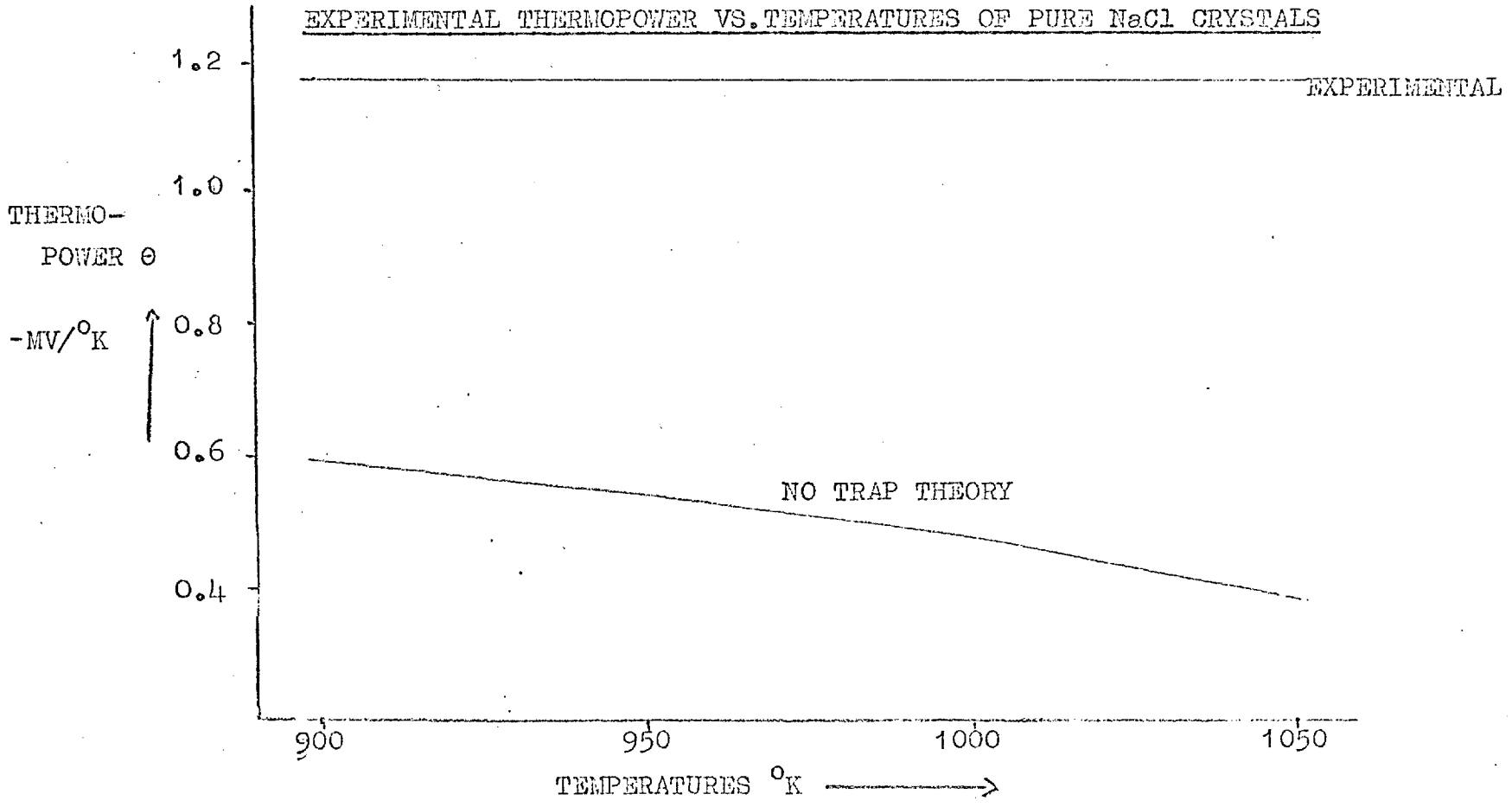

CAPTION: THE THEORETICAL CURVE IS DRAWN FROM EQUATION (VII 1) WITH $Q^{*}_{\pm} = 2E_{\pm}$

FIGURE 14

GRAPH COMPARING THE PREDICTIONS OF THE JACOBS AND MAYCOCK THEORY AND THE EXPERIMENTAL THERMOPOWER VS .TEMPERATURES OF PURE NaCl CRYSTALS.

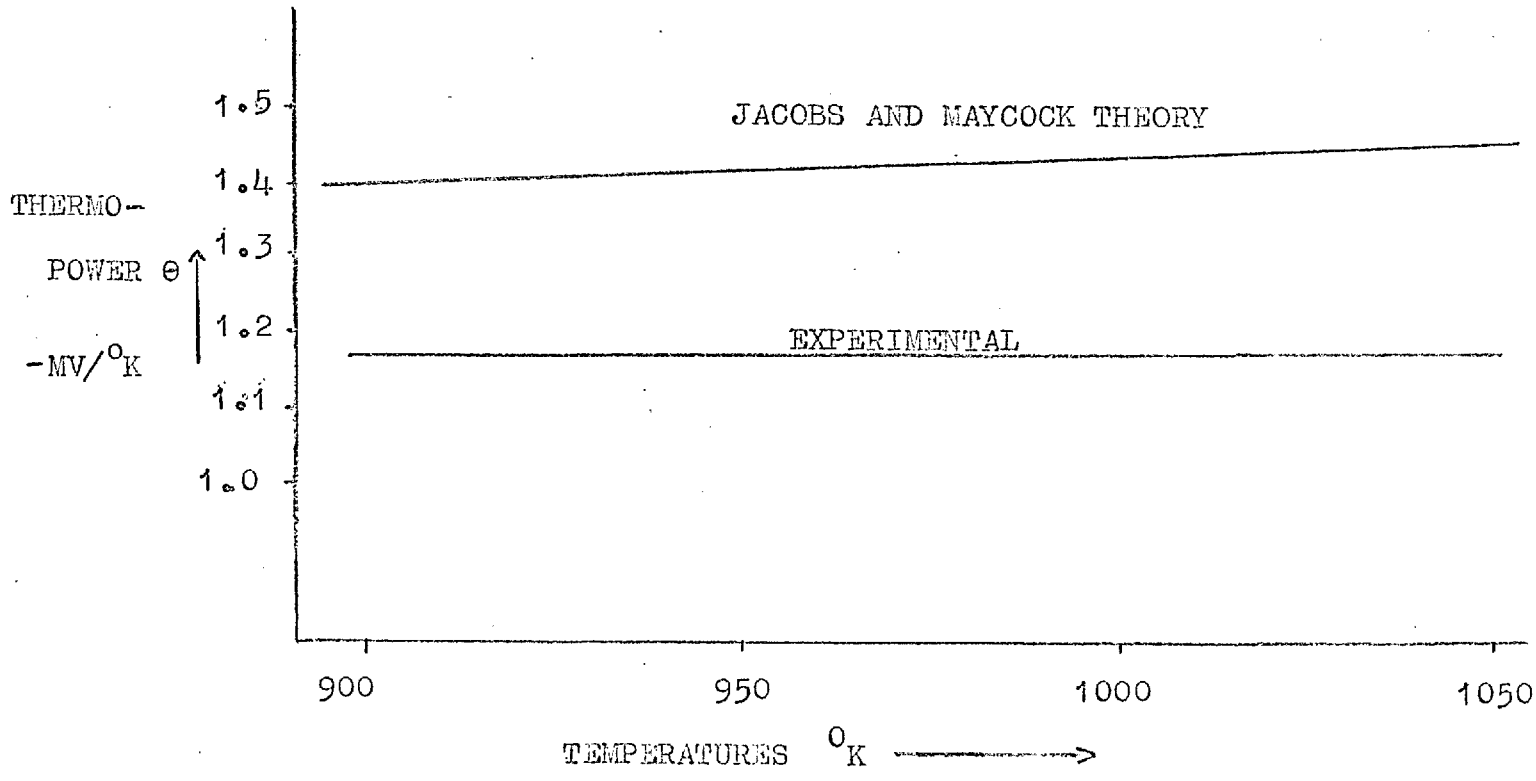

CAPTION : THE THEORETICAL CURVE IS DRAWN FROM EQUATION (II 27)

WITH $Q^{*}_{\pm} = 2E_{\pm}$